

Membrane properties and synaptic
integration of identified neuronal
populations in the developing rodent
neocortex

Dissertation

Zur Erlangung des Grades
Doktor der Naturwissenschaften

Am Fachbereich Biologie
der Johannes Gutenberg-Universität
Mainz

vorgelegt von

Aurel-Bogdan Sava

geb. am 25.01.1979 in Vaslui, Rumänien

Mainz, 2011

Dekan:

1. Berichterstatter:

2. Berichterstatter:

Tag der mündlichen Prüfung: 26.04.2012

Table of contents

Abbreviations.....	3
1. Introduction.....	6
1.1 Development of the nervous central system (CNS).....	6
1.1.1 Role, function and integration of Cajal-Retzius cells	7
1.1.2 Role, function and integration of subplate cells.....	9
1.1.3 Role of the GABAergic system during cortical development	10
1.1.4 Role of the Glycinergic system during development	11
1.2 Aims of the present study	12
2. Material & Methods.....	14
2.1 Preparation of the cortical slices.....	14
2.1.1 Tangential slice preparation.....	14
2.1.2 Coronal slice preparation.....	14
2.1.3 Mini slice preparation.....	15
2.2 Electrophysiological setup.....	15
2.3 Identification of Cajal-Retzius cells.....	16
2.4 Identification of the subplate cells	16
2.5 Electrophysiological procedures	17
2.6 Generation of <i>Dbx1^{cre};ROSA26^{YFP}</i> recombinant mice	18
2.7 Generation of GAD67-GFP transgenic mouse	19
2.8 Solutions and substances	19
2.8.1 Extracellular solution	19
2.8.2 Intracellular solution	19
2.8.3 List of substances used.....	20
2.9 Staining procedures	20
2.10 Statistics	21
3. Results	22
3.1 Electrophysiological and morphological properties of Cajal-Retzius cells with different ontogenetic origins	22
3.1.1 Identification of YFP ⁺ and YFP ⁻ Cajal-Retzius cells	22
3.1.2 Passive and active electrophysiological properties of YFP ⁺ and YFP ⁻ Cajal- Retzius cells.....	24

3.1.3 GABA _A -receptors on CR cells	27
3.1.4 NMDA-receptors on CR cells	28
3.2 Glycine receptors mediate excitation of subplate neurons in neonatal rat cerebral cortex	30
3.2.1 Morphology and membrane properties of the subplate cells (SP cells)	30
3.2.2 Glycine-induced membrane responses in SP cells	31
3.2.3 Activation of glycine receptors by taurine in SP cells	34
3.2.4 Pharmacological properties of glycine-induced responses in SP cells	35
3.2.5 Intrinsic activation of glycine receptors	38
3.3 GABAergic networks in the developing cerebral cortex are activated by taurine	39
3.3.1 Basic properties of the investigated pyramidal cells	39
3.3.2 Effect of taurine on pyramidal neurons	42
3.3.3 Pharmacology of taurine-induced responses in pyramidal neurons	45
3.3.4 Reversal of taurine-induced sPSCs	51
3.3.5 Effect of taurine on GABAergic interneurons	53
3.3.6 Taurine effect on pyramidal neurons in reduced slice preparation	58
3.3.7 Effect of isogavacine and glycine on sPSCs in pyramidal neurons	59
3.3.8 Temporal coherence between taurine-induced PSCs	60
4. Discussion	62
4.1 CR cells of different origins show homogenous electrophysiological properties	62
4.2 Functional expression of glycine receptors in SP cells	65
4.3 Taurine activates GABAergic networks in the immature neocortex	69
4.4 Conclusion	73
5. Summary	74
6. References	75
Acknowledgments	95
Declaration of contribution	96
Curriculum vitae	97

Abbreviations

%	Percent
ACSF	Artificial cerebrospinal fluid
AMPA	α -Amino-3Hydroxy-5-Methyl-4-Isoxazolpropion
ANOVA	Analysis of variance
AP	Action potential
APV	DL-2-Amino-5-phosphonopentanoic acid
Ca ²⁺	Calcium
C _{in}	Input capacitance
cm	Centimetre
CR-cell	Cajal-Retzius cell
nCR-cell	Non Cajal-Retzius cell
CNQX	6-cyano-7-nitroquinoxaline-2,3-dione
CNS	Central nervous system
CP	Cortical plate
CPn	Cortical plate neurons
CPP	3-(2-Carboxypiperazin-4-yl) propyl-1-phosphonic acid
DIC	Differential interference contrast
DMSO	Dimethyl sulfoxide
ES cell	Embryonic stem cell
E _h	Holding potential

GABA	Gamma-amino-butyric acid
GABA _A	Ionotropic gamma-amino-butyric acid receptor
GABA _B	Metabotropic gamma-amino-butyric acid receptor
GAD	Glutamic acid decarboxylase
GES	Guanidinoethyl sulphonate
GFP	Green fluorescent protein
CP neurons	Cortical plate neurons
h	Hour
Hz	Hertz
IR	Infrared-light
K ⁺	Potassium
KCC2	K ⁺ -Cl ⁻ cotransporter
MZ	Marginal zone
mPSCs	Miniature postsynaptic currents
Na ⁺	Sodium
NKCC1	Na ⁺ -K ⁺ -2Cl ⁻ cotransporter
NMDA	N-methyl-D-aspartate
(P) 0-7	Postnatal day 0 to 7
PSCs	Postsynaptic currents
R _{in}	Input resistance
RMP	Resting membrane potential
RT	Room temperature
SEM	Standard error of the mean

SD	Standard deviation
SP	Subplate
SP-cell	Subplate cell
sPSCs	Spontaneous postsynaptic currents
SVZ	Subventricular zone
TTX	Tetrodotoxin
VZ	Ventricular zone
WM	White matter

1. Introduction

1.1 Development of the nervous central system (CNS)

The brain is one of the most sophisticated biological structures. During the first stages of its development a complex and tightly regulated sequence of proliferation, migration and maturation must occur (Sur and Rubenstein, 2005). The formation of CNS starts very early during embryogenesis when it differentiates from the ectoderm, which is one of the three primary germ cell layers. During gastrulation, cellular reorganization of the embryo takes place and the other germ layers, endoderm and mesoderm, invaginate inward, leaving the ectoderm on the surface (Squire, 2003). Following gastrulation in all three newly formed layers, cells begin to generate the anlagen that later develop into the different organ systems. The ectoderm situated at the dorsal side of the embryo, begins to thicken and form the neural plate. During two steps of neurulation (primary and secondary neurulation), a complex morphogenetic process, cells in the neural plate give rise to the neural tube and subsequently, the CNS (Squire, 2003). After formation, the anterior end of the neural tube starts to swell and subdivides into three primary vesicles (the prosencephalon, mesencephalon and rhombencephalon). The prosencephalic vesicle subsequently divides into the telencephalon and the diencephalon, the rhombencephalic vesicle forms the metencephalon and myelencephalon. The telencephalon, which gives rise to the cerebral cortex, is situated at the most rostral part of the vesicles. There two buds appear and form the two telencephalic vesicles which will lead to the formation of the cerebral hemispheres. Due to neuron proliferation the telencephalon expands to form three distinct regions (the cerebral cortex, basal telencephalon and olfactory bulb). The majority of principal cortical neurons are generated in the ventricular zone (VZ)/subventricular zone (SVZ), which develops from the inner, ventricular surface of the neuroepithelium and migrate outward along radial glial fibers (Sidman & Rakic, 1973) into the developing neocortex until they reach the marginal zone (MZ). Radial glia cells are involved in key developmental processes as patterning and neuronal migration. Recently it was discovered that radial glial cells also function as precursors during neurogenesis (Noctor et al., (2001). They arise early in development from neuroepithelial cells and divide asymmetrically in the ventricular zone (VZ) to generate radial glia cells, postmitotic neurons and intermediate

progenitor cells. At the border of the MZ migrating neurons detach from radial glial cells to form the cortical plate in an inside-out manner which later develops into the cortical layers VI to II (Parnavelas et al., 2000; Frotscher et al., 1998). For this process reelin, an extracellular matrix glycoprotein released from Cajal-Retzius cells (CR cells), plays an essential role (D'Arcangelo et al., 1997). A second class of neurons are GABAergic interneurons. In contrast to principal neurons, nearly all cortical GABAergic interneurons originate from the ganglionic eminence in the ventral forebrain and migrate tangentially to the neocortex (Pleasure et al., 2000; Zhu et al., 1999). However, in humans and non-humans primates they originate from both the ganglionic eminence and the SVZ of the dorsal telencephalon (Metin et al., 2006). The early developmental events like proliferation, migration and primary axon ingrowth are thought to depend mainly on genetic programs (Spitzer, 2006). In the last decades experiments on developing neocortical neurons demonstrated that neurotransmitters could also influence developmental processes like proliferation (LoTurco et al., 1995), migration (Behar et al., 1998; Behar et al., 2000; Behar et al., 1999) and differentiation (Altshuler et al., 1993; Fukui et al., 2008).

1.1.1 Role, function and integration of Cajal-Retzius cells

Retzius cells (CR cells) are one of the major neuronal cell types involved in the development of the cortex. These neurons gain much of interest when it was discovered that they secrete the extracellular matrix protein reelin, which is essential for the correct lamination of the brain (D'Arcangelo et al., 1995, Frotscher, 1998). CR cells reside directly below the pial surface in the marginal zone (MZ). They have a unique morphology compared with other cell types, displaying a horizontal orientation with one thick tapered dendrite and a long spanning axon (Mienville, 1999). CR cells are under the first cell types appearing in the developing neocortex (Bayer and Altman, 1991).. Despite their important role in development, CR cells disappear later in development, most probably by apoptosis (Derer and Derer, 1990; Meyer and González-Hernández, 1993; Naqui et al., 1999), although dilution of these cells in the growing cerebral surface or transformation into other cell types are currently discussed (Marin-Padilla, 1990).

The neuronal nature of CR cells is clearly demonstrated by their ability to fire action potentials (Zhou and Hablitz, 1996c; Hestrin and Armstrong, 1996; Kilb and Luhmann, 2000; Kilb et al., 2000). CR cells display electrophysiological properties typical for immature neurons: a relatively positive resting membrane potential (RMP), a high input resistance, and slow action potentials with a high threshold (Zhou and Hablitz, 1996a; Hestrin and Armstrong, 1996). A particular feature of CR cells is the pronounced hyperpolarization-activated voltage sag, which is caused by a hyperpolarization-activated inward current (Zhou and Hablitz, 1996a; Kilb and Luhmann 2000). These cells express a variety of neurotransmitter receptors such as: gamma-amino-butyric acid type A (GABA_A) (Mienville, 1998), N-methyl-D-aspartate (NMDA) (Mienville and Pesold, 1999), α -amino-3-hydroxy-5-methyl-isoxazole-propionic acid (AMPA)/kainate (Kim and Connors, 1993; Aguiló et al., 1999), glycine (Kilb et al., 2002; Okabe et al, 2004) and muscarinic and adrenergic receptors (Schwartz et al., 1998). In the last years, an series of publications indicate that CR cells are integrated into synaptic networks of the immature neocortex (Mienville, 1998; Aguiló et al., 1999; Kilb and Luhmann, 2001;Radnikow et al., 2002;Soda et al., 2003).

The heterogeneity of transcription factors and the different origins of CR cells indicate that the neurons grouped under the term “Cajal–Retzius cell” may actually represent different neuronal populations (Meyer and Wahle, 1999; Bielle et al., 2005). While it was originally thought that CR cells are produced by the local pallium ventricular zone as part of the primordial plexiform layer (Marin-Padilla, 1998) other regions at the borders of the developing pallium were subsequently identified as sources of CR cells, like the cortical hem, the septum, or the retrobulbar ventricular zone (Meyer and Wahle, 1999;Zecevic and Rakic, 2001;Meyer et al., 2002;Shinozaki et al., 2002;Takiguchi-Hayashi et al., 2004). Neurons from these origins most probably populate the entire cortical surface via tangential migration within the marginal zone (Hevner et al., 2003;Takiguchi-Hayashi et al., 2004;Garcia-Moreno et al., 2007). Recently, an additional origin of CR cells at the pallial–subpallial border (PSB) of the ventral pallium was identified by the expression of the transcription factor *Dbx1* (Bielle et al., 2005). The homeodomain transcription factor *Dbx1* is expressed in progenitors at the boundaries between dorsal and ventral parts of the caudal neural tube (Lu et al., 1992;Pierani et al., 1999;Shoji et al., 1996) and in

the telencephalon is restricted to the pallial–subpallial boundary, the septum and the preoptic/anterior entopenduncular area (Medina et al., 2004; Yun et al., 2001). Permanently labeled Dbx1-derived postmitotic cells migrate from the septum and PSB to populate the embryonic MZ, where they express reelin and show the typical location and appearance of CR cell (Bielle et al., 2005).

1.1.2 Role, function and integration of subplate cells

Subplate cells (SP cells) are another particularly important cell type during neocortical development. They are involved in the pathfinding of corticopetal and corticofugal axonal projections (Ghosh and Shatz, 1993; Ghosh et al., 1990; McConnell et al., 1989) and the formation of cortical columns (Kanold et al., 2003). As CR cell, SP cells are born before the majority of the first cortical plate neurons (Luskin and Shatz, 1985; Valverde et al., 1990). SP cells are well integrated in the developing cerebral cortex. They receive synaptic inputs from thalamus, cortical neurons and from other SP cells (Kostovic and Rakic, 1980; Friauf et al., 1990; Hanganu et al., 2002), indicating that they are capable to process information from cortical and subcortical regions. Recently it has been show that SP cells plays important role in the generation of transient oscillatory network activity in the newborn rodent cortex (Dupont et al., 2006). These observations indicate that SP cells are essential for activity-dependent formation of cortical circuits during early stages of development (Kanold, 2004; Kostovic and Judas, 2002; Allendoerfer and Shatz, 1994).

SP cells express functional NMDA, AMPA/kainate and GABA_A receptors and these receptors mediate fast synaptic transmission between cortex and thalamus and within the SP (Hanganu et al., 2002; Kilb and Luhmann, 2001). Furthermore, cholinergic fibers from basal forebrain first accumulates in the subplate and plays a modulatory role via activation of nicotinic (Hanganu and Luhmann, 2004) and muscarinic receptors (Dupont et al., 2006) expressed in SP cells. Unlike CR cells, SP cells display a large variety of morphologies (Hanganu et al., 2002).

1.1.3 Role of the GABAergic system during cortical development

GABA is one of the most important neurotransmitter in the brain (Wang et al., 2009) and acts primarily by binding to GABA_A or GABA_B receptors. GABA can act as excitatory or inhibitory neurotransmitter depending on the stage of the development (Ben-Ari et al., 2007; Wang et al., 2009). The GABA_A receptor is an ionotropic receptor, permeable mostly to Cl⁻ and therefore the reversal potential of GABAergic currents is determined mainly by the Cl⁻ distribution over the membrane. In immature neurons activation of GABA_A receptors will lead to membrane depolarization caused by Cl⁻ efflux and can therefore have an excitatory effect (Luhmann and Prince, 1991). This is due to the high Cl⁻ accumulation into the immature neurons via the Na⁺-K⁺-2Cl⁻ cotransporter NKCC1, expressed from mid-embryonic stages until first week of the postnatal life in rodents (Li et al., 2002; Wang et al., 2002; Plotkin et al., 1997; Wang et al., 2002; Achilles et al., 2007). In the mature brain, Cl⁻ ions are entering into the cell after activation of GABA_A receptors, which will lead to membrane hyperpolarization and therefore inhibitory effect of GABA. This is due to the low intracellular Cl⁻ concentration established by the K⁺-Cl⁻ cotransporter KCC2 (Rivera et al., 1999; Li et al., 2002; Wang et al., 2002). Because GABA_A receptors are expressed early in development in radial glia and migrating neurons, these cells respond to GABA from the beginning of cortical development (Muth-Kohne et al., 2010; Owens et al., 1996; Owens and Kriegstein, 2002). Therefore GABA is involved in most of the developmental steps, mediating the cell proliferation, cell migration and synaptic integration (Wang et al., 2009). Activation of GABA_A receptors decreases cell proliferation (LoTurco et al., 1995; Andäng et al., 2008). In vivo and in vitro studies demonstrated that GABA receptors (GABA_A, GABA_B and GABA_C) are critically involved in the regulation of neuronal migration (Behar et al., 2000; Behar et al., 2001; Heck et al., 2007; Denter et al., 2010). It has been shown that GABA_A receptors are expressed before glutamate receptors in new born neurons of many regions of the developing neocortex and these young neurons receive first GABAergic synaptic inputs before glutamatergic synapses are functional in the neocortex (Owens et al., 1999; Tyzio et al., 1999; Hennou et al., 2002; Ben-Ari, 2006). Therefore spontaneous depolarizations mediated by GABA_A receptor activation may provide the first excitatory drive necessary for activity-dependent synapse formation (Ben-Ari, 2006). In addition to

this excitatory actions, GABA can exert in immature neurons a shunting effect, by clamping the membrane potential near the Cl⁻ reversal potential, thereby preventing long-lasting activation of voltage-gated channels that might lead to Ca²⁺ toxicity. The shunting property of GABA makes this neurotransmitter an ideal regulator for synaptogenesis (Ben Ari et al., 2006).

1.1.4 Role of the Glycinergic system during development

The glycinergic system is another neurotransmitter system that plays an important role in early cortical development (Flint et al., 1998; Kilb et al., 2002; Okabe et al., 2004; Kilb et al., 2008). The effect of glycine is modulated via glycine receptors. The glycine receptor, as the GABA_A receptor, is a ligand-gated chloride channel with the typical pentameric subunit composition. Four highly homologous ligand-binding subunits (α_{1-4}) and one β subunit have been identified so far. Both homomeric glycine receptors containing only α subunits or α/β heteromeric receptors are functional (Vannier and Triller, 1997). Activation of glycine receptors causes a membrane depolarization in immature neurons of the developing cortex (Ito and Cherubini, 1991; Flint et al., 1998; Ehrlich et al., 1999; Kilb et al., 2002; Kilb et al., 2008). Glycine receptors are involved in generation of correlated neuronal activity early in development (Momose-Sato et al., 2005). Taurine, a amino acid which is found in much higher concentration than glycine in the immature cortex (Cutler and Dudzinski, 1974; Davies and Johnston, 1974), is thought to be the endogenous agonist of glycine receptors (Flint et al., 1998). Interestingly, taurine is involved in many neuronal processes as: neuronal neuronal proliferation, migration and differentiation (Sturman et al., 1994; Altshuler et al., 1993; Maar et al., 1995; Palackal et al., 1986), suggesting that glycine may have a possible role during cortical maturation. Functional glycine receptors has been found in different neuronal populations of the developing neocortex: in neurons of the SVZ, in CP neurons and in CR cells and SP cells (Flint et al., 1998; Kilb et al., 2002; Okabe et al., 2004; Kilb et al., 2008), again suggesting an important role of glycine in brain development.

1.2 Aims of the present study

In my PhD work I concentrated on three elementary questions that are essential to understand the interactions between the different neuronal cell populations in the developing neocortex. The questions regarded the identity of CR cells, the ubiquitous expression of glycine receptors in all major cell populations of the immature neocortex, and the role of taurine in the modulation of immature neocortical network activity.

The study of Bielle et al. (2005) provides clear evidence that at least two subpopulations of CR cells with different ontogenetic origins could be identified. The question whether CR cells with different ontogenetic origins display distinct functional properties in the postnatal cortex has not been addressed yet. Therefore, I investigated in the first part of my work the electrophysiological properties of Dbx1-Cre positive and negative neurons using whole-cell patch-clamp recordings. These experiments revealed that no significant differences between CR cells of different ontogenetic origins could be observed.

A series of experiments unraveled the expression of homogeneous glycine receptors with a α_2/β heteromeric subunit composition in neurons of the intermediate zone and the cortical plate and in CR cells (Flint et al., 1998; Kilb et al., 2002; Okabe et al., 2004). However, the questions whether similar glycine receptors are also expressed on SP cells remain unanswered. To address this question, I studied in the second part of my thesis the effect of glycine and glycinergic agonists on SP cells using whole-cell patch-clamp recordings. In addition, the effect of low taurine concentration on the excitability of SP neurons was investigated. These experiments revealed that SP neurons also expressed α_2/β heteromeric glycine receptors, that the activation of these receptors promotes excitation, and that they are not implicated in synaptic transmission.

Since the previous finding, in line with published studies (Flint et al., 1998; Okabe et al., 2004), indicated that glycine receptors mediate extrasynaptic transmission and promote neuronal excitation, I investigated in the third part of this thesis the effect of a tonic activation of glycine receptors on identified pyramidal neurons and GABAergic interneurons of the immature neocortex. These experiments revealed

that a tonic activation of glycine receptors induced a massive increase in the frequency of PSCs that are exclusively mediated via GABA_A receptors. Accordingly, recordings from genetically labeled interneurons showed that glycine and GABA_A receptors mediate an excitatory action on these cells. These findings suggest that low taurine concentrations can tonically activate exclusively GABAergic networks.

2. Material & Methods

2.1 Preparation of the cortical slices

Animal handling was performed in accordance with EU directive 86/609/EEC for the use of animals in research and approved by the local ethical committee (Landesuntersuchungsanstalt RLP, Koblenz, Germany). All efforts were made to minimize the number of animals and their suffering. For electrophysiological experiments tangential, coronal and sagittal slices of the neocortex were prepared from pups of mice or rat at postnatal days 0 - 7 (P0 - P7). Wistar rats and C57Bl/6 mice had been deeply anaesthetized by hypothermia or enflurane (Abbot, Wiesbaden, Germany). After opening of the skull, the brains were quickly removed and placed in ice-cold artificial cerebrospinal fluid (ACSF) (composition given in 2.8.1).

2.1.1 Tangential slice preparation

For preparation of tangential slices the hemispheres of isolated brains were dissected at the midline, and the pia was removed carefully, using fine tweezers. Tangential neocortical slices (maximum thickness 600 μm) of both hemispheres were cut by hand using a razorblade. The slices were subsequently mounted on fine tissue paper (Kodak Lens Paper) to enable the reconstruction of their original orientation in the neocortex and were transferred to an incubation chamber filled with ACSF at room temperature in which they recovered for ≥ 1 h before recording began. These tangential slices covered mainly parietal parts of the developing cortex. Some of the slices may also have contained portions of frontal regions, while occipital or medial parts of the cortex were always absent.

2.1.2 Coronal slice preparation

Whole-brain 400 μm thick coronal slices were cut on a Vibratome (HR2, Sigmund Elektronik, Hüffenhardt, Germany) and cut along the midline to separate the two hemispheres. Only coronal slices that included the primary somatosensory cortex,

according to an atlas of the developing rat brain (Paxinos et al., 1991) were transferred to an incubation-storage chamber. Slices were allowed to recover for at least 1 hour before recording began.

2.1.3 Mini slice preparation

For some experiments a reduced slice preparation was required. Therefore coronal slices with a thickness of 400 μm were placed under a binocular with magnification of 2x, 5x, and 10x. The slices were trimmed with a scalpel blade to a width of approximately 2-3 mm. The trimmed slices were always obtained from somatosensory areas of the cortex. In some of these slices the SP and WM were identified by eye and with a help of scalpel blade the subplate was removed.

2.2 Electrophysiological setup

The videomicroscopic setup consisted of an upright microscope (BW51WI, Olympus) with infrared differential interference contrast (IR-DIC) optics (Dodt et al., 2007), and a CCD-camera (C5405, Hamamatsu, Japan). The video image was contrast enhanced by a video processor (C 2400, Hamamatsu) and visualized on a video-monitor. For whole-cell and cell-attached patch-clamp experiments pipettes were made from borosilicate tubing (2.0 mm outside diameter, 1.16 mm inside diameter; Science Products, Hofheim, Germany) using a vertical puller (PP-83, Narishige, Tokyo, Japan) and filled with pipette solution (see intracellular solution 2.8.2). The patch pipettes were connected to the headstage of a discontinuous voltage-clamp/current-clamp amplifier (SEC05L, NPI, Tamm, Germany). Signals were amplified, low-pass filtered at 3 kHz, visualized on an oscilloscope (HM507, Hameg Instruments), digitized on-line by an AD/DA-board (ITC-18, Heka, Lamprecht, Germany), recorded and processed with the software WINTIDA 5.0 (Heka), and stored on a personal computer. The bathing solution was connected to ground via chloride silver wire. The slices were transferred into a submerged recording chamber, mounted on the fixed stage of the microscope and were superfused with ACSF at a rate of 1-2 ml/min. All experiments were performed at 30

± 1 °C with the help of a peltier-element based temperature controller (Luigs & Neumann, Ratingen, Germany).

2.3 Identification of Cajal-Retzius cells

CR cells were identified in the tangential slice by their location, morphological appearance in the IR-DIC (close to pia surface with an ovoid soma and only one, thick tapered dendrite) and electrophysiological properties (prominent voltage sag and repetitive APs with small amplitude and relatively long duration) (Zhou and Hablitz, 1996c; Zhou and Hablitz, 1996b; Kilb and Luhmann, 2000; Luhmann et al., 2000). Since the YFP fluorescence was washed out during whole-cell recordings, no reliable identification of neurons double stained for biocytin and YFP could be made after the experiment. Because the classification of the CR cells relies only on the YFP fluorescence at the patch-clamp setup, we picked for subsequent experiments only unequivocally YFP⁺ CR cells, in which the location, soma shape and the orientation of the dendrite perfectly matched between DIC and YFP images (see Fig. 1A) and unequivocally YFP⁻ cells, in which clearly no overlap of fluorescence with soma and dendrite of the CR cells occurred (Fig. 1B).

2.4 Identification of the subplate cells

Subplate cells (SP cells) were visualized by infrared differential interference contrast (DIC) videomicroscopy and were identified according to their location directly above the white matter, their morphology and their electrophysiological properties. Neurons were excluded from analysis if their electrophysiological properties and their morphological appearance after subsequent staining of fixed slices did not correspond to those reported previously (Friauf et al., 1990; Hanganu et al., 2001; Hanganu et al., 2002).

2.5 Electrophysiological procedures

Resting membrane potential (RMP) was measured directly after establishing whole-cell configuration. All potentials were corrected for a liquid junction potential of 9.1 mV. The input resistance was calculated from a membrane hyperpolarization induced by a current pulse according to Ohm's law. Input capacitance was calculated from the ratio between time course of the membrane recharging (τ) and input resistance. Action potential (AP) onset was defined as the time point of 50% peak amplitude in the second derivative of the potential trace (Bar-Yehuda and Korngreen, 2007), AP threshold was determined from the membrane potential at this time point. AP amplitude was defined as voltage difference between firing threshold and peak depolarization and AP width was measured at half-maximal amplitude. Amplitude of afterhyperpolarization (AHP) was measured as difference between firing threshold and maximum hyperpolarization following the AP. For the phase plane plots E_m and dE_m/dt were sampled every 0.084 ms, recordings were aligned to AP onset and averaged. In this plot the average trajectories were displayed and for each data point standard error of the mean (SEM) for E_m and dE_m/dt was plotted (Fig. 5). For determination of current densities peak current amplitudes were divided by surface area of the cells, estimated from input capacitance assuming a specific membrane capacitance of $2 \mu\text{F}/\text{cm}^2$ (Barrett and Crill, 1974). For the estimation of binding constants data points were fitted by the equation $I/I_{\text{max}} = c^h/(c^h + EC_{50}^h)$ (with c = agonist concentration, EC_{50} = half-maximal response concentration and h = Hill coefficient) using a least square algorithm.

Spontaneous postsynaptic currents (sPSCs) were recorded in voltage-clamp mode at holding potentials of -60 mV. PSCs were detected and analyzed in continuous recordings lasting at least 180 s up to 600 s in a voltage clamp conditions from a holding potential (V_h) of -60 mV, using the program MiniAnalysis 4.3.3 (Synaptosoft, Leonia, NJ, USA) by adequate program settings followed by visual inspection. Since the occurrence and frequency of sPSCs in CR cells is rather low (Kilb and Luhmann, 2001; Kirmse and Kirischuk, 2006b), PSCs induced by bath application of 100 μM carbachol (CCh-PSCs) were also analyzed (Dupont et al., 2006). GABAergic PSCs were isolated by bath application of 10 μM CNQX/30 μM

APV. Miniature glutamatergic postsynaptic currents (mPSCs) in the SP cells were isolated in 0.2-1 μ M TTX and 10 μ M gabazine.

For dose-response and kinetic analysis experiments, the agonists were applied semi-focally for 2 or 20 sec by a fine capillary (inside diameter 250 μ m, Microfil, WPI, Sarasota, FL, U.S.A.) placed at a distance of 200-600 μ m upstream of the investigated cell. This semi-focal application system allows the delivery of drugs within 0.4-1 s. In all other experiments taurine, glutamate, glycine, isoguvacine or GABA was applied by bath application or focally to the soma of the investigated cells via a patch pipette for 2-100 ms with a pressure of 0.4 bar using a pressure application system (PDES 02T, NPI; LHDA0533115H, Lee, Westbrook, CT, U.S.A.). The analysis of glutamatergic currents in CR cells were made in low-Mg²⁺ solution containing 10 μ M glycine. The reversal potentials were calculated after focal application of the specific agonist to the soma at different holding potentials. Antagonists were applied via the bathing solution for at least 3 min prior to agonist application.

2.6 Generation of *Dbx1^{cre};ROSA26^{YFP}* recombinant mice

Dbx1^{cre} animals were generated by inserting an IRES-CRE-pGK-Hygro^r cassette into the BamH1 site present in the 3' UTR of the *Dbx1* gene (Bielle et al., 2005). In this transgenic line, the *YFP* gene under the control of the ROSA26 ubiquitous promoter is preceded by a sequence preventing translation surrounded by two LoxP sites (Srinivas et al., 2001). Not all *Dbx1*-derived CR cells are labeled in *Dbx1^{cre};ROSA26^{YFP}* animals most likely due to the delay necessary for recombination of the genome allowing expression of the reporter gene. The earliest generated *Dbx1*-derived CRs might escape recombination. All animals are kept on a C57Bl/6 background. Animals were genotyped by PCR using primers specific for the different alleles (*Cre*, *YFP*, *Dbx1*). Mating were performed using *Dbx1^{Cre}* heterozygous males and *ROSA^{loxP-stop-loxP-YFP}* homozygous females. *Dbx1^{cre};ROSA26^{YFP}* recombined embryos were sorted directly with a fluorescence binocular lens. The *Dbx1^{cre};ROSA26^{YFP}* mice were kindly provided by Prof. Alessandra Pierani.

2.7 Generation of GAD67-GFP transgenic mouse

In brief, a cDNA-encoding enhanced GFP (EGFP; ClonTech, Palo Alto, CA) was targeted to the locus encoding GAD67 using homologous recombination. Homologous recombinant embryonic stem (ES) cells were used to generate chimeric male mice by 8-cellstage injection. GAD67-GFP knock-in mice were obtained by breeding the chimeric male mice with C57BL/6 females. Heterozygous progeny were backcrossed to C57BL/6 and referred to as GAD67-GFP mice (Nobuaki et al., 2003).

In the GAD67-GFP knock-in mouse GABAergic neurons are specifically labeled with GFP fluorescence. The GAD67-GFP knock-in mouse was kindly provided by Dr. Thomas Munsch and Prof. Yuchio Yanagawa.

2.8 Solutions and substances

2.8.1 Extracellular solution

As extracellular solution we used (ACSF) containing (in mM) 124 NaCl, 26 NaHCO₃, 1.25 NaH₂PO₄, 1.8 MgCl₂, 1.6 CaCl₂, 3 KCl, 20 glucose (equilibrated with 95% O₂/5% CO₂), osmolarity 333 mOsm. For low-Mg²⁺ solution MgCl₂ was replaced by CaCl₂. For low-Ca²⁺ solution, [Mg²⁺]_e was increased to 3.4 mM while [Ca²⁺]_e was omitted. For hypoosmolar solutions ACSF was diluted with distilled water and the osmolarity was checked using a freezing point osmometer (Knauer, Berlin, Germany).

2.8.2 Intracellular solution

For whole cell recordings the intracellular solution contained (in mM) 50 KCl, 80 K-Gluconate, 1 CaCl₂, 2 MgCl₂, 11 EGTA, 10 HEPES, 2 Na₂-ATP, 0.5 Na-GTP, pH adjusted to 7.4 with KOH and osmolarity to 306 mOsm with sucrose. For the cell attached recordings the intracellular solution was modified to (in mM) 126 K-Gluconate, 4 KCl, 1 CaCl₂, 2 MgCl₂, 11 EGTA, 10 HEPES, 2 Na₂-ATP, 0.5 Na-GTP, pH adjusted to 7.4 with KOH and osmolarity to 306 mOsm with sucrose.

2.8.3 List of substances used

Taurine and β -alanine were dissolved directly in ACSF, while the following substances were diluted from the following stock solutions: 10 mM ifenprodil, 10 mM gabazine (GBZ = SR-95531), 30 mM 6-Cyano-7-nitroquinoxaline-2,3-dione (CNQX) and 30 mM strychnine from a stock solution in DMSO, 1 mM tetrodotoxin (TTX) from a stock solution in citrate buffer, , 100 mM glycine, 30 mM CTB, 10 mM (\pm) R(-)-3-(2-carboxypiperazine-4-yl)-propyl-1-phosphonic acid (CPP) and 300 mM GES from an aqueous stock solution, and 30 mM picrotoxin and 60 mM DL-2-Amino-5-phosphonopentanoic acid (APV) from a stock solution in 0.1 M NaOH. Tetrodotoxin (TTX) was purchased from RBI (Natic, MA), glycine and taurine from Tocris (Ballwin, MO), guanidinoethyl sulphate (GES) from TRC (North York, Canada), and all other substances from Sigma. Cyanotriphenylborate (CTB) was a kind gift from Dr. Till Opatz (Inst. of Organic Chemistry, Univ. of Mainz, Germany). The final DMSO concentration never exceeded 0.5 %.

2.9 Staining procedures

In all whole-cell experiments \sim 0.5 % biocytin (Sigma, Taufkirchen, Germany) was added to the pipette solutions to label the cells on which a whole cell configuration was established for later morphological reconstruction of the cells. Slices were fixed in a 4 % paraformaldehyde solution immediately after recording for more than 24 h. After washing in phosphate buffer, slices were incubated in blocking solution (4.5 % normal goat and 3 % normal bovine serum, 0.5 % Triton, 0.05 % sodium azide in PBS) for 2 h at RT. For reconstruction, patched CR cells biocytin-labeled cells were stained with Cy-3 conjugated streptavidin (Dianova, Hamburg, Germany) as described in detail before (Achilles et al., 2007). Since the YFP fluorescence was not stable during the biocytin-streptavidin reaction, most of these slices were subsequently counterstained for YFP. For YFP staining a GFP antibody raised in rabbit (1:500, Invitrogen, Karlsruhe, Germany) was incubated overnight at RT and was subsequently visualized with a donkey anti-rabbit IgG secondary antibody conjugated with Dylight 488 (1:100; Dianova). The slices were embedded in fluoromount (Sigma).

Immunofluorescence was investigated with a Nipkow spinning disk confocal system (Visitech, Sunderland, U.K.) attached to a conventional fluorescence microscope (Olympus BX51 WI) equipped with water immersion objectives and a cooled CCD camera (CoolSnap HQ, Roper Scientific) controlled by MetaMorph software (Universal Imaging, West Chester, USA). Green and red fluorescence was excited with the 488 nm and the 568 nm lines of a Kr/Ar laser (Laser Physics, Malpas, U.K.).

2.10 Statistics

All values are expressed as mean \pm standard error of the mean (SEM). For statistical analysis Student t-test, Mann-Whitney-U-test, ANOVA tests and Fishers Exact test were used (Systat 11, Systat Inc., Point Richmond, CA). Results were designated significant at a level of $p < 0.05$.

3. Results

3.1 Electrophysiological and morphological properties of Cajal-Retzius cells with different ontogenetic origins

The heterogeneity of transcription factors and the different origins of CR cells indicate that the neurons grouped under the term “Cajal–Retzius cell” may actually represent different neuronal populations (Meyer and Wahle, 1999; Bielle et al., 2005). In order to investigate whether CR cells of different ontogenetic origins have distinct functional properties we used *Dbx1^{cre};ROSA26^{YFP}* mice in which CR cell originating from the septum and at the pallial–subpallial border could be identified by their YFP fluorescence.

3.1.1 Identification of YFP⁺ and YFP⁻ Cajal-Retzius cells

CR cells were identified by their appearance in the DIC image of tangential slices. Only cells in the most superficial layer of the tangential slice preparation and a clear CR cell like appearance, with an ovoid soma and a long tapered dendrite (Fig. 1A, B), were chosen for recordings (Zhou and Hablitz, 1996b). Subsequent visualization of the fluorescence of these cells using an YFP-filter clearly demonstrated that the CR cell was either YFP⁺ (Fig. 1A) or YFP⁻ (Fig. 1B).

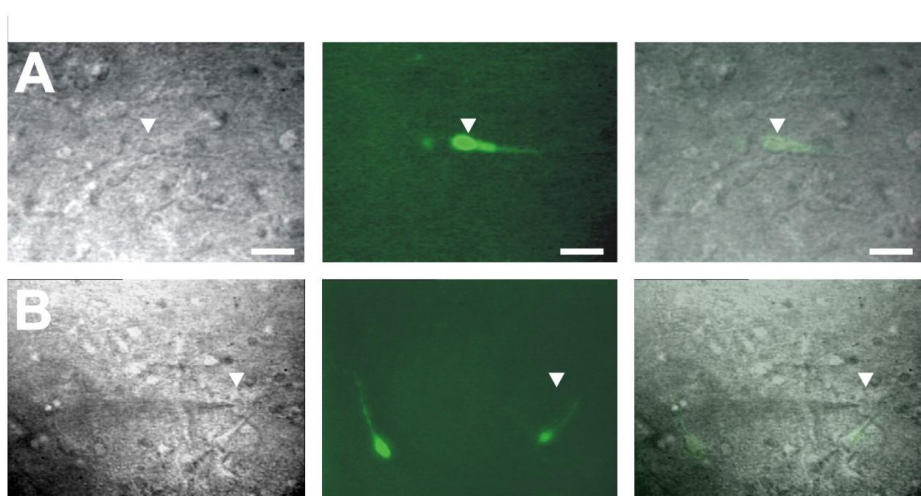


Figure 1: Identification of YFP⁺ and YFP⁻ CR cells. A: Videomicroscopic (left) and fluorescence images (middle) of a living CR cell (marked by a white arrowhead) in an acute tangential slice preparation. Note the close correspondence in the appearance of the ovoid soma and the tapered dendrite of the CR cell in both images. B: Videomicroscopic and fluorescence image of YFP⁻ CR cells (white arrowhead) in an acute tangential slice preparation. A patch pipette is attached to the YFP⁻ CR cell. Note that the YFP fluorescence signal does not overlap with the patched cell. Scale bar represents 20 μ m.

Patched cells displayed the characteristic electrophysiological properties of CR cells (Zhou and Hablitz, 1996c; Luhmann et al., 2000) with relatively broad APs upon depolarization and a prominent voltage sag upon hyperpolarization (Fig. 2A,B).

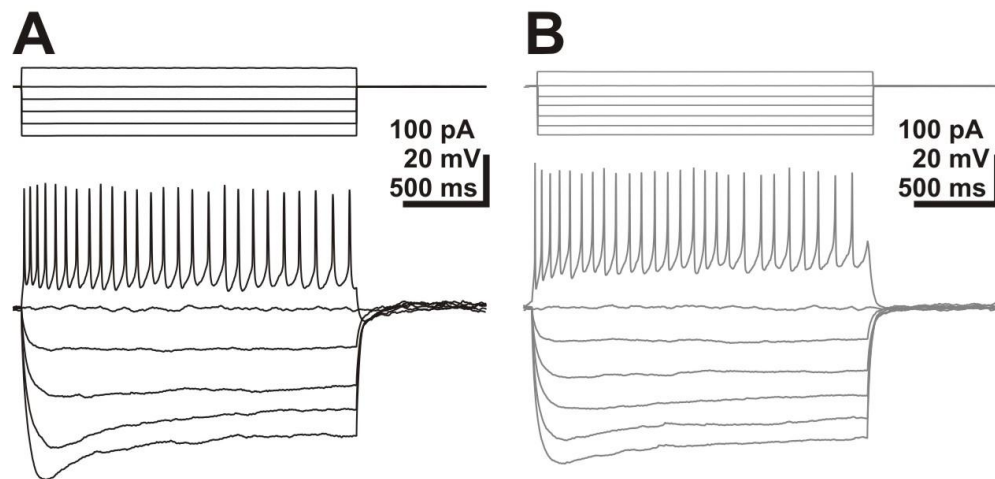


Figure 2: A: Electrophysiological properties of the cell shown in Fig 1A. B: Electrophysiological properties of the cell shown in Fig. 1B. Both CR cells are characterized by repetitive APs with long duration and small amplitudes and a prominent voltage sag.

All neurons that could be stained for biocytin (n=51 of 65 recorded cells) displayed the typical morphological properties of CR cells (Fig. 3), indicating that CR cells can be unequivocally identified by their location, their appearance in the DIC image and their electrophysiological properties in tangential slices.

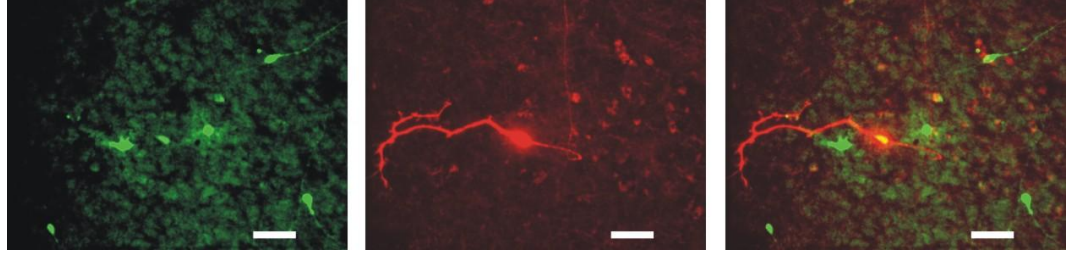


Figure 3: Confocal fluorescence images displaying YFP^+ neurons (left), a biocytin-labeled CR cell (middle) and the merged image (right). The patched biocytin-labeled neuron displays the typical features of a CR cell. Scale bars represent $50 \mu m$.

3.1.2 Passive and active electrophysiological properties of YFP^+ and YFP^- Cajal-Retzius cells

No significant differences in passive membrane properties were observed between YFP^+ and YFP^- CR cells (Table 1).

Membrane properties						
	RMP (mV)	R_{input} ($G\Omega$)	C_{input} (pF)	I_h -Amplitude (pA)	τ of I_h (ms)	
YFP^+	-58.3 ± 1.2 (30)	1.98 ± 0.16	42.6 ± 2.4	21.6 ± 1.6 (26)	688 ± 67	
YFP^-	-59.4 ± 1.3 (37)	2.11 ± 0.12	44.4 ± 3.5	22.5 ± 2.0 (31)	650 ± 52	
p=	0.495	0.605	0.753	0.981	0.892	
Action potential properties						
	Threshold (mV)	Amplitude (mV)	$d_{1/2}$ (ms)	V_{Rise} (V/s)	V_{Decay} (V/s)	AHP-Ampl. (mV)
YFP^+	-40.3 ± 1.0 (30)	41.8 ± 1.4	4.2 ± 0.3	28.7 ± 2.5	-14.3 ± 1.1	-14.8 ± 1.0
YFP^-	-37.8 ± 0.8 (37)	38.4 ± 1.3	3.5 ± 0.3	27.5 ± 2.7	-16.7 ± 1.2	-17.3 ± 1.0
p=	0.108	0.107	0.033	0.413	0.207	0.069
Glutamate receptors and spontaneous synaptic inputs						
	Amplitude Glut.-current (pA)	Frequency sPSCs (Hz)	Amplitude sPSCs (pA)	Rise sPSCs (ms)	Decay sPSCs (ms)	
YFP^+	13.7 ± 3.2 (10)	0.08 ± 0.02 (11)	38.4 ± 18.1	4.4 ± 0.6	16.5 ± 2.3	
YFP^-	15.3 ± 3.0 (9)	0.13 ± 0.03 (13)	36.9 ± 5.5	3.7 ± 0.4	17.6 ± 1.9	
p=	0.591	0.235	0.060	0.235	0.502	
Carbachol-induced synaptic inputs						
	Frequency PSCs (Hz)	CCh-ind. Freq. increase	Amplitude PSCs (pA)	Rise PSCs (ms)	Decay PSCs (ms)	
YFP^+	0.90 ± 0.32 (10)	15.8 ± 7.1	46.2 ± 15.9	4.3 ± 0.7	17.0 ± 2.0	
YFP^-	1.02 ± 0.28 (13)	14.4 ± 6.4	41.2 ± 4.1	3.8 ± 0.2	16.1 ± 1.0	
p=	0.901	0.723	0.174	0.951	0.951	

Table 1: Electrophysiological properties of YFP^+ and YFP^- CR cells

In both CR cells subpopulations APs with typical properties could be elicited. In YFP⁺ CR cells APs with an average amplitude of 41.8 ± 1.4 mV ($n = 30$) and a duration of 4.2 ± 0.3 ms were elicited upon depolarization above a threshold of -40.3 ± 1.0 mV (Fig. 4B). The maximal rate of the rising phase amounted to 28.7 ± 2.5 Vs⁻¹ and of the repolarization to -14.3 ± 1.1 Vs⁻¹. The action potential was followed by a pronounced AHP of -14.8 ± 1.0 mV (Fig. 4B). APs with rather similar properties were observed in YFP⁻ CR cells (Fig. 4C). While neither amplitude (38.4 ± 1.4 mV; $n=37$) nor threshold (-37.8 ± 0.8 mV) or AHP amplitude (-17.3 ± 1.0 mV) was significantly different from YFP⁺ CR cells, AP duration was slightly shorter in YFP⁻ CR cells (3.5 ± 0.3 ms). The maximal rate of the rising phase (27.5 ± 2.7 Vs⁻¹) and of the repolarization (-16.7 ± 1.2 Vs⁻¹) was not significantly different to YFP⁺ CR cells.

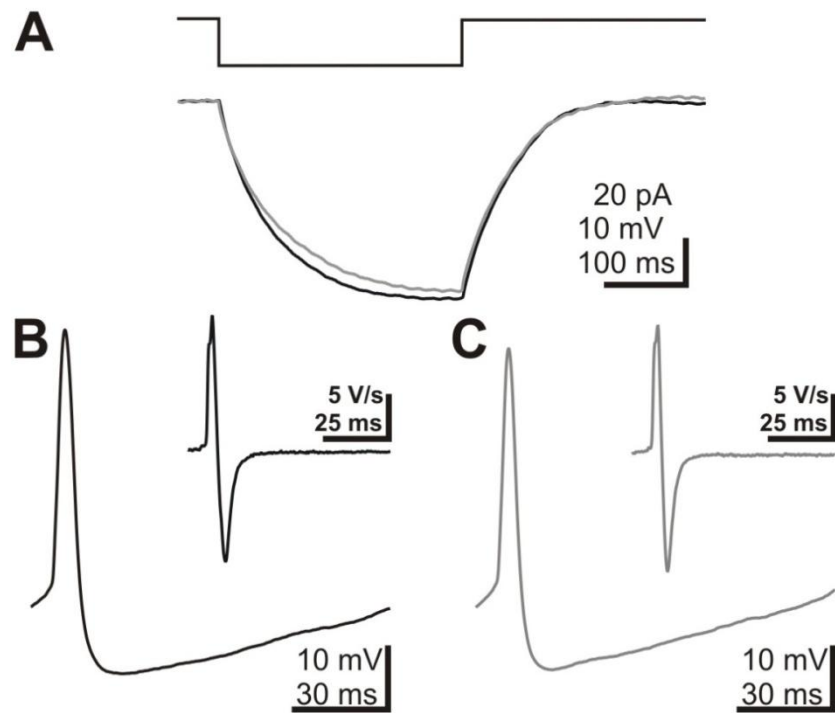


Figure 4: Passive and active membrane properties of YFP⁺ and YFP⁻ CR cells. A: Time course and amplitude of voltage deflections upon injection of small negative currents are similar between YFP⁺ (black trace) and YFP⁻ (gray trace) CR cells. B: Typical action potential of a YFP⁺ CR cell. The inset illustrates the first derivative of the action potential discharge. C: Typical action potential of a YFP⁻ CR cell. The inset illustrates the first derivative of the action potential discharge.

Accordingly, the averaged trajectories in the phase plane were comparable between YFP^+ and YFP^- CR cells (Fig. 5).

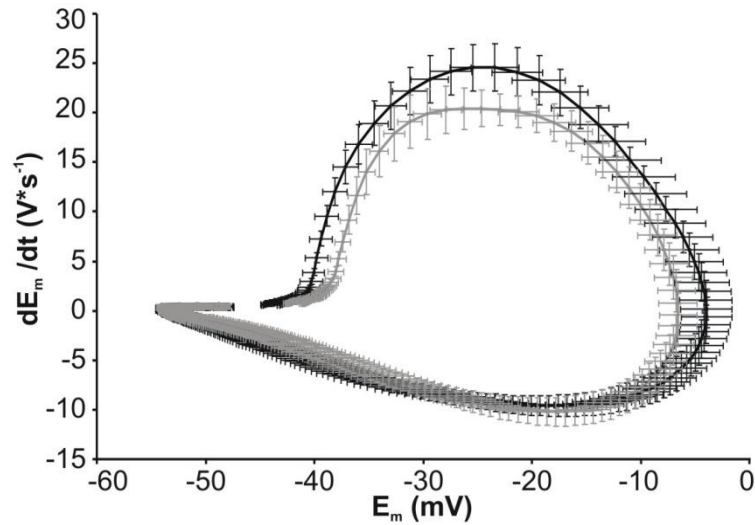


Figure 5: Phase plane plot of averaged APs (\pm SEM) of YFP^+ (black) and YFP^- (gray) CR cells. No significant differences in the trajectories are evident.

A typical feature of CR cells is a prominent voltage sag upon hyperpolarization which is mediated by a hyperpolarization-activated inward current (Kilb and Luhmann, 2000). Hyperpolarization-activated inward current with similar properties (see Table 1) were found in both YFP^+ and YFP^- CR cells (Fig. 6).

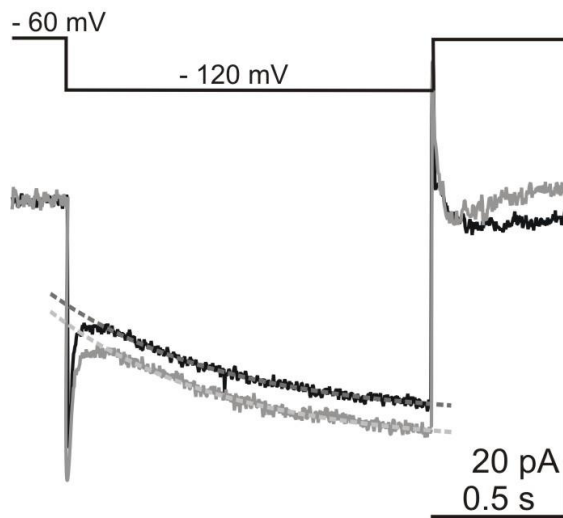


Figure 6: Current traces of YFP^+ (black) and YFP^- (gray) CR cells upon a step in the holding current from -60 mV to -120 mV. Monoexponential

fits are displayed as dashed lines. Note that amplitude and time course of the hyperpolarization induced inward current are similar in both CR cells.

3.1.3 GABA_A-receptors on CR cells

Previous studies demonstrated that the majority of synaptic inputs on CR cells are mediated by GABA_A receptors (Kilb and Luhmann, 2001;Kirmse and Kirischuk, 2006b;Kirmse and Kirischuk, 2006a;Radnikow et al., 2002;Soda et al., 2003). To investigate whether the properties of GABAergic inputs differ between the YFP⁺ and YFP⁻ CR cells population, we analyzed spontaneous postsynaptic currents (sPSCs). In accordance with previous studies (Kilb and Luhmann, 2001;Kirmse and Kirischuk, 2006b), YFP⁺ and YFP⁻ CR cells display sPSCs with a low frequency (0.08 ± 0.02 Hz (n = 11) for YFP⁺ and 0.13 ± 0.03 Hz (n = 13) for YFP⁻CR cells; with no significant difference between both CR cells subpopulations (Table 1). Bath application of 100 μ M carbachol (Dupont et al., 2006) increased the frequency of PSCs by a factor of 15.8 ± 7.1 (n = 10) in YFP⁺ and by 14.4 ± 6.4 (n = 13) in YFP⁻ CR cells. In YFP⁺ CR cells CCh-PSCs with an amplitude of 46.2 ± 18.1 pA (n = 11) and a frequency of 0.90 ± 0.32 Hz could be elicited in 11 out of 13 slices (Fig. 7A). These CCh-PSCs had a rise-time of 4.3 ± 0.7 ms and the decay could be fitted with a single exponential function ($\tau=17 \pm 2.0$ ms). The CCh-PSCs in YFP⁻ CR cells showed similar properties (Table 1). In this CR cells population CCh-PSCs with an amplitude of 41.2 ± 4.1 pA (n = 13), a rise-time of 3.8 ± 0.2 ms, a decay time constant of 16.1 ± 1.0 ms and a frequency of 1.02 ± 0.28 Hz could be elicited in 13 out of 16 slices (Fig. 7B).

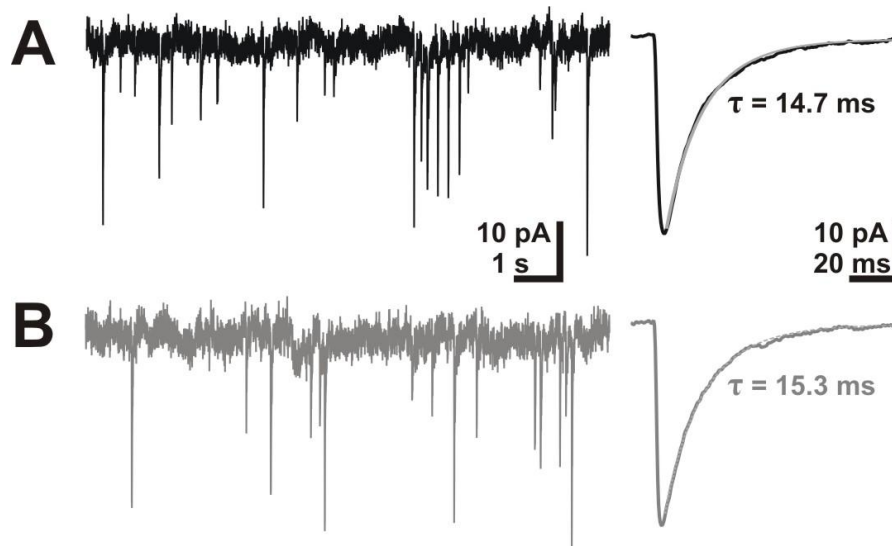


Figure 7: Properties of GABAergic inputs and glutamate receptors of YFP⁺ and YFP⁻ CR cells. A: Typical recording of carchol-induced PSCs in a YFP⁺ CR cell. Next to the recording an average PSC (averaged from 101 PSCs) is displayed. B: Typical recording of carchol-induced PSCs in a YFP⁻ CR cell. Next to the registration an average PSC (averaged from 105 PSCs) is displayed. Note that amplitude, decay and occurrence of carchol-induced PSCs are similar in both CR cells subpopulations.

Both sPSCs and CCh-PSCs were completely blocked by the specific GABA_A receptor antagonist gabazine (3 μ M) in YFP⁺ (n = 7) and YFP⁻ CR cells (n = 7), indicating that synaptic activity was mediated exclusively via GABA_A receptors in both populations.

3.1.4 NMDA-receptors on CR cells

Although glutamatergic synaptic inputs had only infrequently been reported in CR cells (Radnikow et al., 2002), they express NMDA-receptors (Chan and Yeh, 2003; Mienville and Pesold, 1999). Focal application of 100 μ M glutamate in Mg²⁺ free solution containing 10 μ M glycine induced inward currents with similar amplitudes of -13.7 ± 3.2 pA (n = 10) and -15.3 ± 3 pA (n = 9) in YFP⁺ and YFP⁻ CR cells, respectively (Table 1). The glutamatergic inward currents could be blocked by the NMDA specific antagonist CPP (20 μ M) in YFP⁺ (n = 6) and YFP⁻ CR cells (n =

6; Fig. 8), indicating that in both populations only NMDA receptors were functionally expressed.

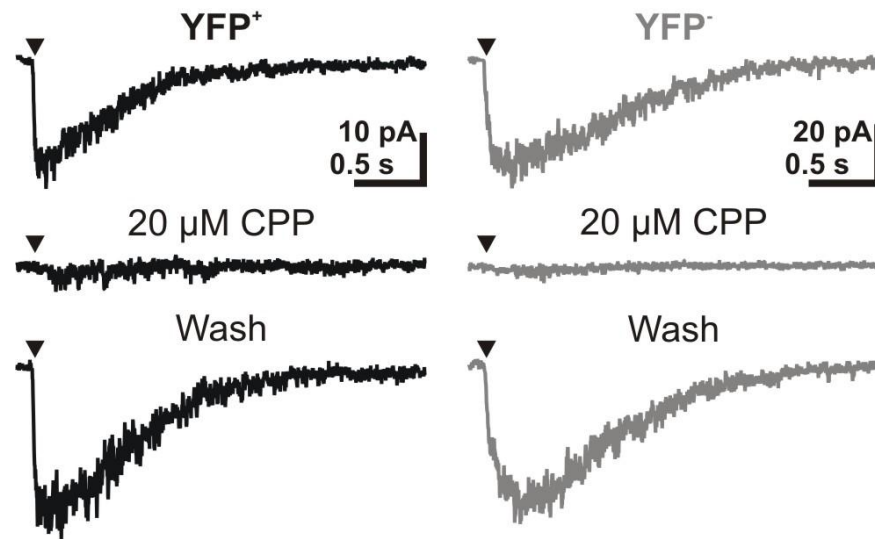


Figure 8: Pharmacological profile of inward currents induced by focal application of 100 μ M glutamate (arrowhead) in a YFP⁺ (black traces) and a YFP⁻ CR cells (gray traces). The glutamatergic current is inhibited by bath application of 20 μ M CPP in both populations.

The NR2B specific antagonist ifenprodil (3 μ M, Williams, 1993) attenuated the amplitude of the glutamatergic inward currents by 52.3 ± 8.6 % (n = 6) in YFP⁺ and by 62.1 ± 4.2 % (n = 7) in YFP⁻ CR cells (Fig. 9).

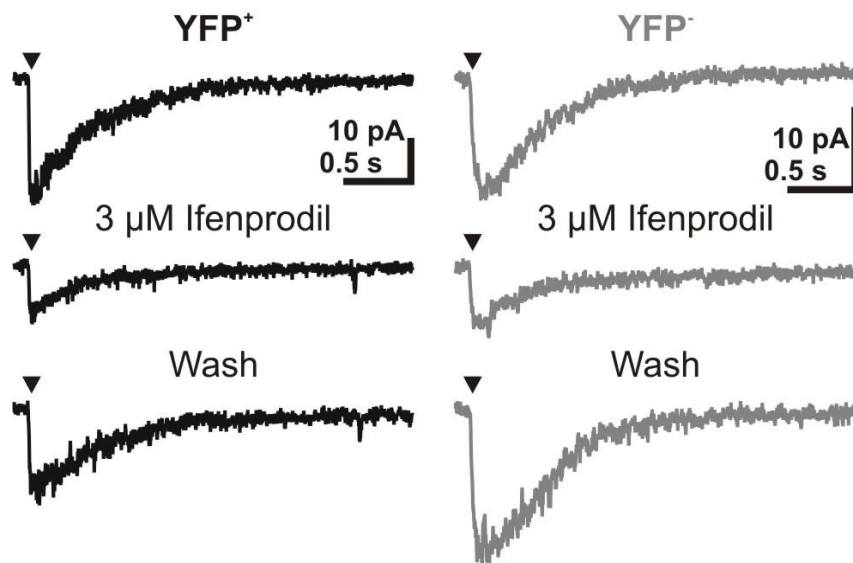


Figure 9: Pharmacological profile of inward currents induced by focal application of 100 μ M glutamate (arrowhead) in a YFP⁺ (black traces) and a YFP⁻ CR cells (gray traces). The NR2B specific antagonist ifenprodil (3 μ M) attenuates glutamatergic inward currents in YFP⁺ (black traces) and YFP⁻ CR cells (gray traces).

The ifenprodil effect was not significantly different between YFP⁺ and YFP⁻ CR cells, suggesting that both populations express NR2B receptor subunits at comparable ratios.

In summary the results of these experiments revealed that the electrophysiological properties are comparable between YFP⁺ and YFP⁻CR cells, suggesting that both subpopulations of CR cells fulfill similar functions in the marginal zone.

3.2 Glycine receptors mediate excitation of subplate neurons in neonatal rat cerebral cortex

In order to investigate whether glycine receptors in SP neurons possess the same properties like in the other neuronal populations of the developing neocortex (Flint et al., 1998; Kilb et al., 2002; Okabe et al., 2004) we analyzed the pharmacological and functional properties of glycinergic currents in visually identified SP cells.

3.2.1 Morphology and membrane properties of the subplate cells (SP cells)

Whole-cell patch-clamp recordings were performed on 112 visually identified SP cells (Fig. 10A). The mean RMP measured under whole-cell conditions was -62.5 ± 1.1 mV and the mean input resistance (R_{in}) was 1245 ± 52.7 M Ω ($n = 112$). Upon depolarization above a threshold of -45.6 ± 0.5 mV ($n = 112$) repetitive APs with a mean amplitude of 54 ± 1.0 mV could be elicited (Fig. 10B).

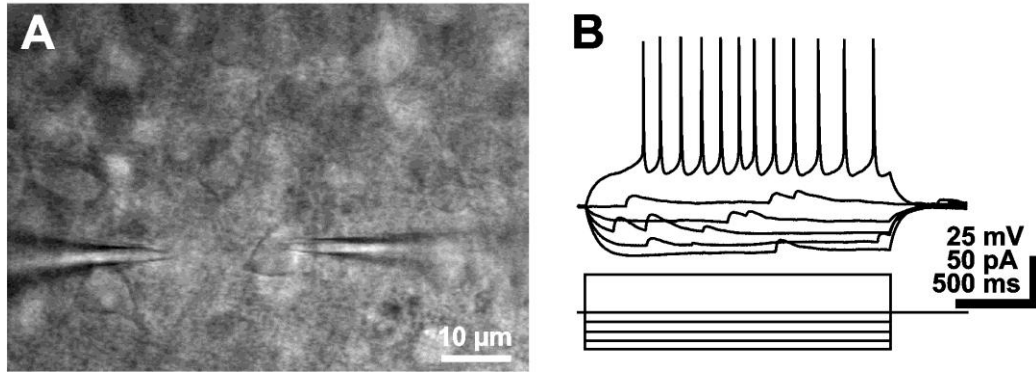


Fig. 10. Identification of subplate cells (SP cells) in coronal slices of the newborn rat cerebral cortex by morphological and electrophysiological properties. A: Videomicroscopic image of a P3 SP cells. The cell was recorded with the patch-clamp pipette displayed to the right, while the pipette for focal glycine application is visible to the left. B: Current-clamp recordings from the cell shown in Fig. 10 A. Holding potential was -60 mV. Injection of a depolarizing current pulse elicits repetitive action potentials, which represents the typical firing pattern of SP cells. Note the high frequency of sPSCs and the absence of a voltage-sag.

3.2.2 Glycine-induced membrane responses in SP cells

Under whole-cell conditions, focal application of 1 mM glycine induced a membrane depolarization of 33.4 ± 2.3 mV ($n = 6$) and reduced R_{in} by 85 ± 4.9 %. Similar results were obtained by focal application of the glycinergic agonist β -alanine (5 mM), which caused a depolarization by 30.3 ± 2.8 mV ($n = 6$) and reduced R_{in} by 80.6 ± 6.8 %. Focal application of 5 mM taurine caused a membrane depolarization of 27.2 ± 3.1 mV ($n = 6$) and a R_{in} decrease by 71.1 ± 7.1 %. Under voltage-clamp conditions, focal glycine application induced in all investigated SP cells inward currents with a mean peak amplitude of 505 ± 51.2 pA ($n = 31$), corresponding to a current density of 16.1 ± 2.2 $\mu\text{A}/\text{cm}^2$. While β -alanine (5 mM) caused inward currents with a mean peak amplitude of 479.9 ± 91.3 pA ($n = 13$), corresponding to a comparable current density (17.3 ± 4.9 $\mu\text{A}/\text{cm}^2$), membrane currents evoked by focal application of 5 mM taurine were significantly ($p=0.025$) smaller (263.9 ± 34.4 pA and 9.1 ± 2.0 $\mu\text{A}/\text{cm}^2$, $n = 15$). The peak amplitudes of the membrane currents

evoked by the glycinergic agonists glycine, taurine and β -alanine showed a clear dose dependency (Fig. 11).

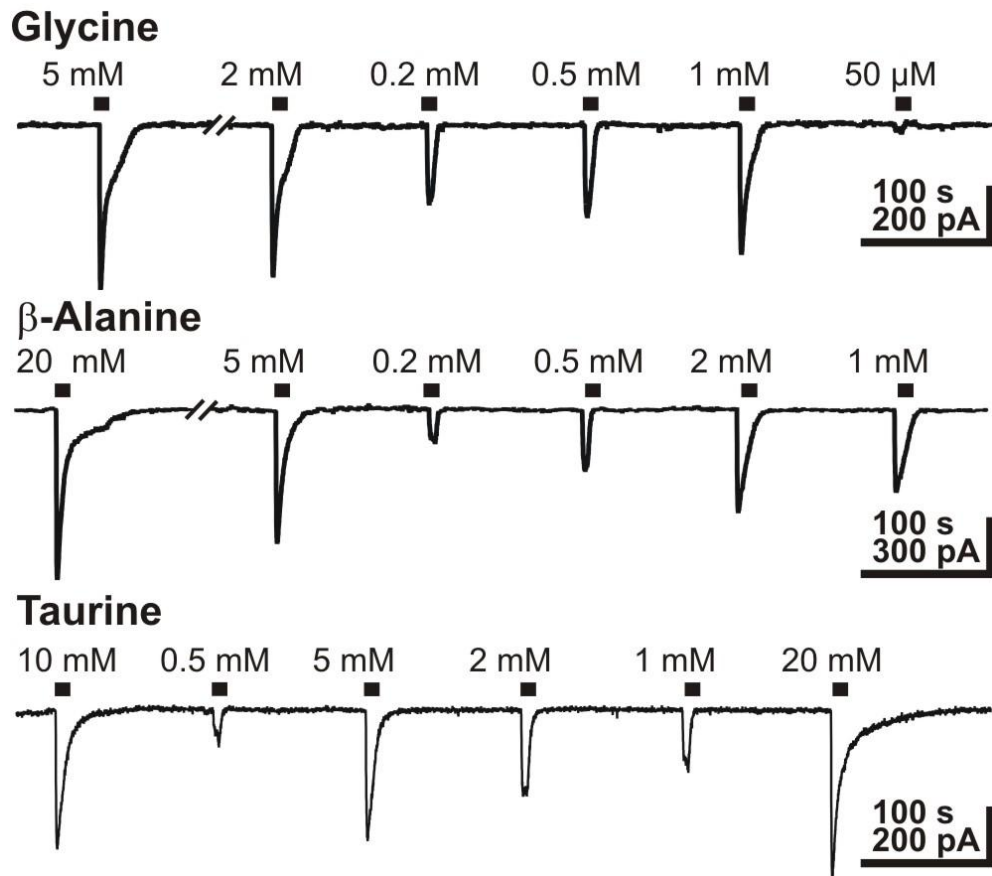


Figure 11: Membrane responses mediated by different glycine receptor agonists in SP cells. A: Inward currents evoked by various concentrations of glycine (upper trace), β -alanine (middle trace) and taurine (lower trace).

The corresponding dose-response curves (Fig. 12) revealed that glycine receptors on SP cells displayed a higher affinity for glycine (0.25 mM) than for taurine and β -alanine (1.67 mM and 1.14 mM, respectively). In these experiments taurine and β -alanine were applied in the continuous presence of 20 μ M bicuculline methiodide to block GABA_A receptors. Because bicuculline at this concentration had been shown to partially block glycine receptors (Shirasaki et al., 1991), the currents induced by β -alanine and taurine may be underestimated.

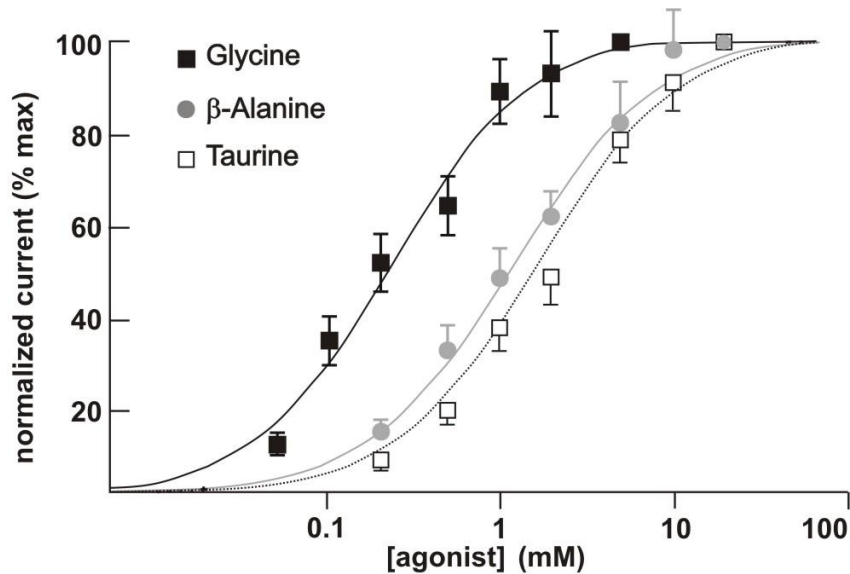


Figure 12. Dose-response curve of the peak currents induced by various concentrations of glycine (black squares), β -alanine (gray circles) and taurine (open squares). Taurine and β -alanine were applied in the presence of 20 μ M bicuculline methiodide. Data points represent mean \pm SEM of at least 6 experiments.

To investigate the kinetics of current desensitization, glycinergic agonists were applied semi-focally for 20 s (Fig.13). Under these conditions, glycinergic currents desensitized to 24.9 ± 3.4 % of the peak amplitude with a time constant of 6 ± 0.5 s ($n=13$, Fig. 13). Similar values were obtained for currents evoked by 5 mM β -alanine, which desensitized to 27.6 ± 2.8 % of the peak amplitude with a time constant of 6.9 ± 0.7 s ($n = 12$). The currents induced by 5 mM taurine showed significantly ($p = 0.002$) less desensitization to 41.5 ± 3.5 % ($n = 14$) with a time constant of 6.9 ± 0.8 s (Fig. 13). Determination of the glycine, β -alanine and taurine reversal potentials revealed that the reduction in current amplitude was partially related to an attenuation of the Cl^- gradient. For all three agonists, the estimated reversal potentials after 15 s applications were negative to the reversal potential calculated for the pipette solution, but there were no significant differences between the agonists. Lowering the taurine concentration to 0.3 mM reduced the degree of desensitization to 66.9 ± 10.3 % ($n = 5$), while with 100 μ M taurine no significant desensitization (5 ± 4.9 %, $n = 4$) was observed (Fig. 13).

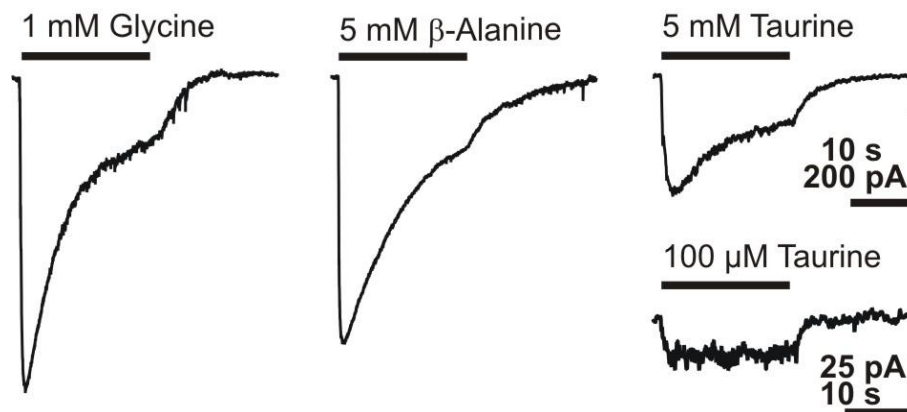


Figure 13: Inward currents elicited by a 20 s application of 1 mM glycine, 5 mM β -alanine and 5 mM taurine. Note smaller peak amplitudes and smaller degree of desensitization of the taurine response. Application of 100 μ M taurine induced non-desensitizing currents with small amplitude.

3.2.3 Activation of glycine receptors by taurine in SP cells

To elucidate whether taurine indeed activates glycine receptors, cross desensitization experiments (Wang et al., 2005) were performed in the presence of 3 μ M gabazine. These experiments revealed that bath application of 5 mM taurine nearly completely abolished (to $1.2 \pm 1\%$; $n = 8$) inward currents induced by focal application of 1 mM glycine (Fig. 14A). Similarly, inward currents induced by focal taurine application were also massively suppressed (by $98 \pm 2\%$; $n = 6$) during bath application of 1 mM glycine (Fig. 14B). Since this reduction may be caused by a decline in Cl^- gradient and/or space-clamp errors in distal parts of dendrites, control experiments analyzing the effect of bath applied glycine on GABAergic currents were performed. In these experiments GABAergic currents were only partially reduced (by $56.6 \pm 10.3\%$; $n = 5$) in the presence of 1 mM glycine (Fig. 14C), indicating that only a fraction of the cross-desensitization between glycine and taurine can be due to a decline in Cl^- gradient and/or space-clamp errors.

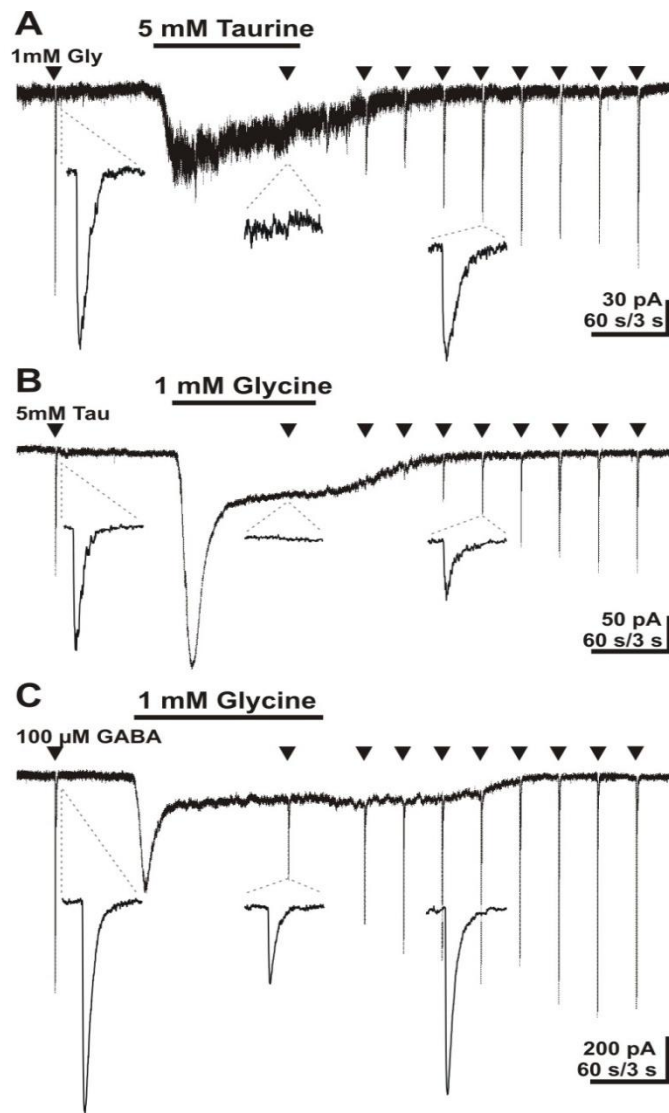


Figure. 14: Cross desensitization between glycine and taurine induced currents in SP cells. A: Inward currents evoked by focal application of 1 mM glycine (arrowheads) were nearly completely abolished during bath application of 5 mM taurine. Current responses are shown at higher temporal resolution below the trace. B: Inward currents evoked by focal application of 5 mM taurine (arrowheads) were nearly completely abolished during bath application of 1 mM glycine. The experiments in A and B were performed in the continuous presence of 3 μ M gabazine.

C: Inward currents evoked by focal application of 100 μ M GABA (arrowheads were only) partially suppressed during bath application of 5 mM taurine. Current responses are shown at higher temporal resolution below the trace.

3.2.4 Pharmacological properties of glycine-induced responses in SP cells

To discriminate pre- and postsynaptic effects of glycine on SP cells, action potentials (APs) were blocked by bath application of 1 μ M TTX and a low extracellular Ca^{2+} concentration was used to suppress activity dependent synaptic vesicle release (Fig. 15A, B). Under these conditions, the amplitude of glycine-induced currents was

similar to the glycine-induced control responses obtained in normal ACSF (97.1 ± 5.4 % of control values, $n = 6$, Fig. 15B), indicating that the glycine-induced currents were predominantly mediated by a direct postsynaptic effect. In the presence of the selective glycine receptor antagonist strychnine ($1 \mu\text{M}$) the glycine-induced currents were inhibited by 92.0 ± 2.1 % ($n = 7$, Fig. 15A,C), suggesting that focal glycine application activates glycine receptors with relatively low strychnine affinity (Ye, 2000; Okabe et al., 2004). Increasing the strychnine concentration to $30 \mu\text{M}$ completely abolished glycine-induced currents ($n = 5$, Fig. 15A,C).

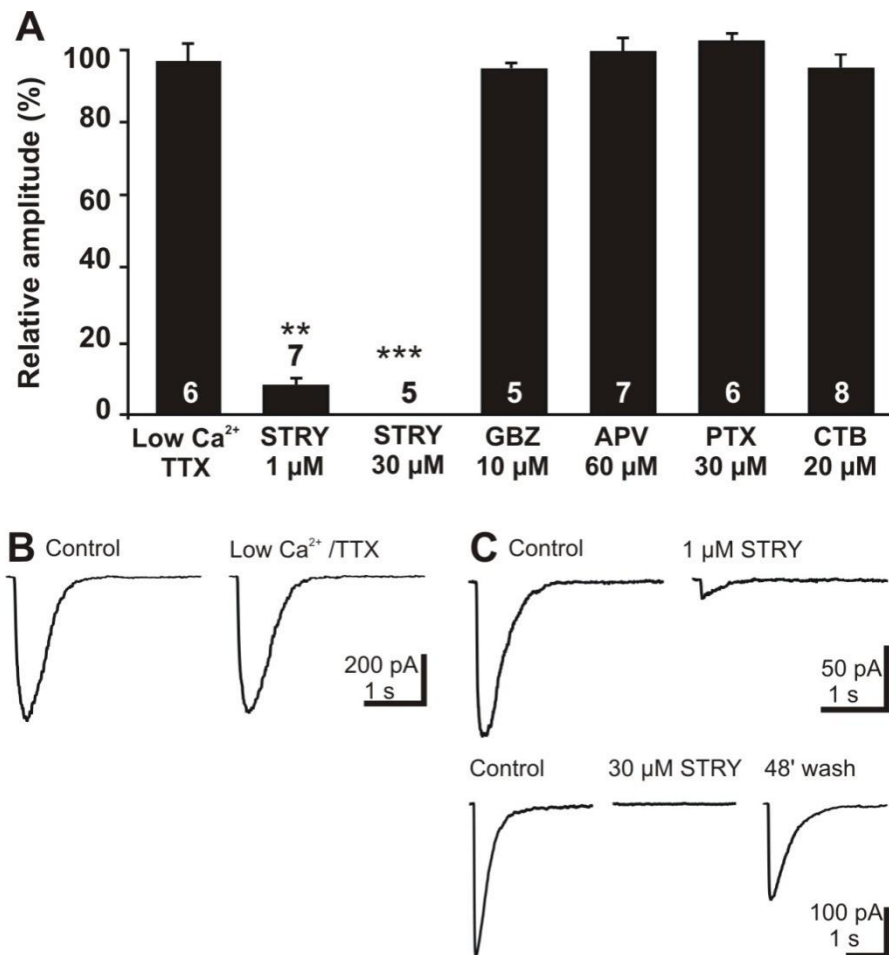


Figure 15: Pharmacological profile of postsynaptic glycine responses in SP cells. A: statistical analysis of the pharmacological experiments. Bars represent means \pm SE of relative peak amplitudes of glycinergic inward currents. Numbers of experiments are given in the bars. B, C: characteristic recordings of inward currents evoked by focal application

of 1 mM glycine before and after bath application of tetrodotoxin (TTX, 1 μ M in nominally Ca^{2+} -free solution) and strychnine (STRY, 1 and 30 μ M).

The specific GABA_A receptor antagonist gabazine (10 μ M) had no significant effect (97.5 ± 0.9 %; $n = 5$) on the amplitude of glycine-induced currents (Fig. 15A and Fig. 16). As it had been shown that glycine application is sufficient for NMDA receptor activation in the absence of an externally applied glutamatergic agonist (Paudice et al., 1998), the effects of NMDA receptor blockade on the glycine-induced response were also investigated (Fig 16). However, bath application of the selective NMDA receptor antagonist APV (60 μ M) had no significant effect on glycine-induced currents in 7 SP cells (99.8 ± 3.8 %; Fig. 15A, 16C). In summary, these results indicate that the glycine-induced membrane responses in SP cells were mediated by postsynaptically located, classical strychnine-sensitive glycine receptors.

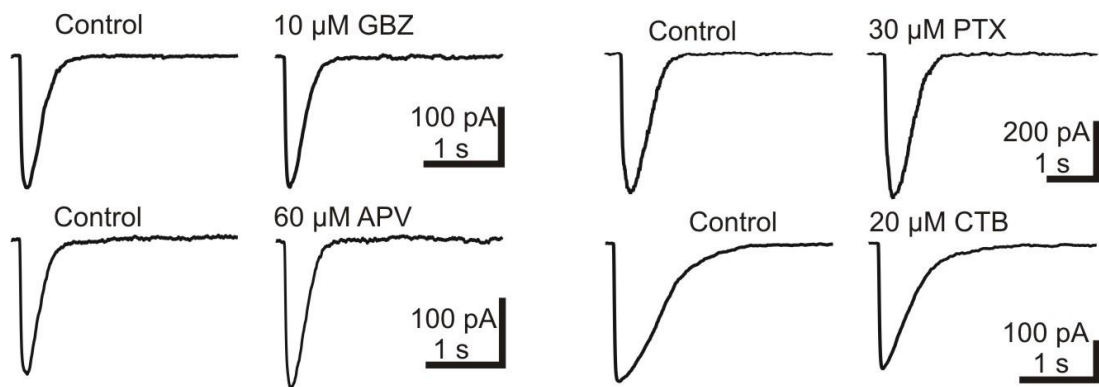


Figure 16: Inward currents evoked by focal application of 1 mM glycine before and after application of 10 μ M gabazine 60 μ M APV, 30 μ M picrotoxin (PTX), and 20 μ M cyanotriphenylborate (CTB).

It had been demonstrated that glycine can directly facilitate glutamate release (Turecek and Trussell, 2001). To rule out such direct effects of glycine or taurine on glutamate release, we examined the effect of these transmitters on miniature glutamatergic postsynaptic currents (mPSCs). Bath application of 10 μ M glycine has no significant effect on amplitude (8.4 ± 1 pA vs. 9.5 ± 1.6 pA) and frequency (0.058

± 0.019 Hz vs. 0.055 ± 0.021 Hz, $n = 5$) of AMPA receptor mediated mPSCs, which were isolated in $0.2 \mu\text{M}$ TTX, $3\text{-}10 \mu\text{M}$ gabazine and $60 \mu\text{M}$ APV. Similar results were observed in the presence of $100 \mu\text{M}$ taurine, where neither amplitude (14 ± 1.1 pA vs. 13 ± 0.9 pA) nor frequency (0.24 ± 0.06 Hz vs. 0.18 ± 0.02 Hz, $n = 8$) of glutamatergic mPSCs (isolated in $10 \mu\text{M}$ GBZ/ $0.2 \mu\text{M}$ TTX) was significantly affected. In summary, these results suggest that neither glycine nor taurine considerably affected glutamate release in synapses at SP cells.

3.2.5 Intrinsic activation of glycine receptors

Finally, we investigated whether intrinsically released glycinergic agonists can activate glycine receptors. To exclude the involvement of GABA_A receptors, all of these experiments were performed in the continuous presence of $3 \mu\text{M}$ gabazine. Application of $30 \mu\text{M}$ strychnine had no effect on the holding current (-1.2 ± 0.9 pA, $n=7$), demonstrating a lack of tonic glycinergic currents. However, in the presence of the endogenous glycinergic agonist taurine ($100 \mu\text{M}$), $30 \mu\text{M}$ strychnine induced a significant ($p=0.028$) shift in the holding current by 4 ± 1.9 pA ($n = 7$; Fig. 17A). Inhibition of taurine uptake with GES ($300 \mu\text{M}$) induced an outward current (-13.9 ± 4 pA; $n = 9$), which was inhibited by $30 \mu\text{M}$ strychnine (Fig. 17B).

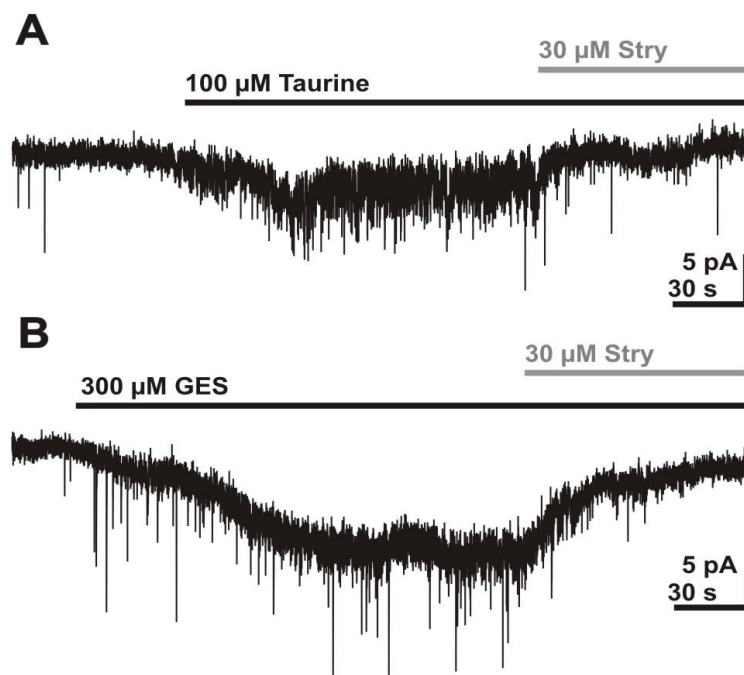


Figure 17: Extrasynaptic activation of glycine receptors. A: Bath application of 100 μ M taurine induced a strychnine sensitive inward current. B: Bath application of the taurine uptake inhibitor GES induced an inward current that could be blocked by strychnine. The experiments displayed in A and B were performed in the continuous presence of 3 μ M gabazine.

In summary, these results in combination with the absence of any glycine-sensitive sPSC suggest that taurine can act as endogenous neurotransmitter activating glycine receptors.

3.3 GABAergic networks in the developing cerebral cortex are activated by taurine

The previous set of experiments and other studies (Flint 1998, Kilb & Luhmann 2002, Okabe et al. 2004) suggest that taurine is the endogenous neurotransmitter acting on the glycine receptors. However, the functional consequences of an activation of these receptors have only partially been resolved. Therefore the influence of a tonic activation of glycine receptors on the excitability of immature networks projecting to pyramidal neurons was further investigated.

3.3.1 Basic properties of the investigated pyramidal cells

In total 20 pyramidal neurons from P0-1, 63 pyramidal neurons from P2, and 513 pyramidal neurons from P3-4 animals were identified by their location in the neocortex and their pyramidal like appearance in IR-DIC image. Threehundredtwo of these neurons could be subsequently stained for biocytin and their location within the total cortical layers could be exactly identified (Fig. 18). Morphological analysis of these neurons revealed that all stained neurons have a pyramidal appearance (Fig. 18B). The soma of the majority of neurons was located between 20 and 50 % of total cortical thickness, indicating that the all neurons used for this analysis were located in supra- and subgranular layers.

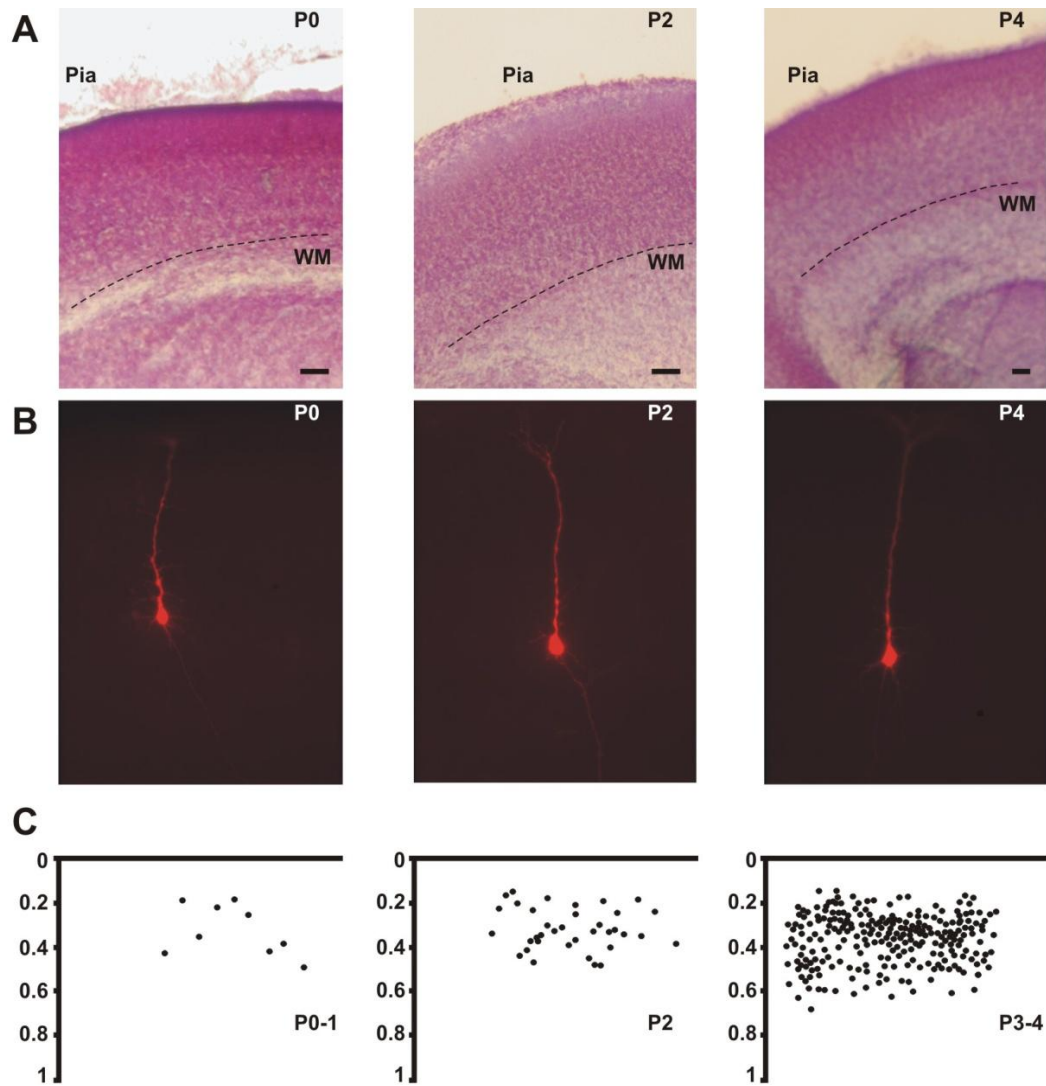


Figure 18: Localization and morphology of biocytin-labeled immature neurons in coronal slices of newborn mice. A: Nissl staining for coronal brain section, showing the developing cerebral cortex at different age stages. Pia is at the top of the figure whereas the beginning of white matter (WM) is marked with dashed lines. Inserted scale bars correspond to 100 μ m. B: Confocal images for the biocytin stained pyramidal neurons reveal that the neurons patched have the same morphological appearance during the early stage of the development. C: Normalized soma location for all biocytin stained neurons within the total cortical thickness for different age groups. In these plots 0 correspond to Pia and 1 to the beginning of the WM.

The pyramidal neurons from P0-1 animals had an average resting membrane potential (RMP) of -56 ± 2.5 mV ($n = 20$), an input resistance (R_{in}) of 1.7 ± 0.14 G Ω and an input capacity (C_{in}) of 55 ± 4 pF (Fig. 19A). In P2 animals a significantly ($p = 0.001$) more hyperpolarized RMP of -67.5 ± 1.1 mV ($n = 63$) was observed. R_{in} in this age group was 1.9 ± 0.1 G Ω and C_{in} 67.7 ± 5.6 pF (Fig. 19A). In P3-4 animals RMP was -68.8 ± 0.4 mV with no significant difference between P2 animals ($p = 0.3$) but significantly more hyperpolarized than P0-1 animals ($p = 0.0001$). The R_{in} of P3-4 animals were 1.6 ± 0.04 G Ω and an input capacity (C_{in}) of 74.6 ± 3 pF (Fig. 19A). In P2 and P3-4 animals the RMP was significantly ($p < 0.001$) more hyperpolarized at -68.8 ± 0.4 mV ($n = 63$) and -67.5 ± 1.1 mV ($n = 513$), respectively. Both R_{in} (1.9 ± 0.1 G Ω ($n = 63$) and 1.6 ± 0.04 G Ω ($n = 509$), respectively) and C_{in} (67.7 ± 5.6 pF and 74.6 ± 3 pF) were significantly ($p = 0.0001$) larger in P2 as compared to P3-4 animals, indicating the developmental increase in membrane surface of these neurons.

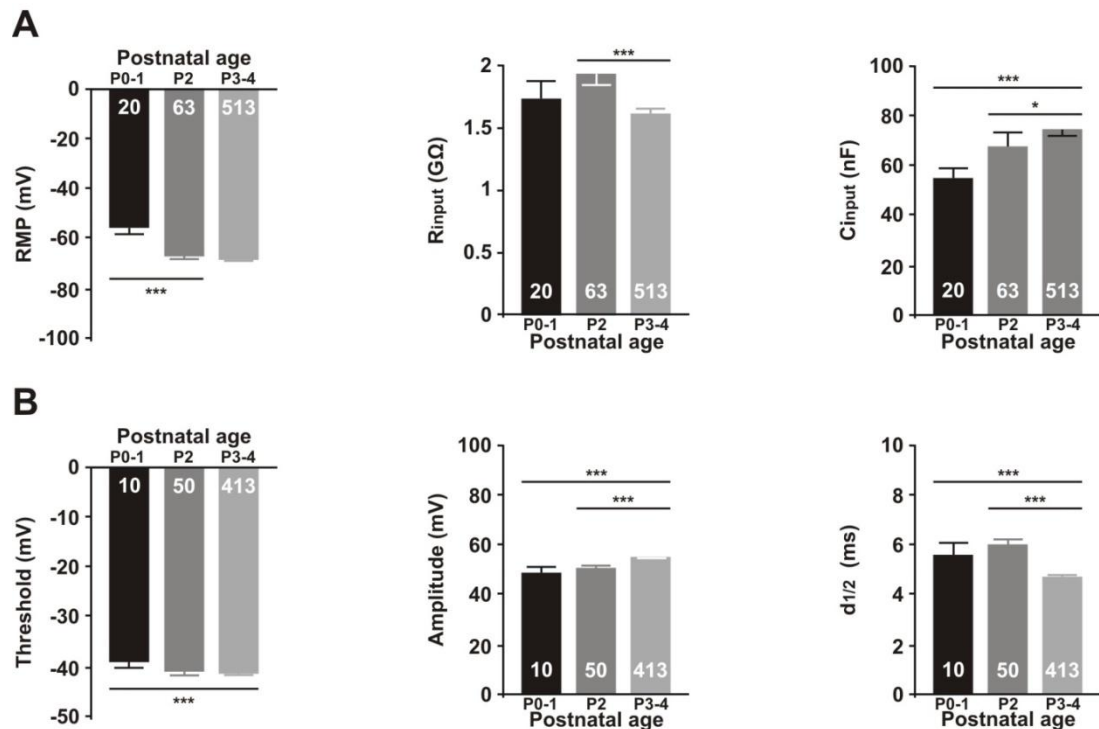


Figure 19: Electrophysiological properties of different postnatal age groups. A: Membrane properties where RMP, R_{in} and C_{in} are represented as histogram bars. Bars represent mean value \pm SEM, with the number of experiments given in the bars. B: Action potential properties with threshold, amplitude and $d_{1/2}$ as histogram bars.

In all three age groups APs could be elicited in pyramidal neurons upon injection of a depolarizing current. In P0-1 pyramidal cell in only 10 out of 20 cells APs with an amplitude of 48.8 ± 2.3 mV ($n = 10$) and an duration ($d_{1/2}$) of 5.6 ± 0.5 ms could be evoked upon a depolarization that crosses the AP-threshold of -39.1 ± 1.2 mV (Fig. 19B). In P2 animals a significantly ($p = 0.003$) larger fraction of pyramidal neurons show APs (50 out of 63 cells). These APs had rather similar properties than in the younger animals (amplitude 50.7 ± 1 mV, AP-threshold of -41 ± 0.8 mV and duration of 6 ± 0.2 ms). In pyramidal neurons from P3-4 animals in 413 out of 513 cells APs with amplitude of 55.1 ± 0.4 mV and duration of 4.7 ± 0.07 ms could be evoked upon a depolarization that crosses the AP-Threshold of -41.4 ± 0.3 mV (Fig. 19B).

3.3.2 Effect of taurine on pyramidal neurons

First we investigated the effect of bath applied taurine on holding potential and frequency of spontaneous postsynaptic currents (sPSCs) in pyramidal neurons. Bath application of taurine induced a dose-dependent induction of an inward current in P3-4 animals (Fig. 20). Maximum current was archived with 3 mM taurine and amounted to 62 ± 8.8 pA ($n = 15$), (Fig. 20C). Similar properties of taurine-induced currents were also observed on pyramidal neurons from P2 animals (Fig. 21A). Here the maximal amplitude amounted to 83 ± 14 pA ($n = 8$). The taurine induced current showed a pronounced desensitization by 27.5 ± 3.8 % ($n = 6$) and 31.4 ± 9 %, ($n = 4$) in 1 mM and 3 mM taurine, respectively, while no obvious desensitization occurred at lower taurine concentrations.

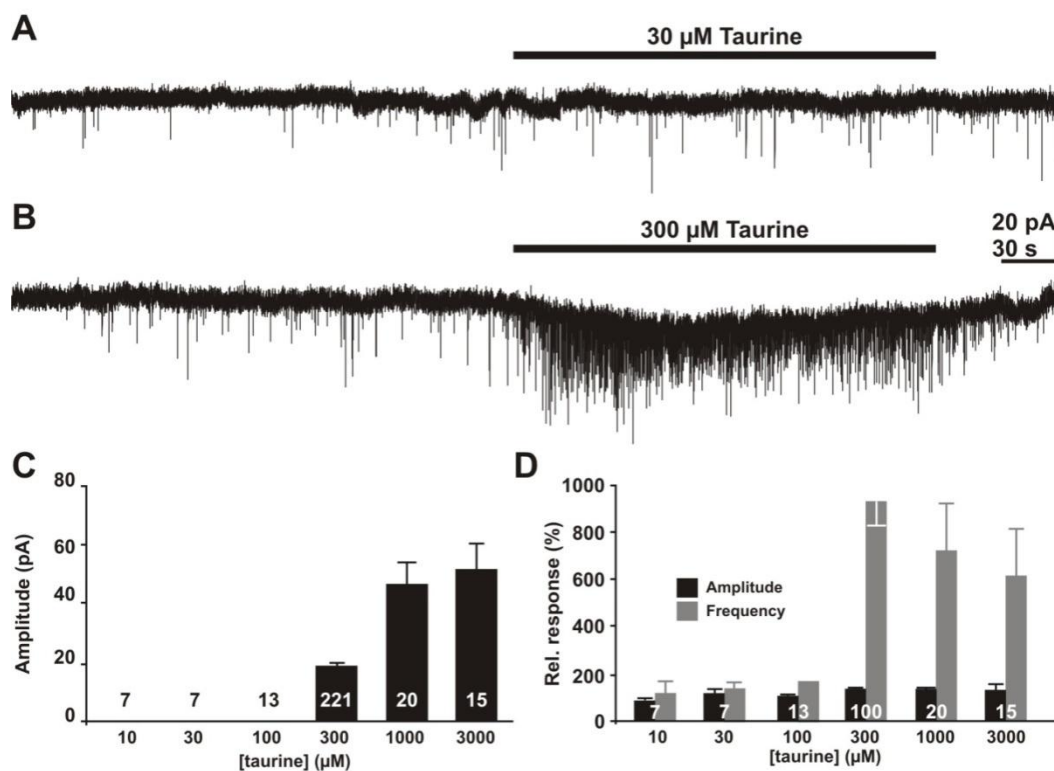


Figure 20: The effect of taurine on pyramidal neurons in P3-4 animals. A: Whole-cell voltage clamp recording from a pyramidal neuron at -60 mV as holding potential. Bath application of 10 μM Taurine do not affect the holding current or the frequency of the PSCs upper trace. B: Bath application of 300 μM taurine clearly induce an inward current and a massive increase in the frequency of the PSCs. C: Dose response relationship for the holding current at different taurine concentration. Bars represent mean ± SEM of the relative steady state amplitudes of taurinergic inward current. Numbers of experiments are given in the bars. D: Dose dependency of relative amplitude and frequency of the PSCs induced by bath application of different taurine concentrations. Bars represent mean ± SEM. Note that the effect of taurine on sPSC frequency displays clear threshold behavior.

In addition to this inward current, bath application of taurine increased the frequency of sPSCs in a considerable fraction of pyramidal neurons (Fig. 20B). In 41% (100 out of 245) of all investigated neurons from P3-4 animals taurine enhanced the frequency of sPSCs by 934.6 ± 102.6 % from 0.1 ± 0.01 Hz to 0.64 ± 0.05 Hz (n = 100). Furthermore these experiments revealed that above the threshold concentration

of 300 μM taurine neither the amplitude nor the frequency was significantly affected by the taurine application ($p = 0.39$, ANOVA, Fig. 20D).

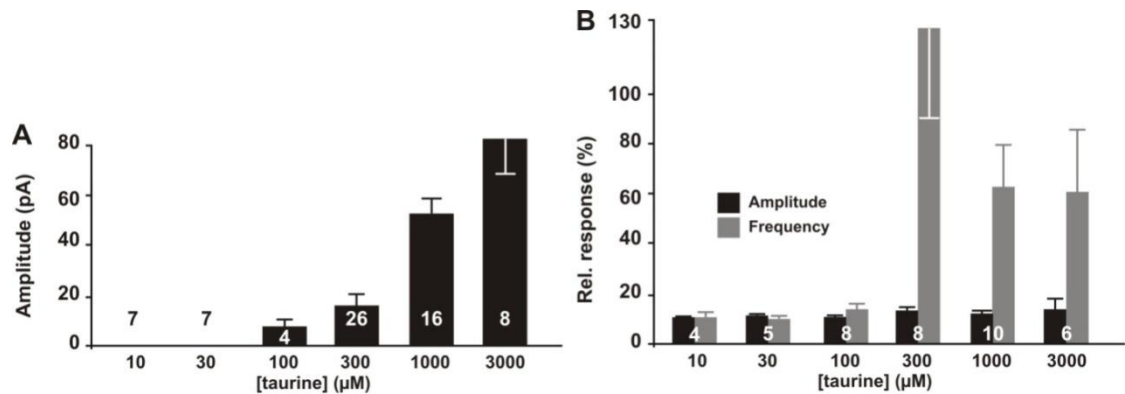


Figure 21: The effect of taurine on pyramidal neurons in P2 animals. A: Dose response for the holding current at different taurine concentration represented as bar histograms. Bars represent mean \pm SEM of the relative steady state amplitudes of taurinergic inward current. Numbers of experiments are given in the bars. B: Dose responses as histogram for the relative amplitude and frequency of the PSCs induced by bath application of different taurine concentrations.

Similar results were also obtained for P2 pyramidal neurons, where a tendentially smaller fraction of 25% ($p = 0.08$) showed an increase in the frequency of sPSCs. In this age group also no significant dose-dependency was observed above a threshold concentration of 300 μM taurine ($p = 0.4$, ANOVA) (Fig. 21B). The increase in the PSCs frequency was also comparable ($p = 0.4$, t-test) to P3-4 animals. In pyramidal neurons of P0-1 animals bath application of 300 μM taurine induced neither an inward current ($n = 12$) nor increases the frequency of sPSCs ($n = 12$). Since in P2-4 animals 300 μM taurine was sufficient to provoke a maximal effect on sPSCs and no obvious differences between both age groups were performed all subsequent experiments with 300 μM taurine in P3-4 pyramidal neurons.

To test if taurine responses are stable during a longer time of measurements, 300 μM taurine was applied repetitively to the same cell. No significant differences in taurine induced inward currents (Fig. 22A) or the amplitude and frequency of taurine-

induced sPSCs was observed between the first, second and third bath application of taurine (Fig. 22B).

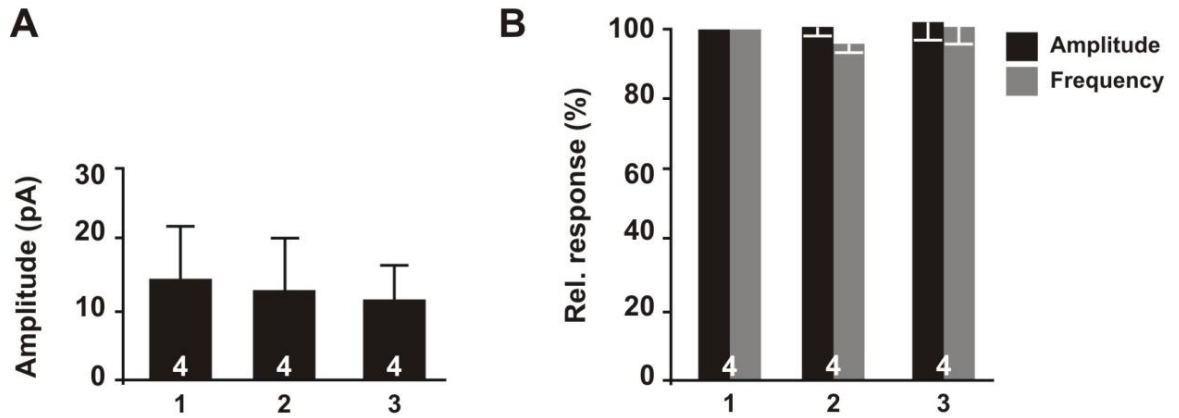


Figure 22: Repetitive taurine application. A: The amplitude of the current induced after bath application of 300 μ M of taurine remains stable throughout 3 repetitive applications. Bars represent mean \pm SEM of the relative steady state amplitudes of taurinergic inward current. Numbers of experiments are given in the bars. B: The amplitude and the frequency of the PSCs do not change after repetitive 300 μ M taurine application.

In summary, these results show that bath application of taurine at a concentration $\geq 300 \mu\text{M}$ increased the frequency of the PSCs in about 45 % of all pyramidal neurons, suggesting that the network activity was considerably increased by the bath application of taurine.

3.3.3 Pharmacology of taurine-induced responses in pyramidal neurons

Next we analyzed the pharmacological properties of the PSCs that are evoked by the bath application of 300 μM taurine in P3-4 pyramidal neurons. In the presence of 0.3-1 μM TTX neither amplitude ($16.8 \pm 2.7 \text{ pA}$ vs $16.9 \pm 2.6 \text{ pA}$) nor frequency (0.2 ± 0.1 vs. $0.2 \pm 0.1 \text{ Hz}$) of sPSCs were significantly ($p = 1$ and $p = 1$ respectively, $n = 3$) affected. This observation indicated that sPSCs represent miniature PSCs and

do not reflect AP dependent activity in the presynaptic cells. However, bath application of TTX (0.3-1 μM) completely blocked the taurine induced increase in PSC frequency (Fig. 23), suggesting that the taurine effect requires the activation of presynaptic networks.

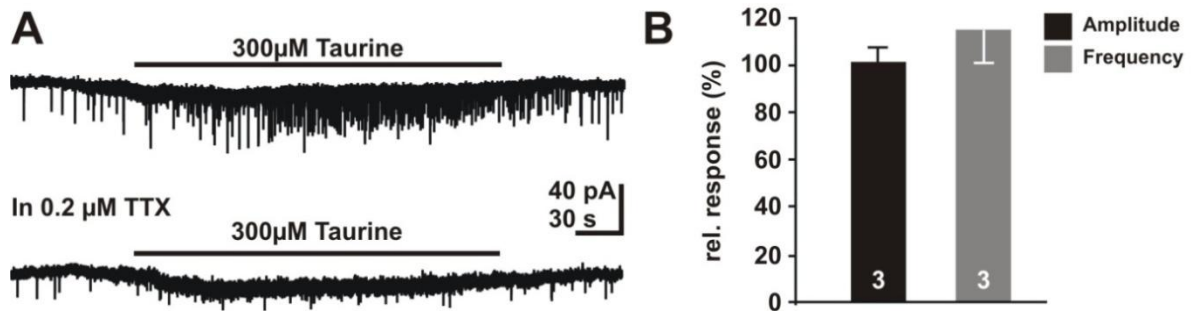


Figure 23: Taurine effect in the presence of TTX. A: Whole-cell voltage clamp recording from a pyramidal neuron at -60mV as holding potential. The taurine-induced increase in PSC frequency was abolished in the presence of 0.2 μM TTX (bottom). Note that taurine induced inward current was unaffected. B: Bar diagrams of the relative response for the amplitude and the frequency of the sPSCs in the presence of 0,2 μM of TTX. Neither of these two parameters was affected by TTX. Histograms represent means \pm SEM of 3 experiments.

Bath application of 10 μM CNQX or 20 μM CPP, blockers of AMPA and NMDA subtypes of glutamate receptors, had no significant effect on the taurine-induced PSCs (Fig. 24B). In the presence of both glutamate antagonists neither amplitude (27.13 ± 3 pA vs. 31.6 ± 6.3 pA) nor the frequency (0.55 ± 0.09 vs. 0.55 ± 0.11 Hz) were significantly ($p = 0,5$ and $p = 1$, respectively, $n = 9$) affected. These results suggest that glutamatergic synapses are not activated by bath application of taurine.

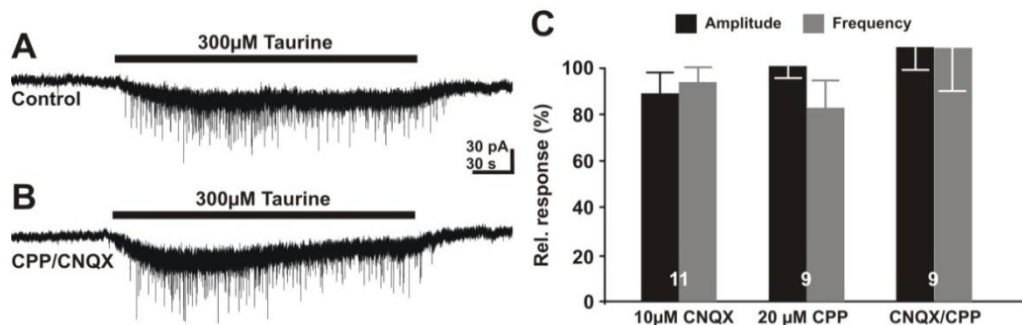


Figure 24: Pharmacology of the glutamate receptors. A, B: Whole-cell voltage clamp recordings from a pyramidal neuron at a holding potential of -60mV . The effect of bath applied taurine was unaltered in the presence of the glutamatergic antagonists CNQX ($10\ \mu\text{M}$) and CPP ($20\ \mu\text{M}$). C: Statistical analysis of the effect of glutamatergic antagonists on frequency and amplitude of taurine induced sPSCs. Bars represent mean \pm SEM. Note that glutamatergic antagonists had no effect on the amplitude or the frequency of taurine induce PSCs.

In the presence of the glycine receptor antagonist strychnine ($0.3\text{-}1\ \mu\text{M}$) the taurine-induced PSC increase was completely suppressed ($n = 12$) (Fig. 25A). Under this conditions bath application of taurine had no effect on the amplitude (13.84 ± 0.9 vs. $16.3 \pm 2.4\ \text{pA}$) and the frequency (0.11 ± 0.01 vs. $0.11 \pm 0.02\ \text{Hz}$) of PSCs (Fig. 25A). On the other hand, strychnine had no significant effect on amplitude (20.4 ± 2.8 vs $13.8 \pm 0.9\ \text{pA}$, corresponding to $92 \pm 11\ \%$, $n = 12$, $p = 0.11$) and frequency (0.17 ± 0.04 vs. $0.1 \pm 0.02\ \text{Hz}$, corresponding to $107 \pm 15\ \%$, $n = 12$; $p = 0.40$) of sPSCs, suggesting that glycine receptors do not directly contribute to sPSCs.

In contrast, bath application of the GABA_A specific antagonist gabazine ($3\ \mu\text{M}$) completely blocked sPSCs in 3 out of 8 pyramidal cells investigated and massively reduced the frequency of sPSCs from 0.14 ± 0.04 to $0.04 \pm 0.004\ \text{Hz}$, corresponding to $79 \pm 8\ \%$ in the remaining 5 neurons (Fig. 25B). These results suggest that a considerably fraction of the sPSCs is mediated by GABA_A receptors. The taurine-induced increase in the frequency of PSCs was abolished ($112 \pm 9\ \%$, $n = 8$, $p = 0.34$) in the presence of $3\ \mu\text{M}$ gabazine. The combined application of $1\ \mu\text{M}$ strychnine and $3\ \mu\text{M}$ gabazine completely blocked the taurine-induced increase in PSC frequency.

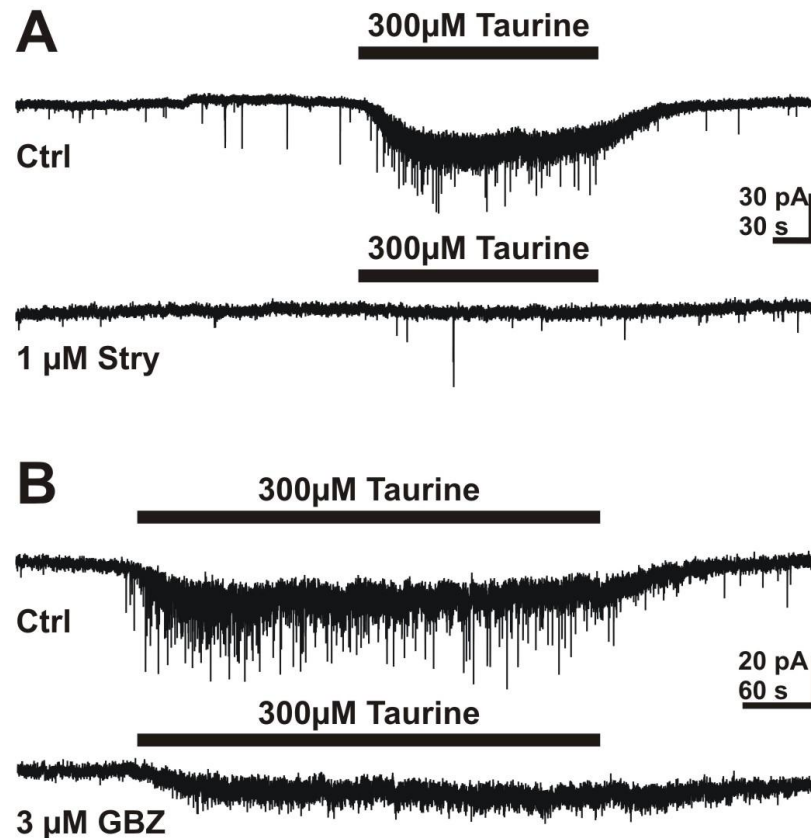


Figure 25: Effect of glycine and GABA_A receptor antagonists on taurine induced responses. A: Whole-cell voltage clamp recordings at a holding potential of -60mV. In the presence of 1µM strychnine the taurine-induced PSCs increases was completely suppressed. Please note that the amplitude of the taurine induce inward current was also reduced in the presence of 1µM strychnine. B: Bath application of 3µM gabazine massively reduced the frequency of taurine induce PSCs and slightly diminished the amplitude of the taurine induced inward current.

The taurine induced inward current was reduced by 73 % (n = 8, Fig. 25) in the presence of 3 µM gabazine, by 55 % (n = 12) in the presence of 1 µM strychnine. The combined application of 1 µM strychnine and 3 µM gabazine completely blocked the taurine-induced inward current. In contrast, glutamatergic antagonists and TTX had no significant effect on this taurine-induced inward current.

Since the later results suggest that taurine induced a direct membrane response in pyramidal neurons, we next directly analyzed these responses using focal-application of 5 mM taurine under whole-cell conditions. Focal taurine application (2-5 ms) at a

holding potential of -60 mV induced in pyramidal neurons an inward current of -260.4 ± 31.9 pA ($n = 12$) (Fig. 26A), which reversed at -22.3 ± 1.5 mV ($n = 10$) (Fig. 26C), in accordance with the Cl^- concentration of the pipette solution.

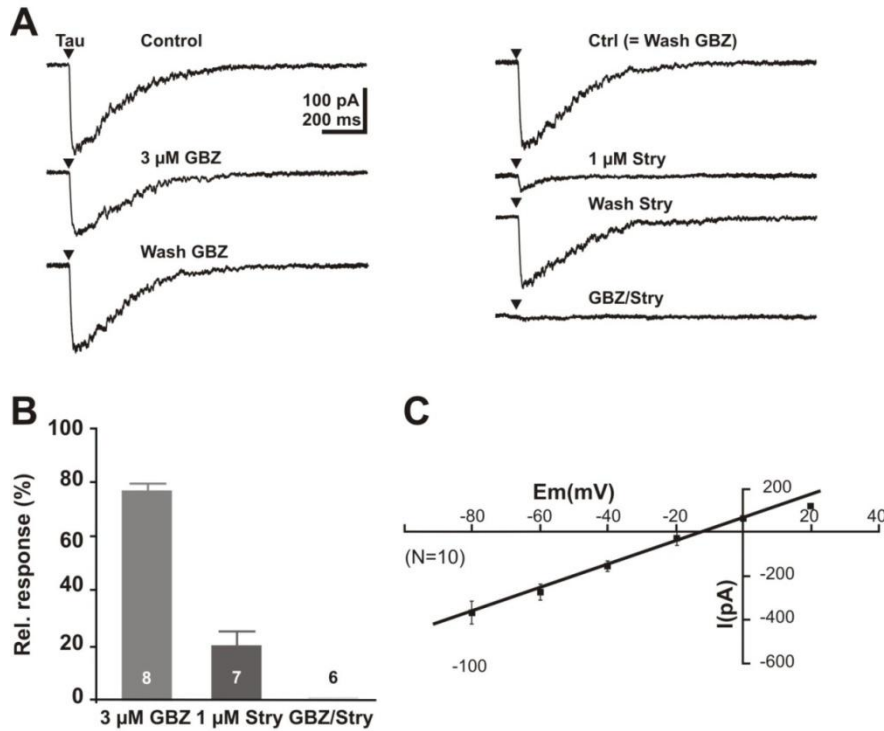


Figure 26: Activation of GABA_A and glycine receptors by focal application of 5mM taurine on pyramidal neurons: B: Inward currents elicited by a 5 ms of 5mM taurine. The left traces illustrate the effect of 3 μM gabazine, the right traces the effect of strychnine. After a partially washout of strychnine, the combined application of gabazine and strychnine completely suppressed the taurine-induced current. C: Bar histograms demonstrating the effect of gabazine and strychnine on taurine-induced currents. Bars represent mean \pm SEM of the relative responses. A: I-V plot of the inward current after focal application of 5mM taurine at different voltages.

Bath application of 1 μM strychnine significantly ($p < 0.001$) reduced the amplitude of taurine-induced currents by 80 ± 5.2 % ($n = 7$, Fig. 26B). Bath application of 3 μM gabazine reduced the amplitude of taurine induced currents by 22 ± 2.5 % ($n = 8$),

and the combined application of 1 μM strychnine and 3 μM gabazine completely blocked taurine induced currents ($n = 6$, Fig. 26A, B). In summary these results suggest that the taurine-induced inward currents were carried by both GABA_A and glycine receptors with the GABA_A receptors mediating approximately 20% and glycine receptors approximately 80% of the responses.

As it had been shown that the pharmacological properties of glycine and GABA_A systematically change during development (Aguayo et al., 2004, Carlson et al., 1998), we performed control experiments to prove the efficacy of glycinergic and GABA_A agonists in immature pyramidal cells. In these experiments focal application of 100 μM glycine induced an inward current of -180.2 ± 42.5 pA ($n = 9$) that was completely blocked by 1 μM strychnine ($n = 6$), while 3 μM gabazine ($n = 7$) had no effect ($103 \pm 7.4\%$, $n = 7$, Fig. 27A).

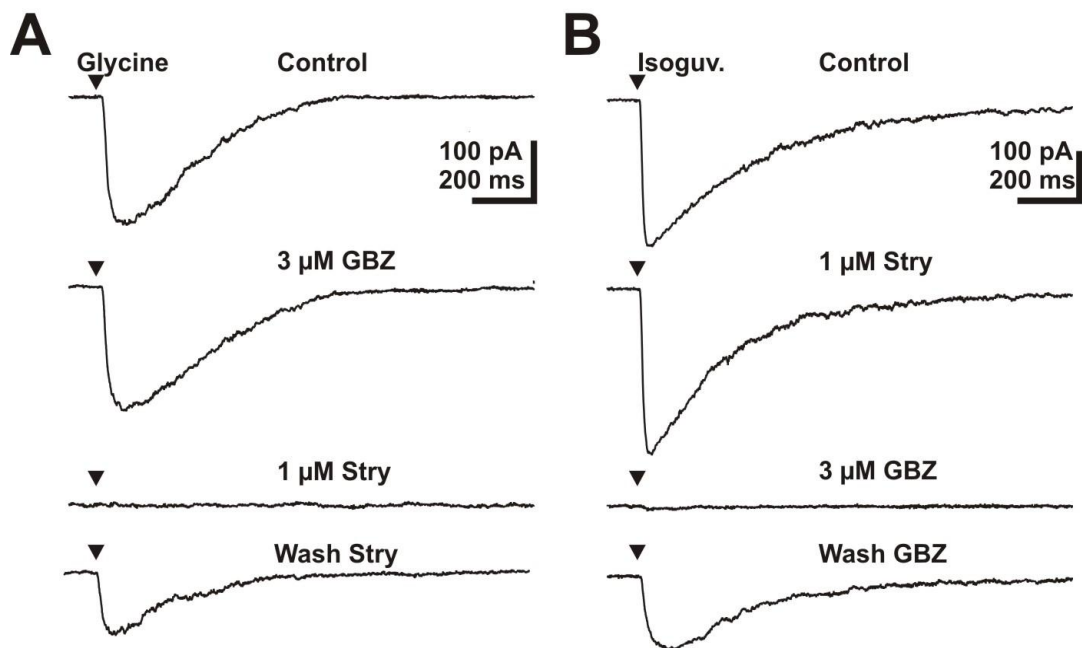


Figure 27: Pharmacological profile of glycine and GABA_A receptors. A: Focal application of 100 μM glycine induce an inward current that was unaffected in the presence of 3 μM gabazine and completely blocked in the presence of 1 μM strychnine. B: Focal application of 100 μM isoguvacine (top) induce an inward current that was unaffected by 1 μM

strychnine (middle) and completely blocked in the presence of 3 μ M gabazine.

Focal application of the GABAergic agonist isoguvacine (100 μ M) induced an inward current of -382.3 ± 37.9 pA ($n = 7$) that was completely blocked by 3 μ M gabazine ($n = 6$), while 1 μ M strychnine had no effect (99 ± 1.8 %, $n = 4$, Fig. 27B). In summary these experiments revealed that 1 μ M strychnine and 3 μ M gabazine could be used as specific antagonists for glycine and GABA_A receptors, respectively, already in P3-4 neocortical pyramidal neurons.

3.3.4 Reversal of taurine-induced sPSCs

To strengthen our previous finding, that GABA_A and glycine receptors are underlying the taurine-induced sPSCs, in the next voltage-clamp experiments a pipette-solution with a $[Cl^-]_p$ of 8 mM was used, to shift E_{GABA} to values around -60 mV (Fig. 28). In these experiments E_{GABA} was determined experimentally for each cell by a series of focal GABA pulses at different holding potentials. Subsequently the cells were clamped exactly to this experimentally determined E_{GABA} to unravel PSCs that were not driven by ligand-gated Cl⁻ channels.

These experiments revealed that the frequency of sPSCs was reduced to about 50% if the membrane was clamped to E_{GABA} , indicating that a substantial fraction of sPSCs may be mediated by glutamatergic receptors. However, at this holding potential bath application of 300 μ M taurine had no significant ($p = 0.35$) effect on the frequency of PSCs (Fig. 28A). In contrast, under conditions when the holding potential was negative (-85 mV) or positive (0 mV) to E_{GABA} a significant increase in the frequency of PSCs was observed during the application of 300 μ M taurine, indicating that taurine exclusively initiates PSCs that are mediated via ligand-gated Cl⁻ channels. Accordingly the voltage dependence of the taurine-induced PSCs reversed approximately at the estimated E_{GABA} (Fig. 28B).

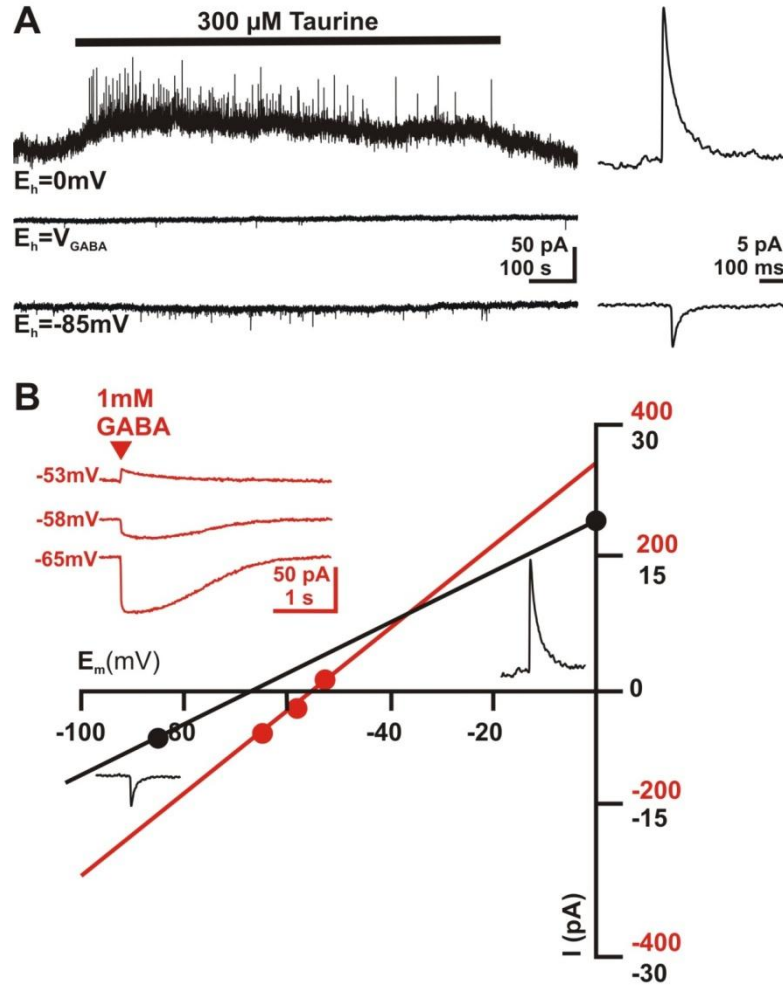


Figure 28: Taurine induces Cl^- dependent PSCs. A: Current traces recorded at $E_h = 0\text{mV}$ (upper trace), $E_h = E_{\text{GABA}}$ (middle trace) and at $E_h = -85\text{mV}$ (bottom trace). Note that no taurine-induced PSCs were visible if $E_h = E_{\text{GABA}}$ and that the PSCs reverse their direction at this potential. B: Determination of the reversal potential of GABAergic currents (E_{GABA}) induced by focal GABA application (red trace) and of average taurine-induced PSCs (black trace).

Since it had been reported by a variety of studies that ligand-gated Cl^- channels mediate depolarizing membrane responses in immature pyramidal neurons, we next investigated whether taurine-induced membrane responses mediate excitatory actions under physiological conditions. Therefore we performed cell-attached recordings to investigate this effects under conditions in which the $[\text{Cl}^-]_i$ remained undisturbed. These experiments revealed that bath application of $300\ \mu\text{M}$ taurine enhances the AP frequency of pyramidal neurons by $780 \pm 320\ \%$ from $0.16 \pm 0.05\ \text{Hz}$ to 0.76 ± 0.09

Hz ($n = 5$). In summary these results strongly suggest, that the taurine-effects mediate an excitatory action of pyramidal neurons (Fig. 29).

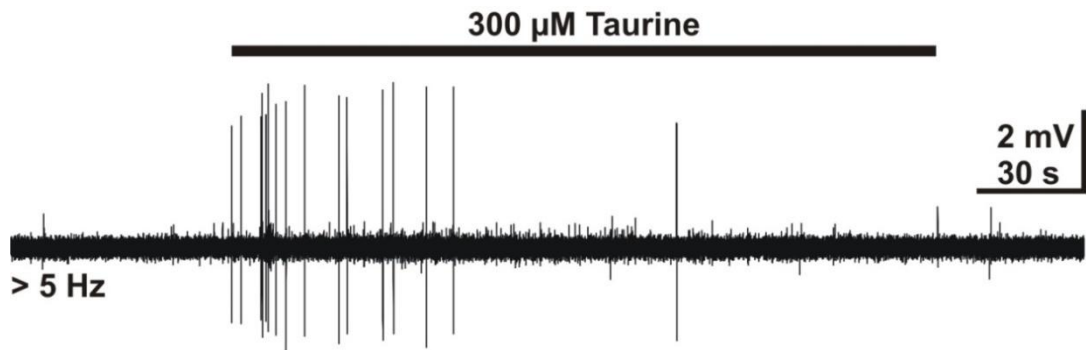


Figure 29: Cell-attached recording from a pyramidal neuron. Bath application of 300 μM taurine induced APs. The recorded data were highpass-filtered at 5Hz.

3.3.5 Effect of taurine on GABAergic interneurons

As the previous results strongly suggested that taurine enhanced the frequency of GABAergic and/or glycinergic PSCs and because no evidences for synaptic release of glycine in the immature cortex had been reported so far, we next concentrated on the role of GABAergic interneurons. Therefore we performed whole-cell measurements on 55 interneurons identified by GFP expression under the control of GAD67 (Fig. 30).

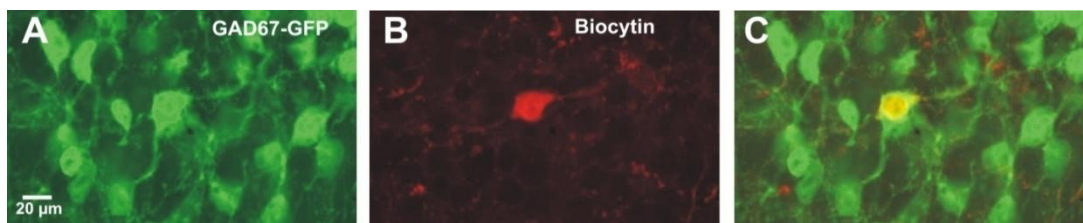


Figure 30: Identification of GABAergic interneurons. A: Confocal fluorescence image displaying GFP^+ interneurons. B: Confocal image for a biocytin-labeled interneuron. C: Merged image.

In total 32 YFP⁺ GABAergic interneurons were recorded. These GABAergic interneurons had an average RMP of -65.7 ± 2 mV (n = 32), a R_{in} of 4 ± 1.5 G Ω and a C_{in} of 37 ± 5.2 pF. In 60 % of the GABAergic interneurons APs could be elicited upon injection of a depolarizing current. These APs had an amplitude of 41.4 ± 2.5 mV (n = 19), a duration of 2.4 ± 0.2 ms and could be evoked upon a depolarization that crosses the AP-threshold of -48 ± 1 mV. Upon persistent injection of depolarizing currents these cell could discharge with a frequency of 53 ± 5.8 Hz (n = 17). Focal application of 100 μ M of glycine induce in GABAergic interneurons a current of -91.4 ± 21.2 pA (n = 7) that was completely blocked by 1 μ M strychnine (n = 7), whereas 3 μ M gabazine had no effect 106.2 \pm 5.3% (Fig. 31B). Focal application of 100 μ M of isoguvacine induces in GABAergic interneurons a current of -131.6 ± 40.7 pA (n = 7) current that was completely blocked by 3 μ M gabazine (n=7), whereas 1 μ M strychnine had no effect 96.3 \pm 3.8% (Fig. 31C). Interestingly, in GABAergic interneurons the current that was induced by focal application of 5mM taurine (-154.8 ± 22 pA; n = 10) was completely blocked by 1 μ M strychnine (n = 9), while 3 μ M gabazine (n = 8) had no effect (99.3 \pm 6.6 %; Fig. 31A).

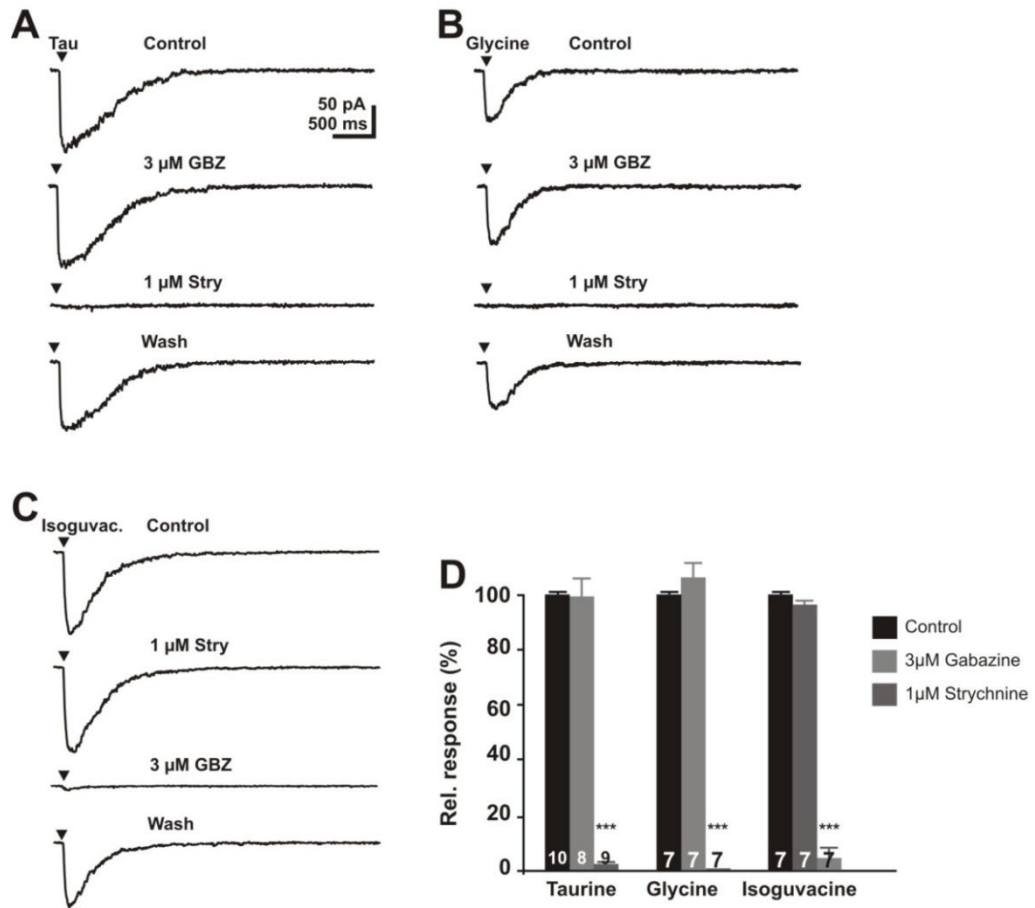


Figure 31: Activation of GABA_A and glycine receptors on interneurons
A: Focal application of 5mM taurine induces an inward current that is unaffected by 3μM gabazine and completely blocked in the presence of 1μM strychnine. **B:** Focal application of 100μM glycine induces an inward current that is unaffected by 3μM gabazine, but completely blocked in the presence of 1μM strychnine. **C:** Focal application of 100μM isoguvacine induces an inward current that is completely blocked by 3μM gabazine, but unaffected in the presence of 1μM strychnine. **D:** Bar histograms representing mean ± SEM of the relative amplitude of the inward current after focal application of taurine, glycine and isoguvacine in the presence of GABA_A receptor antagonist gabazine or glycine receptor antagonist strychnine. The numbers of experiments are given in bars.

The tonic activation of the GABA_A and glycine receptors in these cells by 300 μM taurine induced an inward current of 8.9 ± 2.5 pA (n = 7). This inward current was

blocked by $72 \pm 12\%$ ($n = 7$) in the presence of $1 \mu\text{M}$ strychnine and by $49 \pm 10\%$ ($n = 7$) in the presence of $3 \mu\text{M}$ gabazine (Fig. 32).

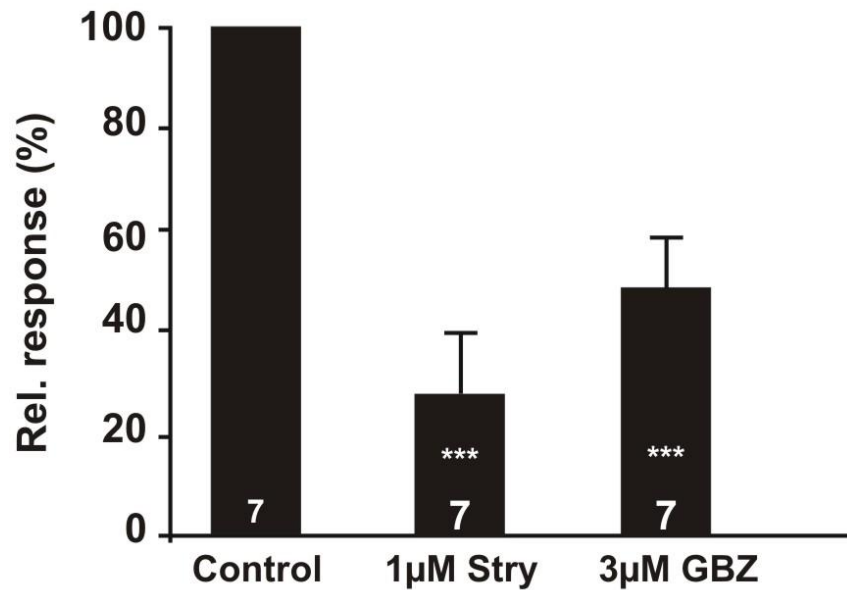


Figure 32: Tonic effect of taurine on interneurons. Bar diagrams of the relative response for the amplitude of the tonic current induced by bath application of $300\mu\text{M}$ taurine in the presence of $1\mu\text{M}$ Strychnine or $3\mu\text{M}$ gabazine. Histograms represent means \pm SEM of 7 experiments.

To uncover the effect of this taurine-induced inward current under conditions with undisturbed $[\text{Cl}^-]_i$ we performed cell-attached experiments. These experiments revealed that in 4 out of 9 recorded GABAergic interneurons bath application of $300 \mu\text{M}$ taurine induced an increase in AP frequency by $995 \pm 55\%$ (Fig. 33A, D). This increase in the frequency could be reduced by $28 \pm 18\%$ ($n = 3$) in the presence of $1 \mu\text{M}$ strychnine and by $54 \pm 20\%$ ($n = 3$) in the presence of $3 \mu\text{M}$ gabazine and $1\mu\text{M}$ strychnine (Fig. 33D).

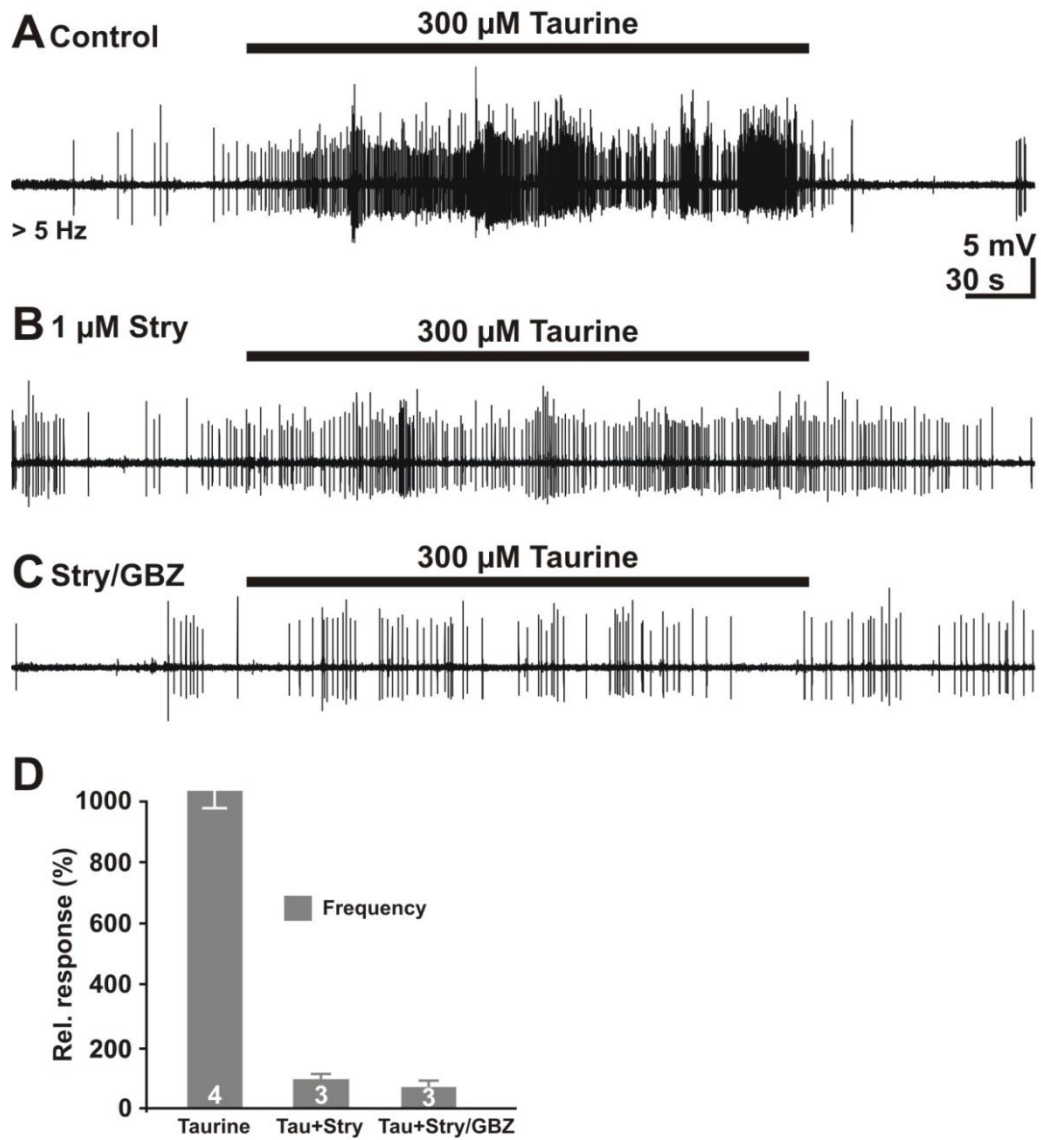


Figure 33: Effect of taurine on GABAergic interneurons under cell-attached conditions. A: Bath application of 300 μ M of taurine increase the frequency of the APs. B: In the presence of 1 μ M strychnine taurine has smaller effect on the AP frequency C: In the presence of strychnine and gabazine taurine had no effect on AP frequency. D: Statistical analysis of the taurine effect on AP frequency revealed that taurine has no effect in the presence of strychnine and gabazine. Bars represent mean \pm SEM, number of experiments is given in the bars.

In summary these results suggest that bath application of taurine excites GABAergic interneurons and that this activity was mediated mainly via glycine receptors.

3.3.6 Taurine effect on pyramidal neurons in reduced slice preparation

In an additional approach, we used a reduced slices preparation to unravel whether SP cells, which comprised of a significant fraction of GABAergic neurons, contribute to this activity induced a comparison of reduced slice preparations either containing the SP or lacking the showed that in both preparations bath application of 300 μ M taurine induced in a comparable fraction of pyramidal neurons (531 ± 138 % vs. 697 ± 170 %, $p=0.45$, $n = 6$) PSC activity (Fig. 34A). The taurine-induced PSCs had comparable properties in both preparations (amplitude 14.4 ± 1.9 vs. 18.8 ± 1.8 pA, frequency 0.19 ± 0.02 vs. 0.26 ± 0.05 Hz for slices including SP vs. slices w/o SP, respectively).

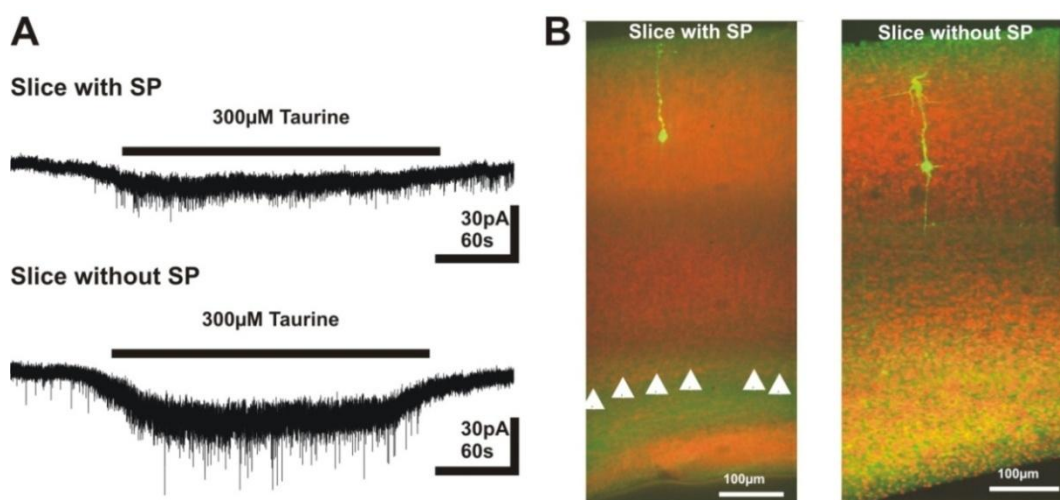


Figure 34: Taurine effect on pyramidal neurons in reduced slice preparation. A: Bath application of taurine in reduced slice preparation with subplate (top) and without subplate (bottom). B: Confocal images of the biocytin-labeled neurons (green) used for the current recordings in A, counter-stained with propidium iodide. Note the absence of the subplate (white arrowheads) in the right slice.

No differences in the frequency of PSCs were observed between slices which contained a SP (531 ± 138 %) and slices without SP (697 ± 170 %). However, both values were significantly smaller when compared to a conventional coronal slice (934.6 ± 102 %, $n = 6$).

3.3.7 Effect of isoguvacine and glycine on sPSCs in pyramidal neurons

Since these results indicate that glycine and/or GABA_A receptors of GABAergic interneurons mediate the effect of taurine on the sPSC_s activity, we next investigated whether a selective activation of GABA_A receptors with 10 μ M isoguvacine or 100 μ M glycine can induce comparable effects on the frequency of PSCs in pyramidal neurons. These experiments in P3-4 animals revealed that bath application of 100 μ M glycine induced an inward current (Fig. 35) of 37.6 ± 4.6 pA (in 23 out of 24 cells) whereas bath application of 3 μ M isoguvacine induce an inward current with an amplitude of 44.4 ± 5.3 pA in 13 out of 14 cells (Fig. 35A).

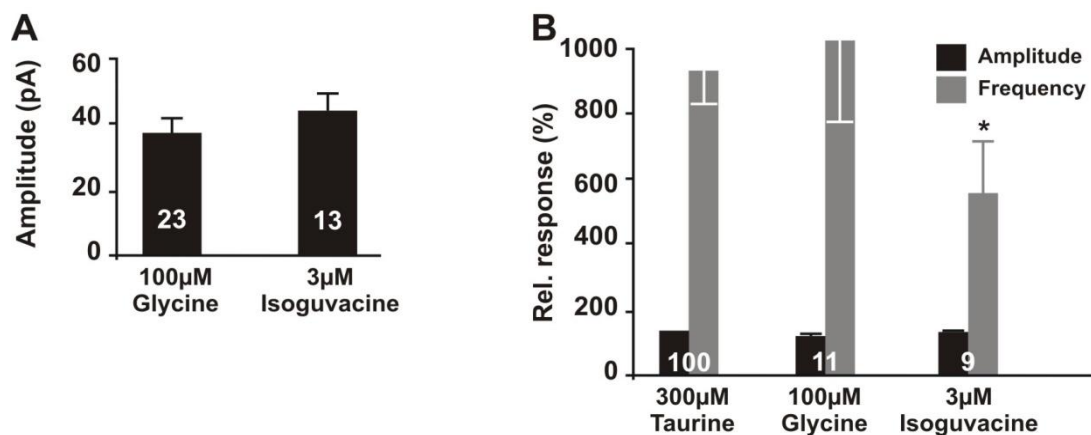


Figure 35: The effect of bath applied glycine and isoguvacine on pyramidal neurons. A: Bar diagram summarizing the steady-state inward currents induced by bath application of 100 μ M of glycine or 3 μ M isoguvacine. Bars represent mean \pm SEM, numbers of experiments are given in the bars. B: Bar diagram illustrating the effect of 100 μ M glycine and 3 μ M isoguvacine on PSCs. For comparison the effect of 300 μ M taurine was added to this graph. Note that the effects of taurine, glycine are not significantly different, while the frequency of isoguvacine induced PSCs was significantly smaller. Bars represent means \pm SEM, numbers of experiments are given in bars.

In addition to this inward current, bath application of 100 μ M glycine increased the frequency of sPSCs in a considerable fraction of pyramidal neurons. In 45 % (11 out of 24) of all investigated neurons 100 μ M glycine enhanced the frequency of PSCs by 1027 ± 250 % from 0.19 ± 0.05 to 0.71 ± 0.2 Hz ($n = 18$, Fig. 35B). This effect was not significantly different ($p = 0.74$, t-test), from the effect of 300 μ M taurine on PSCs. Bath application of 3 μ M isoguvacine also increased the frequency of PSCs in 64 % (9 out of 14) of all investigated neurons by 559 ± 146 % from 0.11 ± 0.03 to 0.34 ± 0.08 Hz ($n = 10$, Fig. 35B), which was significantly ($p=0.005$, t-test) smaller than the effect of 300 μ M taurine. The relative amplitude of the PSCs induced by glycine and isoguvacine application was not significantly different (122 ± 7.7 % vs. 133 ± 16 %, $p = 0.5$, pair t-test), (Fig. 35B).

To test if the glycine-induced PSCs were mediated via GABA_A receptors in the postsynaptic membrane, we bath applied 100 μ M glycine in the presence of 3 μ M of gabazine, under this conditions all PSCs were completely blocked ($n = 3$, Fig.36), suggesting that glycine induced exclusively GABAergic PSCs.

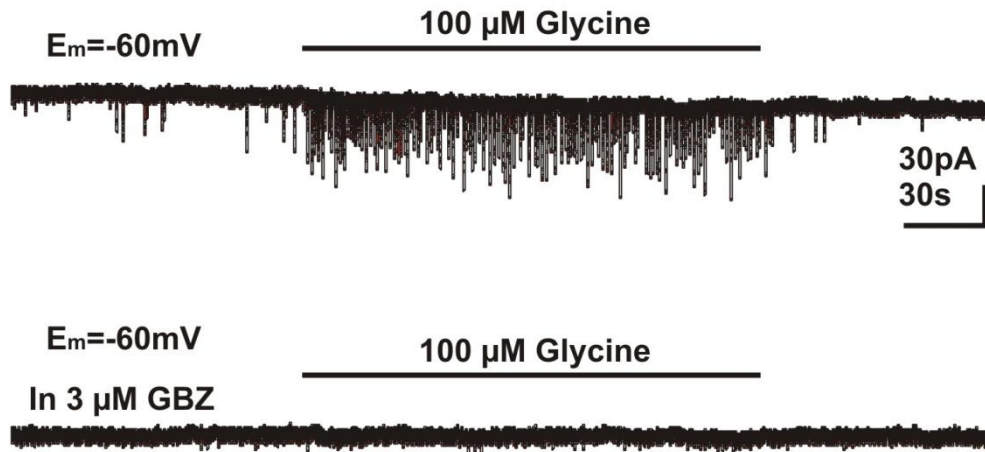


Figure 36: The PSCs induced by bath application of 100 μ M glycine are completely suppressed in the presence of 3 μ M gabazine (GBZ).

3.3.8 Temporal coherence between taurine-induced PSCs

As the previous results indicate, that GABAergic interneurons respond to the bath-application of 300 μ M taurine with suprathreshold responses, we next performed

simultaneous recordings from in total 10 pairs of pyramidal neurons. In 5 of these simultaneous recordings both neurons showed a taurine-induced increase in the PSCs. In 3 out of these 5 simultaneous recordings a rather high cross correlation between taurine-induced PSCs was observed (Fig. 37), while only 2 cells lack tight correlation. In the cells with a close correlation $12 \pm 4 \%$ ($n = 3$) of all PSCs occurred highly correlated with a latency of 6.7 ± 3.3 ms between the PSCs. In summary, these results suggest that a rather small subset of the GABAergic interneurons project to pyramidal neurons to induce GABAergic PSCs in these neurons.

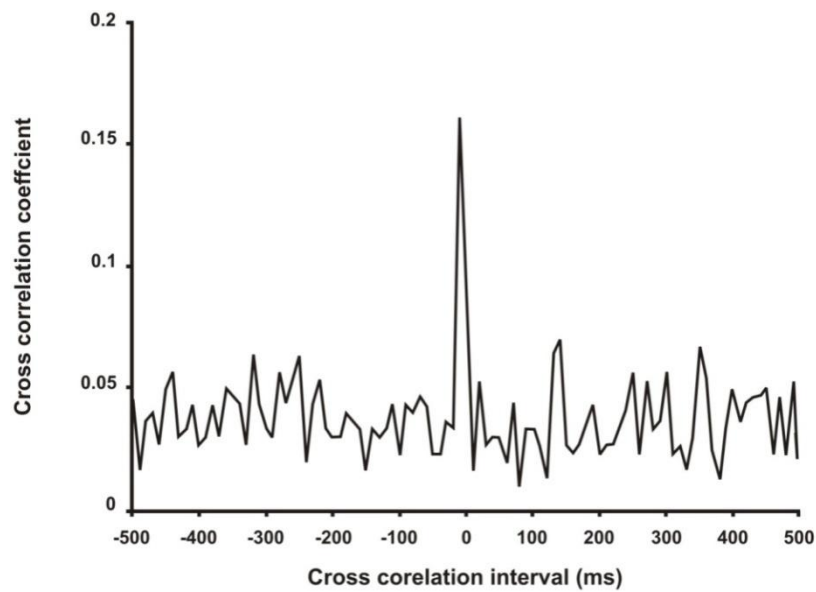


Figure 27: Temporal coherence between taurine-induced PSCs in a simultaneous recordings from two pyramidal neurons.

4. Discussion

4.1 CR cells of different origins show homogenous electrophysiological properties

The finding that all neurons selected by their morphological appearance and electrophysiological parameters could be characterized as CR cells after biocytin staining indicates that CR cells can be unequivocally identified in the tangential slice preparation by their appearance in the videomicroscopic image and their electrophysiological properties, as already discussed in previous studies (Kilb and Luhmann, 2000; Kilb and Luhmann, 2001; Kilb et al., 2002; Achilles et al., 2007). YFP⁺ and YFP⁻ CR cells were classified in our study only by the YFP fluorescence observed at the patch-clamp setup, since a reliable classification of YFP⁺ and YFP⁻ CR cells after biocytin/YFP immunostaining was not possible, probably caused by a washout of YFP fluorescence during whole-cell recordings. Therefore we used only cells that could be unequivocally classified as YFP⁺ or YFP⁻ CR cells before recording in subsequent experiments (Fig. 1A). The YFP⁺ and the YFP⁻ subpopulation both might represent CR cells with heterogeneous origin. While the YFP⁺ CR cells derive from Dbx1-expressing progenitors and thus originate from the septum and PSB (Bielle et al., 2005), the YFP⁻ CR cells derive from caudomedial portions of the pallial border (cortical hem) (Zecevic and Rakic, 2001; Shinozaki et al., 2002; Takiguchi-Hayashi et al., 2004). In addition, some Dbx1-derived CRs might not be labeled in *Dbx1^{cre}; ROSA26^{YFP}* animals due to a delay in recombination or recombination escape in *Dbx1^{cre}; ROSA26^{YFP}* animals and, thus, be included in the YFP⁻ population (see experimental procedures). However, hem-derived CR cells have been shown to represent the majority of CR cells in parietal cortex (Yoshida et al., 2006), where most recorded neurons were located, while very few, if any, septum Dbx1-derived CR cells populate this area (Bielle et al., 2005). Therefore it is likely that YFP⁺ and YFP⁻ represent two fairly homogeneous subpopulations, namely PSB Dbx1-derived and hem-derived CR cells, respectively. On the other hand, the present study can make no prediction whether CR subpopulations in medial or more lateral regions of the cortex may display different morphological or electrophysiological properties, how YFP⁺ and YFP⁻ CR cells differ in these properties during prenatal development, and whether other properties, like their life span, differ between these CR cells subpopulations.

This study is the first direct comparison of electrophysiological properties between different subpopulations of CR cells. No considerable differences between YFP⁺ and YFP⁻ CR cells in any of the aspects investigated were found. RMP and input resistance observed in the present study for both populations are comparable with values reported previously (Zhou and Hablitz, 1996c; Mienville, 1998; Kilb and Luhmann, 2000; Kilb and Luhmann, 2001; Kilb et al., 2002; Radnikow et al., 2002; Kilb et al., 2004). Due to short circuit effects of the leak conductance between cell membrane and patch pipette, the measured membrane potential most probably underestimated the RMP (Fricker et al., 1999; Tyzio et al., 2003). If the measured potential was corrected for seal and input resistance (both values were determined for all CR cells) according to the formula delivered by Tyzio et al. (2003) a RMP of -83 ± 5.2 mV ($n = 30$) for YFP⁺ and of -80 ± 5.6 mV ($n = 37$) for YFP⁻ CR cells was obtained. These values were not significantly ($P < 0.427$) different and are close to the RMP determined from reversal potential of NMDA receptor currents for CR cells (Achilles et al., 2007) and other immature neurons (Hirsch and Luhmann, 2008; Tyzio et al., 2003). AP potential tended to be shorter in YFP⁻ CR cells, however, this difference was not significant after a Bonferroni–Holm adjustment of the error-level α . The other AP parameters as well as the properties of the I_h current were also not significantly different between both CR cells subpopulations.

Many reports found that CR cells receive synaptic inputs that are mainly or exclusively mediated by GABA_A receptors (Kilb and Luhmann, 2001; Kilb et al., 2004; Kirmse and Kirischuk, 2006a; Soda et al., 2003; Dvorzhak et al., 2008). Since the GABA reversal potential is positive to action potential threshold in CR cells, GABAergic PSCs can mediate excitatory responses (Achilles et al., 2007; Mienville, 1998). In the present study spontaneous and CCh-induced synaptic activity were completely suppressed by the GABA_A specific antagonist gabazine in both YFP⁺ and YFP⁻ CR cells, indicating that in both CR cells subpopulations synaptic activity was primarily mediated via GABA_A receptors. In addition, the properties of sPSCs and CCh-induced PSCs were similar between both subpopulations, indicating that YFP⁺ and YFP⁻ neurons express GABA_A receptors with similar characteristics and that cholinergic activation of network activity in the immature cortex (Dupont et al., 2006) mediates similar activity in both CR cells subpopulations. However, whether

the different CR cells subpopulations receive specific GABAergic inputs from distinct sources could not be resolved by our study.

This study also demonstrated the functional expression of NMDA receptors in both YFP⁺ and YFP⁻ cell populations, in accordance with other studies revealing NMDA receptors in the membrane of CR cells (Chan and Yeh, 2003; Lu et al., 2001; Mienville and Pesold, 1999; Radnikow et al., 2002). In the presence of the NMDA specific antagonist CPP all glutamatergic responses were blocked, supporting the finding that functional AMPA receptors are absent in rodent CR cells (Lu et al., 2001; Radnikow et al., 2002). The observation that 3 μ M ifenprodil inhibits NMDA receptors in YFP⁺ and YFP⁻ CR cells with similar efficacy suggests that in both populations NR2B receptor subunits are expressed at comparable ratios (Williams, 1993). A comparable inhibition of glutamatergic currents has been previously reported in other CR cells studies using 1–10 μ M ifenprodil (Mienville and Pesold, 1999; Lu et al., 2001; Radnikow et al., 2002). The observation, that NMDA receptors are equally expressed in both CR cells populations suggests that these populations are most probably not differentially affected by glutamate.

In addition to their electrophysiological parameters, the morphological organization of neurons is also an important factor for their functional role within neuronal networks by virtue of the constraints it imposes on the input-output features. Therefore the morphological properties of YFP⁺ and YFP⁻ CR cells were also analyzed. These studies revealed that most morphological properties are comparable between YFP⁺ and YFP⁻ CRc, with a slightly larger dendritic compartment in YFP⁺ CR (Sava et al., 2010). However, even in YFP⁺ CR cells the dendritic compartment covers a rather small area, in accordance with previous findings (Zhou and Hablitz, 1996b; Kilb and Luhmann, 2001; Radnikow et al., 2002). Such a larger dendritic compartment suggests a larger capacity for synaptic integration of YFP⁺ CR cells, but the result of the electrophysiological experiments revealed no evidence that this CR cells subpopulation received more synaptic inputs. Thus the morphological difference between both CR cells subpopulations did most probably not reflect any functional difference in the amount of synaptic integration between both CR cells subpopulations.

Because CR cells are an integral part of neuronal networks in the marginal zone of the developing cortex, their synaptic inputs and membrane properties will influence the activity in these neuronal networks (Aguiló et al., 1999; Soda et al., 2003). In particular, the activity of CR cells may provide the synaptic input to developing pyramidal neurons that is essential to attach the dendritic bouquets of pyramidal neurons to the most apical part of the developing cortex (Marin-Padilla, 1998; Radnikow et al., 2002). The findings that the electrophysiological properties and synaptic integration, representing the physiological substrate for neuronal activity, are similar in YFP⁺ and YFP⁻ CR cells and that no considerable differences in the morphological appearance, representing the anatomical basis for connectivity and neuronal information processing, were found, suggest that both neuronal populations are equally implicated in the regulation of neuronal activity in the immature cortex. The recruitment of additional origins for CR cells at the pallial–subpallial boundary and the resulting increase in number of available reelin positive neurons has been proposed as an essential step for the evolution of the laminated mammalian cortex (Pierani and Wassef, 2009). The dynamic distribution of these molecularly distinct CR subtypes in pallial territories at early stages of development appears to influence early cortical regionalization/arealization and each individual CR subtype appears to play a specific role in this process (A. Griveau and A. Pierani unpublished results). However, the results of the present study propose that CR cells originating from these additional sources fulfill similar tasks within transient neuronal networks in the marginal zone of the early postnatal cortex

4.2 Functional expression of glycine receptors in SP cells

The application of glycine and the glycinergic agonists taurine and β -alanine evoked membrane responses in all SP cells, with a higher affinity for glycine than for taurine and β -alanine. The obvious cross desensitization between glycine and taurine suggests that both substances act on similar receptors. The affinities for glycine, β -alanine and taurine observed in the present study were comparable to those in other immature cortical neurons (Okabe et al., 2004) and resembles the values found in *Xenopus* oocytes expressing α_2 subunit-containing glycine receptors (Schmieden et al., 1992). Because glycinergic responses were blocked by the glycine receptor

antagonist strychnine and since the GABA_A receptor antagonist gabazine and the NMDA receptor antagonist APV were without effect, the glycine-induced currents were mediated exclusively by classical strychnine sensitive glycine receptors in the SP cells. The SP cells glycine receptors showed a rather low strychnine sensitivity, which is a characteristic property of glycine receptors during early development (Ye, 2000). Although β -alanine is known to block GABA transporters expressed in immature neurons GAT3, (Liu et al., 1993), a significant contamination of the membrane currents by altered transporter currents could be excluded because of their low turnover rates resulting in currents below the resolution of patch-clamp recordings in vertebrate neurons (Masson et al., 1999).

The glycinergic currents recorded in SP cells showed a significant desensitization. The slow time-constant of this desensitization is in the range observed for α_2 subunit-containing glycine receptors (Kungel and Friauf, 1997). Estimation of the reversal potentials, as well as the reduction of GABAergic currents in the presence of glycine, revealed that part of the desensitization was caused by an attenuation of the Cl⁻ gradient. In SP cells, the time-constant of desensitization was similar for all three glycinergic agonists tested. In contrast, in CR cells or CP neurons, a significantly slower desensitization was observed for taurine (Okabe et al., 2004). Since the kinetics of glycine receptor desensitization depend on agonist concentration (Gisselmann et al., 2002), this finding may indicate that the effective taurine concentration at the receptor site may vary between SP cells, CR cells and CP neurons. A more effective taurine uptake or a denser extracellular matrix in the cortical plate and marginal zone may explain different taurine concentrations and glycine receptor desensitization kinetics. In any case, reducing the taurine concentration attenuated the desensitization in SP cells. At a taurine concentration of 100 μ M no significant desensitization was observed, suggesting that taurine is capable to induce stable tonic currents in SP cells.

Pharmacological evidences suggest the functional expression of α/β heteromeric glycine receptors, which did not contain α_1 subunits, in SP cells. The lack of inhibition by 30 μ M picrotoxin, which at this concentration predominantly inhibits homomeric α receptors (Pribilla et al., 1992;Kungel and Friauf, 1997), argues against the expression of homomeric α receptors in SP cells. The α_1 subunit specific

inhibitor CTB was also without effect on the glycine responses, demonstrating that α_1 subunit containing glycine receptors did not significantly contribute to the observed glycinergic effects. The pharmacological properties of glycine receptors on SP cells were similar to receptors found in other cell types of the developing cerebral cortex (Kilb et al., 2002;Okabe et al., 2004) and other parts of the immature CNS (Ye, 2000). Since previous studies demonstrate the predominant expression of α_2 and β glycine receptor subunits in all layers of the immature cortex (Malosio et al., 1991;Fujita et al., 1991;Sato et al., 1991;Flint et al., 1998;Okabe et al., 2004), glycine receptors in SP cells most probably have mainly an α_2/β heteromeric composition. Glycine, taurine and β -alanine are capable to activate α_2/β heteromeric glycine receptors (Farroni and McCool, 2004).

While glycine evokes hyperpolarizing membrane responses in the adult nervous system (Curtis et al., 1967;Vannier and Triller, 1997), glycine receptors mediate a depolarizing action in immature neurons (Ito and Cherubini, 1991;Kandler and Friauf, 1995;Singer et al., 1998;Flint et al., 1998;Ehrlich et al., 1999;Kilb et al., 2002). Since activation of GABA_A receptors depolarizes SP cells (Hanganu et al., 2002), the glycinergic responses in this cell type should also have a depolarizing effect. Indeed, depolarizing membrane responses were induced by glycine receptor activation in all investigated SP cells. The depolarizing action of glycine most probably reflects an increased intracellular Cl⁻ concentration in immature cortical neurons (Cherubini et al., 1991;Owens et al., 1996;Ehrlich et al., 1999;Rivera et al., 1999;Shimizu-Okabe et al., 2002;Yamada et al., 2004), although a contribution of HCO₃⁻ fluxes has been suggested in fetal motoneurons (Kulik et al., 2000, for review see Kaila, 1994;Payne et al., 2003). From the reversal potential of glycine-induced currents in SP cells (-36.7 ± 2 mV) an intracellular Cl⁻ concentration of 34.3 ± 2.7 mM can be estimated, which is higher than the passive Cl⁻ distribution (~ 15 mM at a membrane potential of -60 mV). Thus, an active uptake mechanism for Cl⁻ ions must exist in SP cells. There is strong evidence that the Na⁺-K⁺-2Cl⁻-transporter (isoform NKCC-1) mediates this active Cl⁻ accumulation in immature cortical neurons (Sun and Murali, 1999;Yamada et al., 2004;Achilles et al., 2007), although a NKCC-1 independent regulation of intracellular Cl⁻ has been observed in other brain regions (Balakrishnan et al., 2003;Titz et al., 2003).

Depolarizing membrane responses mediated by ligand-gated Cl⁻ channels do not elicit excitatory responses *per se*, but may also mediate an inhibitory action due to shunting of membrane currents (Staley and Mody, 1992; Lamsa et al., 2000). In fact, it has been demonstrated in the immature cortex that the glycine-induced membrane depolarization mediates shunting inhibition in postnatal Cajal-Retzius cells (Kilb et al., 2002). However, glycine application elicited APs in the majority of SP cells. In addition, subthreshold glycine-induced depolarizations reduced the injection currents required to evoke APs. The generation of APs by AMPA-EPSPs was also facilitated by simultaneous application of glycine in SP cells. However, since no glycinergic synaptic currents had been observed in SP cells (Hanganu et al., 2001), this stimulation paradigm do not mimic the effect of physiological glycine receptor activation. As taurine is the endogenous agonist of glycine receptors in the immature cortex (Flint et al., 1998) and is acting mainly via glycine receptors in the immature cortex (Yoshida et al., 2004), it is also highly significant that low concentrations of this agonist also reduced the thresholds to elicit APs by current injection or synaptic activation. In summary, these results demonstrate a robust excitatory effect of glycine receptor activation in this cell type, which may contribute to the maintenance of adequate activity levels in SP cells to facilitate neuronal information processing in the immature cortex. Whether an excitatory effect of SP cells will increase the activity level within the cortex cannot be predicted from our experiments due to the heterogeneity of subplate neurons (Antonini and Shatz, 1990) and possible implication of inhibitory interneurons. It had been demonstrated at corticostriatal and hippocampal synapses that taurine can induce long-lasting enhancements of synaptic efficiency (Sergeeva et al., 2003). But since this phenomenon is pronounced in adults and much smaller in animals between the second and fourth postnatal week (Chepkova et al., 2002) it may not occur in the early postnatal neocortex.

Because a synaptic activation of glycine receptors does not occur under physiological conditions in SP cells, as suggested by the complete suppression of synaptic activity in the presence of GABA_A and glutamate receptor blockers (Hanganu et al., 2001; Hanganu et al., 2002), glycine receptors are most probably activated by non-synaptic processes. One possibility is the tonic activation of these receptors by the presumable endogenous neurotransmitter taurine, which can be released by non-synaptic processes (Flint et al., 1998). In contrast to this publication, an inhibition of

glycine receptors with strychnine had no effect on holding currents, indicating the lack of tonic glycine receptor-mediated currents in our slice preparations. While we cannot rule out that experimental differences like the different pipette solutions, temperature or solution exchange rates contribute to this diverse findings, the lower density of SP cells, as compared with the cortical plate neurons investigated by Flint et al. (1998), may result in lower extracellular taurine levels. However, the conditions used in both studies did not exactly reproduce the *in-vivo* situation, where extracellular neurotransmitter levels are sufficient to maintain tonic activation of receptors (Chadderton et al., 2004). Indeed, addition of low taurine concentrations to the bathing solution uncovered a strychnine sensitive tonic current. The observation that this current did not desensitized demonstrates that taurine at a physiological concentration, which is probably less than 100 μ M (Andiné et al., 1991), can indeed induce stable tonic currents. The strychnine sensitive currents induced by the taurine uptake blocker GES indicates that functional taurine transporters are present in the immature cortex and suggests that these transporters may contribute to the regulation of extracellular taurine concentrations.

4.3 Taurine activates GABAergic networks in the immature neocortex

The previous results demonstrate that activation of glycine receptors by taurine, even at concentrations that could not elicit action potentials by themselves, had an excitatory influence on SP cells. This excitatory effect of taurine on SP cells influence the neuronal activity of this important neuronal population but can subsequently also modulate neuronal activity in downstream neocortical networks (Dupont et al., 2006; Friauf and Shatz, 1991). Taurine should thus interfere with activity-dependent modifications of early cortical networks (Allendoerfer and Shatz, 1994; Ghosh and Shatz, 1994; Anderson and Price, 2002; Antonini and Shatz, 1990; Kanold et al., 2003). In addition, activation of glycine receptors also provide an excitatory action on other cortical cell types (Flint et al., 1998; Kilb et al., 2002), which can also promote activity within immature neuronal networks. Therefore I investigated in the third part of my PhD work the affect of a tonic activation of glycine receptors on the network activity in the immature neocortex. In this study PSCs recorded in pyramidal neurons of the P0-4 neocortex, which are generated

mainly by presynaptic action potential activity, directly represent the activity level in the immature network.

A direct comparison between the cortical depth of the investigated pyramidal neurons and Nissl-stained slices suggested that most neurons are located in supragranular layers or within Layer IV. The morphological and electrophysiological properties of these neurons and their gradual developmental progress within the investigated interval are comparable to previous studies (Luhmann et al., 2000; McCormick and Prince, 1987). Both, the increasing R_{In} and C_{In} will influence dendritic filtering of GABAergic currents (Rall, 1977; Rose and Call, 1992), therefore disabling a direct comparison between the amplitudes and kinetic properties. However, dendritic filtering has no influence on the frequency of PSCs.

The main finding of this study is that bath application of taurine increases the frequency of PSCs. Since the taurine-induced increase in PSCs frequency was absent in the presence of TTX, these PSCs reflect an increased network activity rather than an increased release probability of presynaptic neurotransmitter vesicles (Hessler et al., 1993; Kirmse and Kirischuk, 2006a). Interestingly, the taurine-induced increase in PSC frequency can be mimicked by bath application of either glycine or the GABAergic agonist isoguvacine. These results suggest that taurine acts on both, GABA_A and glycine receptors to increase the network activity. This observation is a clear indication that GABA_A and glycine receptor activation has an excitatory action on neocortical networks. On the other hand, the taurine induced PSCs could be completely abolished by the glycinergic antagonist strychnine. However, this observation most probably reflects an insufficient activation of GABA_A receptors on presynaptic cells under this condition, because we used only a relatively small taurine concentration of 300 μ M and GABA_A receptors have a relatively low affinity for taurine (Bureau and Olsen, 1991). The observation that activation of GABA_A receptors induces network activity is in line with observations in the early postnatal hippocampus, where GABA clearly triggers network activity (Ben-Ari et al., 1997; Sipila et al., 2005). In the neocortex spontaneous GABA_A receptor mediated network activity occurs later in development around the end of the first postnatal week (Allene et al., 2008), while in the first postnatal week spontaneous network activity was clearly independent of GABA_A receptors (Garaschuk et al., 2000). On

the other hand, despite the observation that glycine evokes depolarizing responses in a variety of immature neuronal cell types (Flint et al., 1998; Ehrlich et al., 1999; Kilb et al., 2002), direct experimental evidence for the involvement of glycine receptors in immature network activity has been delivered only for the spinal cord (Jean-Xavier et al., 2007; Sibilla and Ballerini, 2009). However, since my experiments demonstrate the absence of spontaneous GABAergic activity in the slice, these results only indicate that GABA_A and glycine receptors can potentially contribute to network activity. On the other hand, under *in-vivo* conditions the GABAergic PSCs occurred at rather high frequencies, suggesting that under this condition these receptors contribute to network activity (Hanganu et al., 2006; Khazipov et al., 2004).

Astonishingly, the results of experiments suggest that taurine enhanced only the frequency of GABA_A receptor mediated PSCs. Several lines of evidence support this suggestion. First, the taurine-induced increase in PSC frequency was virtually unaffected in the presence of glutamate receptor antagonists, but completely suppressed in the presence of a GABA_A receptor antagonists. While the later finding may indicate that an activation of GABA_A receptors on the presynaptic cells is required for the activation of these cells, the observation that bath-application of glycine induced a similar gabazine-sensitive increase in PSC frequency strongly suggest that a taurine-mediated glycine-receptor activation is sufficient to induce these PSCs. And third, no increase in the frequency of PSCs was observed when the holding potential was set exactly to the GABA reversal potential. Under this condition, existing GABAergic PSCs could not be detected due to the fact that the driving force for any current through this receptor was abolished. The frequency of remaining PSCs, which were most probably mediated by glutamate receptors, were unaltered under this condition, again emphasizing that exclusively GABAergic PSCS were increased by taurine. And finally, gabazine drastically reduced spontaneous PSCs while strychnine was without effect, suggesting that glycinergic PSCs are absent in pyramidal neurons. To my knowledge, this observation is the first report of a specific activation of GABAergic presynaptic networks by GABAergic agonists or by glycine.

It has been shown by various groups that GABA_A receptors mediate depolarizing membrane responses in pyramidal neurons of the immature neocortex (Owens et al.,

1996;Rheims et al., 2008). This depolarizing membrane responses reflect the elevated $[Cl^-]_i$ due to the absence of Cl^- extrusion transporters like the neuron specific K^+-Cl^- -cotransporter KCC2 (Rivera et al., 1999;Lee et al., 2005) and Cl^- -accumulation by the Na^+ -dependent K^+-2Cl^- -cotransporter NKCC1 (Rohrbough and Spitzer, 1996;Delpire, 2000;Zhu et al., 2008). In accordance with this publications, cell-attached recordings revealed that the GABAergic PSCs evoked by taurine indeed massively increase action potential frequency in pyramidal neurons, unraveling that under native conditions these PSCs mediate an excitatory effect. This observation indicates that bath application of taurine will also enhance the activity of pyramidal neurons, which are glutamatergic. However, our observation that glutamatergic antagonists had no effect on frequency and amplitude of the taurine induced PSCs suggest that this action potential firing of pyramidal neurons is not reflected in synaptic inputs towards pyramidal neurons. This observation may indicate that in the neocortex GABAergic connections dominate before the onset of glutamatergic connections (Hennou et al., 2002;Ben-Ari et al., 2004;Gozlan and Ben-Ari, 2003).

The fact that bath application of taurine, glycine or GABA induced GABAergic PSCs clearly indicate that GABAergic interneurons are activated by these substances. Recordings from genetically labeled and visually identified GABAergic interneurons indeed revealed that they express both $GABA_A$ and glycine receptors. This observation is in line with previous report showing the expression of $GABA_A$ and glycine receptors on adult interneurons (Xiang et al., 1998;Chattipakorn and McMahon, 2002). While $GABA_A$ receptors had already been described in interneurons of the immature hippocampus (Gozlan and Ben-Ari, 2003) no evidences for glycine receptors on cortical interneurons were published so far. The taurine-induced current was in interneurons mediated by both $GABA_A$ and glycine receptors. The observation that strychnine reduced the amplitude of the tonic taurine-induced current to a larger extend than gabazine is in line with the observation that strychnine can effectively abolish the PSCs recorded in pyramidal neurons. In contrast, focal application of high taurine concentration resulted in a large gabazine insensitive current, which is probably mediated mainly by $GABA_A$ receptors (Bureau and Olsen, 1991). In accordance with the excitatory role of ligand-gated Cl^- channels like $GABA_A$ and glycine receptors in the immature CNS (Ben-Ari et al., 2007), bath

application of taurine increases the frequency of action potentials in interneurons, which strongly suggested an excitatory action of GABA and/or glycine in these cells. Therefore also GABAergic synapses on interneurons (Gozlan and Ben-Ari, 2003) will have an excitatory influence on the activity within the GABAergic network. These GABAergic synapses may also contribute to the amount of GABAergic activity induced by the activation of glycine and GABA_A receptors on interneurons.

In summary, the results of this part of my thesis demonstrated for the first time that an activation of glycine or GABA_A receptors induced network activity, which was exclusively mediated via GABAergic interneurons. As many studies demonstrated an effect of depolarizing GABA_A receptor responses on a variety of developmental events, like neurogenesis (Haydar et al., 2000;LoTurco et al., 1995), neuronal migration (Behar et al., 1996;Behar et al., 2000;Denter et al., 2010;Heck et al., 2007) or differentiation (Maric et al., 2001) the glycine and GABA mediated increase in GABAergic activity can profoundly influence the development of neocortical circuits and corticofugal connections (Nguyen et al., 2001;Owens and Kriegstein, 2002). In particular, the excitatory effect of taurine may contribute to the crucial role of taurine during neuronal development (Palackal et al., 1986;Sturman et al., 1994;Maar et al., 1995).

4.4 Conclusion

In summary, the results of all these experiments complemented the knowledge about the neuronal interactions in the immature neocortex and provide additional evidence for the important role of taurine as nonsynaptic neurotransmitter during development. These findings improve our understanding of cellular processes that guide neuronal development and thus shape the brain.

5. Summary

In my PhD work I concentrated on three elementary questions that are essential to understand the interactions between the different neuronal cell populations in the developing neocortex. The questions regarded the identity of Cajal-Retzius (CR) cells, the ubiquitous expression of glycine receptors in all major cell populations of the immature neocortex, and the role of taurine in the modulation of immature neocortical network activity.

To unravel whether CR cells of different ontogenetic origin have divergent functions I investigated the electrophysiological properties of YFP⁺ (derived from the septum and borders of the pallium) and YFP⁻ CR cells (derived from other neocortical origins). This study demonstrated that the passive and active electrophysiological properties as well as features of GABAergic PSCs and glutamatergic currents are similar between both CR cell populations. These findings suggest that CR cells of different origins most probably support similar functions within the neuronal networks of the early postnatal cerebral cortex.

To elucidate whether glycine receptors are expressed in all major cell populations of the developing neocortex I analyzed the functional expression of glycine receptors on subplate (SP) cells. Activation of glycine receptors by glycine, β -alanine and taurine elicited membrane responses that could be blocked by the selective glycinergic antagonist strychnine. Pharmacological experiments suggest that SP cells express functional heteromeric glycine receptors that do not contain α_1 subunits. The activation of glycine receptors by glycine and taurine induced a membrane depolarization, which mediated excitatory effects. Considering the key role of SP cells in immature cortical networks and the development of thalamocortical connections, this glycinergic excitation may influence the properties of early cortical networks and the formation of cortical circuits.

In the third part of my project I demonstrated that tonic taurine application induced a massive increase in the frequency of PSCs. Based on their reversal potential and their pharmacological properties these taurine-induced PSCs are exclusively transmitted via GABA_A receptors to the pyramidal neurons, while both GABA_A and glycine receptors were implicated in the generation of the presynaptic activity. Accordingly, whole-cell and cell-attached recordings from genetically labeled interneurons revealed the expression of glycine and GABA_A receptors, which mediated an excitatory action on these cells. These findings suggest that low taurine concentrations can tonically activate exclusively GABAergic networks. The activity level maintained by this GABAergic activity in the immature nervous system may contribute to network properties and can facilitate the activity dependent formation of adequate synaptic projections.

In summary, the results of my studies complemented the knowledge about neuronal interactions in the immature neocortex and improve our understanding of cellular processes that guide neuronal development and thus shape the brain.

6. References

Achilles K, Okabe A, Ikeda M, Shimizu-Okabe C, Yamada J, Fukuda A, Luhmann HJ, Kilb W (2007) Kinetic properties of Cl uptake mediated by Na⁺-dependent K⁺-2Cl cotransport in immature rat neocortical neurons. *J Neurosci* 27: 8616-8627.

Aguayo LG, van Zundert B, Tapia JC, Carrasco MA, Alvarez FJ (2004) Changes on the properties of glycine receptors during neuronal development. *Brain Res Rev* 47: 33-45.

Aguiló A, Schwartz TH, Kumar VS, Peterlin ZA, Tsiola A, Soriano E, Yuste R (1999) Involvement of Cajal-Retzius neurons in spontaneous correlated activity of embryonic and postnatal layer 1 from wild-type and reeler mice. *J Neurosci* 19: 10856-10868.

Allendoerfer KL, Shatz CJ (1994) The subplate, a transient neocortical structure: Its role in the development of connections between thalamus and cortex. *Annu Rev Neurosci* 17: 185-218.

Allene C, Cattani A, Ackman JB, Bonifazi P, Aniksztejn L, Ben Ari Y, Cossart R (2008) Sequential Generation of Two Distinct Synapse-Driven Network Patterns in Developing Neocortex. *J Neurosci* 28: 12851-12863.

Altshuler D, LoTurco JJ, Rush J, Cepko C (1993) Taurine promotes the differentiation of a vertebrate retinal cell type in vitro. *Development* 119: 1317-1328.

Altshuler D, LoTurco JJ, Rush J, Cepko C (1993) Taurine promotes the differentiation of a vertebrate retinal cell type in vitro. *Development* 119: 1317-1328.

Andäng M, Hjerling-Leffler J, Moliner A, Lundgren TK, Castelo-Branco G, Nanou E, Pozas E, Bryja V, Halliez S, Nishimaru H, Wilbertz J, Arenas E, Koltzenburg M, Charnay P, El Manira A, Ibanez CF, Ernfors P (2008) Histone H2AX-dependent GABA(A) receptor regulation of stem cell proliferation. *Nature* 451: 460-464.

Anderson G, Price DJ (2002) Layer-specific thalamocortical innervation in organotypic cultures is prevented by substances that alter neural activity. *Eur J Neurosci* 16: 345-349.

Andiné P, Sandberg M, Bågenholm R, Lehmann A, Hagberg H (1991) Intra- and extracellular changes of amino acids in the cerebral cortex of the neonatal rat during hypoxic-ischemia. *Dev Brain Res* 64: 115-120.

Antonini A, Shatz CJ (1990) Relation between putative transmitter phenotypes and connectivity of subplate neurons during cerebral cortical development. *Eur J Neurosci* 2: 744-761.

Balakrishnan V, Becker M, Lohrke S, Nothwang HG, Guresir E, Friauf E (2003) Expression and function of chloride transporters during development of inhibitory neurotransmission in the auditory brainstem. *J Neurosci* 23: 4134-4145.

Barrett JN, Crill WE (1974) Specific membrane properties of cat motoneurons. *J Physiol* 239: 301-324.

Bar-Yehuda D, Korngreen A (2007) Cellular and network contributions to excitability of layer 5 neocortical pyramidal neurons in the rat. *PLoS ONE* 2: e1209.

Bayer SA, Altman J (1991) *Neocortical Development*. New York: Raven Press.

Behar TN, Li YX, Tran HT, Ma W, Dunlap V, Scott C, Barker JL (1996) GABA stimulates chemotaxis and chemokinesis of embryonic cortical neurons via calcium-dependent mechanisms. *J Neurosci* 16: 1808-1818.

Behar TN, Schaffner AE, Scott CA, Greene CL, Barker JL (2000) GABA receptor antagonists modulate postmitotic cell migration in slice cultures of embryonic rat cortex. *Cereb Cortex* 10: 899-909.

Behar TN, Schaffner AE, Scott CA, O'Connell C, Barker JL (1998) Differential response of cortical plate and ventricular zone cells to GABA as a migration stimulus. *J Neurosci* 18: 6378-6387.

Behar TN, Scott CA, Greene CL, Wen XL, Smith SV, Maric D, Liu QY, Colton CA, Barker JL (1999) Glutamate acting at NMDA receptors stimulates embryonic cortical neuronal migration. *J Neurosci* 19: 4449-4461.

Behar TN, Smith SV, Kennedy RT, McKenzie JM, Maric I, Barker AL (2001) GABA_B receptors mediate motility signals for migrating embryonic cortical cells. *Cerebral Cortex* 11: 744-753.

Ben-Ari Y (2002) Excitatory actions of GABA during development: the nature of the nurture. *Nat Rev Neurosci* 3: 728-739.

Ben-Ari Y (2006) Basic developmental rules and their implications for epilepsy in the immature brain. *Epileptic Disord* 8: 91-102.

Ben-Ari Y, Gaiarsa JL, Tyzio R, Khazipov R (2007) GABA: a pioneer transmitter that excites immature neurons and generates primitive oscillations. *Physiol Rev* 87: 1215-1284.

Ben-Ari Y, Khalilov I, Represa A, Gozlan H (2004) Interneurons set the tune of developing networks. *Trends Neurosci* 27: 422-427.

Ben-Ari Y, Khazipov R, Leinekugel X, Caillard O, Gaiarsa JL (1997) GABA_A, NMDA and AMPA receptors: a developmentally regulated 'menage a trois'. *Trends in Neurosciences* 20: 523-529.

Bielle F, Griveau A, Narboux-Neme N, Vigneau S, Sigrist M, Arber S, Wassef M, Pierani A (2005) Multiple origins of Cajal-Retzius cells at the borders of the developing pallium. *Nat Neurosci* 8: 1002-1012.

Bormann J, Rundstrom N, Betz H, Langosch D (1993) Residues within transmembrane segment M2 determine chloride conductance of glycine receptor homo- and hetero-oligomers. *EMBO J* 12: 3729-3737.

Bureau MH, Olsen RW (1991) Taurine acts on a subclass of GABA_A receptors in mammalian brain in vitro. *Eur J Pharmacol* 207: 9-16.

Carlson BX, Elster L and Arne Schousboe (1998) Pharmacological and functional implications of developmentally-regulated changes in GABA_A receptor subunit expression in the cerebellum. *European Journal of Pharmacology* 352: 1–14.

Chadderton P, Margrie TW, Hausser M (2004) Integration of quanta in cerebellar granule cells during sensory processing. *Nature* 428: 856-860.

Chan CH, Yeh HH (2003) Enhanced GABA(A) receptor-mediated activity following activation of NMDA receptors in Cajal-Retzius cells in the developing mouse neocortex. *J Physiol* 550: 103-111.

Chattipakorn SC, McMahon LL (2002) Pharmacological characterization of glycine-gated chloride currents recorded in rat hippocampal slices. *J Neurophysiol* 87: 1515-1525.

Chepkova AN, Doreulee N, Yanovsky Y, Mukhopadhyay D, Haas HL, Sergeeva OA (2002) Long-lasting enhancement of corticostriatal neurotransmission by taurine. *Eur J Neurosci* 16: 1523-1530.

Cherubini E, Gaiarsa JL, Ben-Ari Y (1991) GABA: An excitatory transmitter in early postnatal life. *Trends Neurosci* 14: 515-519.

Curtis DR, Hosli L, Johnston GA (1967) Inhibition of spinal neurons by glycine. *Nature* 215: 1502-1503.

Cutler RW, Dudzinski DS (1974) Regional changes in amino acid content in developing rat brain. *J Neurochem* 23: 1005-1009.

D'Arcangelo G, Miao GG, Chen SC, Soares HD, Morgan JI, Curran T (1995) A protein related to extracellular matrix proteins deleted in the mouse mutant *reeler*. *Nature* 374: 719-723.

D'Arcangelo G, Nakajima K, Miyata T, Ogawa M, Mikoshiba K, Curran T (1997) Reelin is a secreted glycoprotein recognized by the CR-50 monoclonal antibody. *J Neurosci* 17: 23-31.

Davies LP, Johnston GA (1974) Postnatal changes in the levels of glycine and the activities of serine hydroxymethyltransferase and glycine:2-oxoglutarate aminotransferase in the rat central nervous system. *J Neurochem* 22: 107-112.

Del Rio JA, Soriano E, Ferrer I (1992) Development of GABA-immunoreactivity in the neocortex of the mouse. *J Comp Neurol* 326: 501-526.

Delpire E (2000) Cation-Chloride Cotransporters in Neuronal Communication. *News Physiol Sci* 15: 309-312.

Denter DG, Heck N, Riedemann T, White R, Kilb W, Luhmann HJ (2010) GABA(C) receptors are functionally expressed in the intermediate zone and regulate radial migration in the embryonic mouse neocortex. *Neuroscience* 167: 124-134.

Derer P, Derer M (1990) Cajal-Retzius cell ontogenesis and death in mouse brain visualized with horseradish peroxidase and electron microscopy. *Neuroscience* 36: 839-856.

Dodt HU, Leischner U, Schierloh A, Jahrling N, Mauch CP, Deininger K, Deussing JM, Eder M, Zieglgansberger W, Becker K (2007) Ultramicroscopy: three-dimensional visualization of neuronal networks in the whole mouse brain. *Nat Methods* 4: 331-336.

Dupont E, Hanganu IL, Kilb W, Hirsch S, Luhmann HJ (2006) Rapid developmental switch in the mechanisms driving early cortical columnar networks. *Nature* 439: 79-83.

Dvorzhak A, Myakhar O, Kamkin A, Kirmse K, Kirischuk S (2008) Postsynaptically different inhibitory postsynaptic currents in Cajal-Retzius cells in the developing neocortex. *Neuroreport* 19: 1213-1216.

Ehrlich I, Löhrike S, Friauf E (1999) Shift from depolarizing to hyperpolarizing glycine action in rat auditory neurones is due to age-dependent Cl⁻ regulation. *J Physiol (Lond)* 520: 121-137.

Farroni JS, McCool BA (2004) Extrinsic factors regulate partial agonist efficacy of strychnine-sensitive glycine receptors. *BMC Pharmacol* 4: 16.

- Flint AC, Liu XL, Kriegstein AR (1998) Nonsynaptic glycine receptor activation during early neocortical development. *Neuron* 20: 43-53.
- Friauf E, McConnell SK, Shatz CJ (1990) Functional synaptic circuits in the subplate during fetal and early postnatal development of cat visual cortex. *J Neurosci* 10: 2601-2613.
- Friauf E, Shatz CJ (1991) Changing patterns of synaptic input to subplate and cortical plate during development of visual cortex. *J Neurophysiol* 66: 2059-2071.
- Fricker D, Verheugen JA, Miles R (1999) Cell-attached measurements of the firing threshold of rat hippocampal neurones. *J Physiol* 517 (Pt 3): 791-804.
- Frotscher M (1998) Cajal-Retzius cells, Reelin, and the formation of layers. *Curr Opin Neurobiol* 8: 570-575.
- Fujita M, Sato K, Sato M, Inoue T, Kozuka T, Tohyama M (1991) Regional distribution of the cells expressing glycine receptor beta subunit mRNA in the rat brain. *Brain Res* 560: 23-37.
- Fukui M, Nakamichi N, Yoneyama M, Ozawa S, Fujimori S, Takahata Y, Nakamura N, Taniura H, Yoneda Y (2008) Modulation of cellular proliferation and differentiation through GABA(B) receptors expressed by undifferentiated neural progenitor cells isolated from fetal mouse brain. *J Cell Physiol* 216: 507-519.
- Garaschuk O, Linn J, Eilers J, Konnerth A (2000) Large-scale oscillatory calcium waves in the immature cortex. *Nat Neurosci* 3: 452-459.
- Garcia-Moreno F, Lopez-Mascaraque L, De Carlos JA (2007) Origins and migratory routes of murine Cajal-Retzius cells. *J Comp Neurol* 500: 419-432.
- Ghosh A, Antonini A, McConnell SK, Shatz CJ (1990) Requirements of subplate neurons in the formation of thalamocortical connections. *Nature* 347: 179-181.
- Ghosh A, Shatz CJ (1993) A role for subplate neurons in the patterning of connections from thalamus to neocortex. *Development* 117: 1031-1047.

- Ghosh A, Shatz CJ (1994) Segregation of geniculocortical afferents during the critical period: A role for subplate neurons. *J Neurosci* 14: 3862-3880.
- Gisselmann G, Galler A, Friedrich F, Hatt H, Bormann J (2002) Cloning and functional characterization of two glycine receptor alpha-subunits from the perch retina. *Eur J Neurosci* 16: 69-80.
- Gozlan H, Ben-Ari Y (2003) Interneurons are the source and the targets of the first synapses formed in the rat developing hippocampal circuit. *Cereb Cortex* 13: 684-692.
- Hanganu IL, Ben Ari Y, Khazipov R (2006) Retinal waves trigger spindle bursts in the neonatal rat visual cortex. *J Neurosci* 26: 6728-6736.
- Hanganu IL, Kilb W, Luhmann HJ (2001) Spontaneous synaptic activity of subplate neurons in neonatal rat somatosensory cortex. *Cereb Cortex* 11: 400-410.
- Hanganu IL, Kilb W, Luhmann HJ (2002) Functional Synaptic Projections onto Subplate Neurons in Neonatal Rat Somatosensory Cortex. *J Neurosci* 22: 7165-7176.
- Hanganu IL, Luhmann HJ (2004) Functional nicotinic acetylcholine receptors on subplate neurons in neonatal rat somatosensory cortex. *J Neurophysiol* 92: 189-198.
- Haydar TF, Wang F, Schwartz ML, Rakic P (2000) Differential modulation of proliferation in the neocortical ventricular and subventricular zones. *J Neurosci* 20: 5764-5774.
- Heck N, Kilb W, Reiprich P, Kubota H, Furukawa T, Fukuda A, Luhmann HJ (2007) GABA-A receptors regulate neocortical neuronal migration in vitro and in vivo. *Cereb Cortex* 17: 138-148.
- Hennou S, Khalilov I, Diabira D, Ben-Ari Y, Gozlan H (2002) Early sequential formation of functional GABA(A) and glutamatergic synapses on CA1 interneurons of the rat foetal hippocampus. *Eur J Neurosci* 16: 197-208.
- Hessler NA, Shirke AM, Malinow R (1993) The probability of transmitter release at a mammalian central synapse. *Nature* 366: 569-572.

Hestrin S, Armstrong WE (1996) Morphology and physiology of cortical neurons in layer I. *J Neurosci* 16: 5290-5300.

Hevner RF, Neogi T, Englund C, Daza RA, Fink A (2003) Cajal-Retzius cells in the mouse: transcription factors, neurotransmitters, and birthdays suggest a pallial origin. *Brain Res Dev Brain Res* 141: 39-53.

Hirsch S, Luhmann HJ (2008) Pathway-specificity in N-methyl-d-aspartate receptor-mediated synaptic inputs onto subplate neurons. *Neuroscience* 153: 1092-1102.

Ito S, Cherubini E (1991) Strychnine-sensitive glycine responses of neonatal rat hippocampal neurones. *J Physiol (Lond)* 440: 67-83.

Jean-Xavier C, Mentis GZ, O'Donovan MJ, Cattaert D, Vinay L (2007) Dual personality of GABA/glycine-mediated depolarizations in immature spinal cord. *Proc Natl Acad Sci U S A* 104: 11477-11482.

Kaila K (1994) Ionic basis of GABA_A receptor channel function in the nervous system. *Prog Neurobiol* 42: 489-537.

Kandler K, Friauf E (1995) Development of glycinergic and glutamatergic synaptic transmission in the auditory brainstem of perinatal rats. *J Neurosci* 15: 6890-6904.

Kanold PO (2004) Transient microcircuits formed by subplate neurons and their role in functional development of thalamocortical connections. *Neuroreport* 15: 2149-2153.

Kanold PO, Kara P, Reid RC, Shatz CJ (2003) Role of subplate neurons in functional maturation of visual cortical columns. *Science* 301: 521-525.

Khazipov R, Sirota A, Leinekugel X, Holmes GL, Ben-Ari Y, Buzsáki G (2004) Early motor activity drives spindle bursts in the developing somatosensory cortex. *Nature* 432: 758-761.

Kilb W, Hanganu IL, Okabe A, Sava BA, Shimizu-Okabe C, Fukuda A, Luhmann HJ (2008) Glycine receptors mediate excitation of subplate neurons in neonatal rat cerebral cortex. *J Neurophysiol* 100: 698-707.

- Kilb W, Hartmann D, Saftig P, Luhmann HJ (2004) Altered morphological and electrophysiological properties of Cajal-Retzius cells in cerebral cortex of embryonic Presenilin-1 knockout mice. *Eur J Neurosci* 20: 2749-2756.
- Kilb W, Ikeda M, Uchida K, Okabe A, Fukuda A, Luhmann HJ (2002) Depolarizing glycine responses in Cajal-Retzius cells of neonatal rat cerebral cortex. *Neuroscience* 112: 299-307.
- Kilb W, Luhmann HJ (2000) Characterization of a hyperpolarization-activated inward current in Cajal-Retzius cells in rat neonatal neocortex. *J Neurophysiol* 84: 1681-1691.
- Kilb W, Luhmann HJ (2001) Spontaneous GABAergic postsynaptic currents in Cajal-Retzius cells in neonatal rat cerebral cortex. *Eur J Neurosci* 13: 1387-1390.
- Kim HG, Connors BW (1993) Apical dendrites of the neocortex: Correlation between sodium- and calcium-dependent spiking and pyramidal cell morphology. *J Neurosci* 13: 5301-5311.
- Kirmse K, Kirischuk S (2006a) Ambient GABA constrains the strength of GABAergic synapses at Cajal-Retzius cells in the developing visual cortex. *J Neurosci* 26: 4216-4227.
- Kirmse K, Kirischuk S (2006b) N-ethylmaleimide increases release probability at GABAergic synapses in layer I of the mouse visual cortex. *Eur J Neurosci* 24: 2741-2748.
- Kostovic I, Judas M (2002) The role of the subplate zone in the structural plasticity of the developing human cerebral cortex. *Neuroembryology* 1: 145-153.
- Kostovic I, Rakic P (1980) Cytology and time of origin of interstitial neurons in the white matter in infant and adult human and monkey telencephalon. *J Neurocytol* 9: 219-242.
- Kulik A, Nishimaru H, Ballanyi K (2000) Role of bicarbonate and chloride in GABA- and glycine-induced depolarization and $[Ca^{2+}]_i$ rise in fetal rat motoneurons *in situ*. *J Neurosci* 20: 7905-7913.

Kungel M, Friauf E (1997) Physiology and pharmacology of native glycine receptors in developing rat auditory brainstem neurons. *Dev Brain Res* 102: 157-165.

Lamsa K, Palva JM, Ruusuvuori E, Kaila K, Taira T (2000) Synaptic GABA(A) activation inhibits AMPA-kainate receptor-mediated bursting in the newborn (P0-P2) rat hippocampus. *J Neurophysiol* 83: 359-366.

Latsari M, Dori I, Antonopoulos J, Chiotelli M, Dinopoulos A (2002) Noradrenergic innervation of the developing and mature visual and motor cortex of the rat brain: a light and electron microscopic immunocytochemical analysis. *J Comp Neurol* 445: 145-158.

Lee H, Chen CX, Liu YJ, Aizenman E, Kandler K (2005) KCC2 expression in immature rat cortical neurons is sufficient to switch the polarity of GABA responses. *Eur J Neurosci* 21: 2593-2599.

Li H, Tornberg J, Kaila K, Airaksinen MS, Rivera C (2002) Patterns of cation-chloride cotransporter expression during embryonic rodent CNS development. *Eur J Neurosci* 16: 2358-2370.

Liu QR, Lopez-Corcuera B, Mandiyan S, Nelson H, Nelson N (1993) Molecular characterization of four pharmacologically distinct gamma-aminobutyric acid transporters in mouse brain [corrected]. *J Biol Chem* 268: 2106-2112.

LoTurco JJ, Owens DF, Heath MJ, Davis MB, Kriegstein AR (1995) GABA and glutamate depolarize cortical progenitor cells and inhibit DNA synthesis. *Neuron* 15: 1287-1298.

Lu S, Bogarad LD, Murtha MT, Ruddle FH (1992) Expression pattern of a murine homeobox gene, *Dbx*, displays extreme spatial restriction in embryonic forebrain and spinal cord. *Proc Natl Acad Sci U S A* 89: 8053-8057.

Lu SM, Zecevic N, Yeh HH (2001) Distinct NMDA and AMPA receptor-mediated responses in mouse and human Cajal-Retzius cells. *J Neurophysiol* 86: 2642-2646.

Luhmann HJ, Prince DA (1991) Postnatal maturation of the GABAergic system in rat neocortex. *J Neurophysiol* 65: 247-263.

Luhmann HJ, Reiprich RA, Hanganu I, Kilb W (2000) Cellular physiology of the neonatal rat cerebral cortex: Intrinsic membrane properties, sodium and calcium currents. *J Neurosci Res* 62: 574-584.

Luskin MB and Shatz CJ (1985) Studies of the early generated cells of the cat's visual cortex: cogeneration of the subplate and migrational zones. *J Neurosci* 5, 1062-1075

Maar T, Moran J, Schousboe A, Pasantés-Morales H (1995) Taurine deficiency in dissociated mouse cerebellar cultures affects neuronal migration. *Int J Dev Neurosci* 13: 491-502.

Malosio ML, Marqueze-Pouey B, Kuhse J, Betz H (1991) Widespread expression of glycine receptor subunit mRNAs in the adult and developing rat brain. *EMBO J* 10: 2401-2409.

Maric D, Liu QY, Maric I, Chaudry S, Chang YH, Smith SV, Sieghart W, Fritschy JM, Barker JL (2001) GABA expression dominates neuronal lineage progression in the embryonic rat neocortex and facilitates neurite outgrowth via GABA_A autoreceptor/Cl⁻ channels. *J Neurosci* 21: 2343-2360.

Marin-Padilla M (1990) Three-dimensional structural organization of layer I of the human cerebral cortex: a Golgi study. *J Comp Neurol* 299: 89-105.

Marin-Padilla M (1998) Cajal-Retzius cells and the development of the neocortex. *Trends Neurosci* 21: 64-71.

Masson J, Sagne C, Hamon M, El Mestikawy S (1999) Neurotransmitter transporters in the central nervous system. *Pharmacol Rev* 51: 439-464.

McConnell SK, Ghosh A, Shatz CJ (1989) Subplate neurons pioneer the first axon pathway from the cerebral cortex. *Science* 245: 978-982.

McCormick DA, Prince DA (1987) Post-natal development of electrophysiological properties of rat cerebral cortical pyramidal neurones. *J Physiol (Lond)* 393: 743-762.

- Mechawar N, Descarries L (2001) The cholinergic innervation develops early and rapidly in the rat cerebral cortex: a quantitative immunocytochemical study. *Neuroscience* 108: 555-567.
- Medina L, Legaz I, Gonzalez G, De Castro F, Rubenstein JL, Puelles L (2004) Expression of Dbx1, Neurogenin 2, Semaphorin 5A, Cadherin 8, and Emx1 distinguish ventral and lateral pallial histogenetic divisions in the developing mouse claustramygdaloid complex. *J Comp Neurol* 474: 504-523.
- Metin C, Baudoin JP, Rakic S, Parnavelas JG (2006) Cell and molecular mechanisms involved in the migration of cortical interneurons. *Eur J Neurosci* 23: 894-900.
- Meyer G, González-Hernández T (1993) Developmental changes in layer I of the human neocortex during prenatal life: A DiI-tracing and AChE and NADPH-d histochemistry study. *J Comp Neurol* 338: 317-336.
- Meyer G, Perez-Garcia CG, Abraham H, Caput D (2002) Expression of p73 and Reelin in the developing human cortex. *J Neurosci* 22: 4973-4986.
- Meyer G, Soria JM, Martínez-Galán JR, Martín-Clemente B, Fairén A (1998) Different origins and developmental histories of transient neurons in the marginal zone of the fetal and neonatal rat cortex. *J Comp Neurol* 397: 493-518.
- Meyer G, Wahle P (1999) The paleocortical ventricle is the origin of reelin-expressing neurons in the marginal zone of the foetal human neocortex. *Eur J Neurosci* 11: 3937-3944.
- Mienville JM (1998) Persistent depolarizing action of GABA in rat Cajal-Retzius cells. *J Physiol (Lond)* 512: 809-817.
- Mienville JM (1999) Feature article cajal-retzius cell physiology: Just in time to bridge the 20th century. *Cerebral Cortex* 9: 776-782.
- Mienville JM, Pesold C (1999) Low resting potential and postnatal upregulation of NMDA receptors may cause Cajal-Retzius cell death. *J Neurosci* 19: 1636-1646.
- Momose-Sato Y, Honda Y, Sasaki H, Sato K (2005) Optical imaging of large-scale correlated wave activity in the developing rat CNS. *J Neurophysiol* 94: 1606-1622.

Muth-Kohne E, Terhag J, Pahl S, Werner M, Joshi I, Hollmann M (2010) Functional excitatory GABAA receptors precede ionotropic glutamate receptors in radial glia-like neural stem cells. *Mol Cell Neurosci* 43: 209-221.

Naqui SZH, Harris BS, Thomaidou D, Parnavelas JG (1999) The noradrenergic system influences the fate of Cajal-Retzius cells in the developing cerebral cortex. *Dev Brain Res* 113: 75-82.

Nguyen L, Rigo JM, Rocher V, Belachew S, Malgrange B, Rogister B, Leprince P, Moonen G (2001) Neurotransmitters as early signals for central nervous system development. *Cell Tissue Res* 305: 187-202.

Nobuaki T, Yuchio Y, Ryohei T, Jun-ichi M, Kunihiko O and Takeshi K (2003) Green Fluorescent Protein Expression and Colocalization with Calretinin, Parvalbumin, and Somatostatin in the GAD67-GFP Knock-In Mouse. *The journal of comparative neurology* 467:60–79.

Noctor SC, Flint AC, Weissman TA, Dammerman RS, Kriegstein AR (2001) Neurons derived from radial glial cells establish radial units in neocortex. *Nature*. 409:714-20.

Okabe A, Kilb W, Shimizu-Okabe C, Hanganu IL, Fukuda A, Luhmann HJ (2004a) Homogenous glycine receptor expression in cortical plate neurons and Cajal-Retzius cells of neonatal rat cerebral cortex. *Neuroscience* 123: 715-724.

Owens DF, Boyce LH, Davis MB, Kriegstein AR (1996) Excitatory GABA responses in embryonic and neonatal cortical slices demonstrated by gramicidin perforated-patch recordings and calcium imaging. *J Neurosci* 16: 6414-6423.

Owens DF, Kriegstein AR (2002) Is there more to GABA than synaptic inhibition? *Nat Rev Neurosci* 3: 715-727.

Owens DF, Liu XL, Kriegstein AR (1999) Changing properties of GABA_A receptor-mediated signaling during early neocortical development. *J Neurophysiol* 82: 570-583.

Palackal T, Moretz R, Wisniewski H, Sturman J (1986) Abnormal visual cortex development in the kitten associated with maternal dietary taurine deprivation. *J Neurosci Res* 15: 223-239.

Parnavelas JG (2000) The origin and migration of cortical neurones: new vistas. *Trends Neurosci* 23: 126-131.

Parnavelas JG, Papadopoulos GC, Cavanagh ME (1988) Changes in neurotransmitters during development. In: *Cerebral Cortex* (Peters A, Jones EG, eds), pp 177-209. New York, London: Plenum Press.

Paudice P, Gemignani A, Raiteri M (1998) Evidence for functional native NMDA receptors activated by glycine or D- serine alone in the absence of glutamatergic coagonist. *Eur J Neurosci* 10: 2934-2944.

Paxinos G, Törk I, Tecott LH, Valentino KL (1991) *Atlas of the developing rat brain*. San Diego: Academic Press.

Payne JA, Rivera C, Voipio J, Kaila K (2003) Cation-chloride co-transporters in neuronal communication, development and trauma. *Trends Neurosci* 26: 199-206.

Pierani A, Brenner-Morton S, Chiang C, Jessell TM (1999) A sonic hedgehog-independent, retinoid-activated pathway of neurogenesis in the ventral spinal cord. *Cell* 97: 903-915.

Pierani A, Wassef M (2009) Cerebral cortex development: From progenitors patterning to neocortical size during evolution. *Dev Growth Differ* 51: 325-342.

Pleasure SJ, Anderson S, Hevner R, Bagri A, Marin O, Lowenstein DH, Rubenstein JLR (2000) Cell migration from the ganglionic eminences is required for the development of hippocampal GABAergic interneurons. *Neuron* 28: 727-740.

Plotkin MD, Snyder EY, Hebert SC, Delpire E (1997) Expression of the Na-K-2Cl cotransporter is developmentally regulated in postnatal rat brains: A possible mechanism underlying GABA's excitatory role in immature brain. *J Neurobiol* 33: 781-795.

Pribilla I, Takagi T, Langosch D, Bormann J, Betz H (1992) The atypical M2 segment of the beta subunit confers picrotoxinin resistance to inhibitory glycine receptor channels [published erratum appears in EMBO J 1994 Mar 15;13(6):1493]. EMBO J 11: 4305-4311.

Radnikow G, Feldmeyer D, Lubke J (2002) Axonal projection, input and output synapses, and synaptic physiology of cajal-retzius cells in the developing rat neocortex. J Neurosci 22: 6908-6919.

Rall W (1977) Core conductor theory and cable properties of neurons. Handbook of Physiology -The Nervous System 1 in Handbook of Physiology, E. R. Kandel, Ed. Bethesda, MD: American Physiological Society, 1977.

Rheims S, Minlebaev M, Ivanov A, Represa A, Khazipov R, Holmes GL, Ben-Ari Y, Zilberter Y (2008) Excitatory GABA in rodent developing neocortex in vitro. J Neurophysiol 100: 609-619.

Rivera C, Voipio J, Payne JA, Ruusuvuori E, Lahtinen H, Lamsa K, Pirvola U, Saarma M, Kaila K (1999) The K^+/Cl^- co-transporter KCC2 renders GABA hyperpolarizing during neuronal maturation. Nature 397: 251-255.

Rohrbough J, Spitzer NC (1996) Regulation of intracellular Cl^- levels by Na^+ -dependent Cl^- cotransport distinguishes depolarizing from hyperpolarizing GABA receptor-mediated responses in spinal neurons. J Neurosci 16: 82-91.

Rose GJ, Call SJ (1992) Evidence for the role of dendritic spines in the temporal filtering properties of neurons: The decoding problem and beyond. Proc Natl Acad Sci USA 89: 9662-9665.

Sarnat HB, Flores-Sarnat L (2002) Cajal-Retzius and subplate neurons: their role in cortical development. Eur J Paediatr Neurol 6: 91-97.

Sato K, Zhang JH, Saika T, Sato M, Tada K, Tohyama M (1991) Localization of glycine receptor alpha 1 subunit mRNA-containing neurons in the rat brain: an analysis using in situ hybridization histochemistry. Neuroscience 43: 381-395.

- Schmieden V, Kuhse J, Betz H (1992) Agonist pharmacology of neonatal and adult glycine receptor alpha subunits: identification of amino acid residues involved in taurine activation. *EMBO J* 11: 2025-2032.
- Schwartz TH, Rabinowitz D, Unni V, Kumar VS, Smetters DK, Tsiola A, Yuste R (1998) Networks of coactive neurons in developing layer 1. *Neuron* 20: 541-552.
- Sergeeva OA, Chepkova AN, Doreulee N, Eriksson KS, Poelchen W, Monnighoff I, Heller-Stilb B, Warskulat U, Häussinger D, Haas HL (2003) Taurine-induced long-lasting enhancement of synaptic transmission in mice: role of transporters. *J Physiol* 550: 911-919.
- Shimizu-Okabe C, Yokokura M, Okabe A, Ikeda M, Sato K, Kilb W, Luhmann HJ, Fukuda A (2002) Layer-specific expression of Cl⁻ transporters and differential [Cl⁻]_i in newborn rat cortex. *Neuroreport* 13: 2433-2437.
- Shinozaki K, Miyagi T, Yoshida M, Miyata T, Ogawa M, Aizawa S, Suda Y (2002) Absence of Cajal-Retzius cells and subplate neurons associated with defects of tangential cell migration from ganglionic eminence in *Emx1/2* double mutant cerebral cortex. *Development* 129: 3479-3492.
- Shirasaki T, Klee MR, Nakaye T, Akaike N (1991) Differential blockade of bicuculline and strychnine on GABA- and glycine-induced responses in dissociated rat hippocampal pyramidal cells. *Brain Res* 561: 77-83.
- Shoji H, Ito T, Wakamatsu Y, Hayasaka N, Ohsaki K, Oyanagi M, Kominami R, Kondoh H, Takahashi N (1996) Regionalized expression of the *Dbx* family homeobox genes in the embryonic CNS of the mouse. *Mech Dev* 56: 25-39.
- Sibilla S, Ballerini L (2009) GABAergic and glycinergic interneuron expression during spinal cord development: dynamic interplay between inhibition and excitation in the control of ventral network outputs. *Prog Neurobiol* 89: 46-60.
- Sidman RL, Rakic P (1973) Neuronal migration, with special reference to developing human brain: a review. *Brain Res* 62: 1-35.

Singer JH, Talley EM, Bayliss DA, Berger AJ (1998) Development of glycinergic synaptic transmission to rat brain stem motoneurons. *J Neurophysiol* 80: 2608-2620.

Sipila ST, Huttu K, Soltesz I, Voipio J, Kaila K (2005) Depolarizing GABA acts on intrinsically bursting pyramidal neurons to drive giant depolarizing potentials in the immature hippocampus. *J Neurosci* 25: 5280-5289.

Soda T, Nakashima R, Watanabe D, Nakajima K, Pastan I, Nakanishi S (2003) Segregation and coactivation of developing neocortical layer 1 neurons. *J Neurosci* 23: 6272-6279.

Spitzer NC (2006) Electrical activity in early neuronal development. *Nature* 444: 707-712.

Squier LR (2003) *Fundamental Neuroscience*. Second edition. Chapter 14 Neural induction and pattern formation. San Diego, Academic Press.

Srinivas S, Watanabe T, Lin CS, Williams CM, Tanabe Y, Jessell TM, Costantini F (2001) Cre reporter strains produced by targeted insertion of EYFP and ECFP into the ROSA26 locus. *BMC Dev Biol* 1: 4.

Staley KJ, Mody I (1992) Shunting of excitatory input to dentate gyrus granule cells by a depolarizing GABA_A receptor-mediated postsynaptic conductance. *J Neurophysiol* 68: 197-212.

Sturman JA, Lu P, Xu YX, Imaki H (1994) Feline maternal taurine deficiency: effects on visual cortex of the offspring. A morphometric and immunohistochemical study. *Adv Exp Med Biol* 359: 369-384.

Sturman JA, Lu P, Xu YX, Imaki H (1994) Feline maternal taurine deficiency: effects on visual cortex of the offspring. A morphometric and immunohistochemical study. *Adv Exp Med Biol* 359: 369-384.

Sun D, Murali SG (1999) Na⁺-K⁺-2Cl⁻ cotransporter in immature cortical neurons: A role in intracellular Cl⁻ regulation. *J Neurophysiol* 81: 1939-1948.

Sur M, Rubenstein JL (2005) Patterning and plasticity of the cerebral cortex. *Science* 310: 805-810.

Takiguchi-Hayashi K, Sekiguchi M, Ashigaki S, Takamatsu M, Hasegawa H, Suzuki-Migishima R, Yokoyama M, Nakanishi S, Tanabe Y (2004) Generation of reelin-positive marginal zone cells from the caudomedial wall of telencephalic vesicles. *J Neurosci* 24: 2286-2295.

Titz S, Hans M, Kelsch W, Lewen A, Swandulla D, Misgeld U (2003) Hyperpolarizing inhibition develops without trophic support by GABA in cultured rat midbrain neurons. *J Physiol* 550: 719-730.

Turecek R, Trussell LO (2001) Presynaptic glycine receptors enhance transmitter release at a mammalian central synapse. *Nature* 411: 587-590.

Tyzio R, Ivanov A, Bernard C, Holmes GL, Ben Ari Y, Khazipov R (2003) Membrane potential of CA3 hippocampal pyramidal cells during postnatal development. *J Neurophysiol* 90: 2964-2972.

Tyzio R, Represa A, Jorquera I, Ben-Ari Y, Gozlan H, Aniksztejn L (1999) The establishment of GABAergic and glutamatergic synapses on CA1 pyramidal neurons is sequential and correlates with the development of the apical dendrite. *J Neurosci* 19: 10372-10382.

Valverde F, Facal Valverde MV, Santacana M and Heredia M (1989) Development and differentiation of the early generated cells of sublayer VIb in the somatosensory cortex of the rat: a correlated Golgi and autoradiographic study. *J. Comp. Neurol.* 209, 118-140.

Vannier C, Triller A (1997) Biology of the postsynaptic glycine receptor. *Int Rev Cytol* 176: 201-244.

Wang C, Shimizu-Okabe C, Watanabe K, Okabe A, Matsuzaki H, Ogawa T, Mori N, Fukuda A, Sato K (2002) Developmental changes in KCC1, KCC2, and NKCC1 mRNA expressions in the rat brain. *Brain Res Dev Brain Res* 139: 59-66.

Wang F, Xiao C, Ye JH (2005) Taurine activates excitatory non-synaptic glycine receptors on dopamine neurones in ventral tegmental area of young rats. *J Physiol* 565: 503-516.

- Wang DD, Kriegstein AR (2009) Defining the role of GABA in cortical development. *J Physiol* 587: 1873-1879.
- Williams K (1993) Ifenprodil discriminates subtypes of the N-methyl-D-aspartate receptor: selectivity and mechanisms at recombinant heteromeric receptors. *Mol Pharmacol* 44: 851-859.
- Xiang ZX, Huguenard JR, Prince DA (1998) GABA_A receptor-mediated currents in interneurons and pyramidal cells of rat visual cortex. *J Physiol (Lond)* 506: 715-730.
- Yamada J, Okabe A, Toyoda H, Kilb W, Luhmann HJ, Fukuda A (2004) Cl⁻ uptake promoting depolarizing GABA actions in immature rat neocortical neurones is mediated by NKCC1. *J Physiol* 557: 829-841.
- Ye J (2000) Physiology and pharmacology of native glycine receptors in developing rat ventral tegmental area neurons. *Brain Res* 862: 74-82.
- Yoshida M, Assimacopoulos S, Jones KR, Grove EA (2006) Massive loss of Cajal-Retzius cells does not disrupt neocortical layer order. *Development* 133: 537-545.
- Yoshida M, Fukuda S, Tozuka Y, Miyamoto Y, Hisatsune T (2004) Developmental shift in bidirectional functions of taurine-sensitive chloride channels during cortical circuit formation in postnatal mouse brain. *J Neurobiol* 60: 166-175.
- Yun K, Potter S, Rubenstein JL (2001) Gsh2 and Pax6 play complementary roles in dorsoventral patterning of the mammalian telencephalon. *Development* 128: 193-205.
- Zecevic N, Rakic P (2001) Development of layer I neurons in the primate cerebral cortex. *J Neurosci* 21: 5607-5619.
- Zhou FM, Hablitz JJ (1996a) Layer I neurons of rat neocortex. I. Action potential and repetitive firing properties. *J Neurophysiol* 76: 651-667.
- Zhou FM, Hablitz JJ (1996b) Morphological properties of intracellularly labeled layer I neurons in rat neocortex. *J Comp Neurol* 376: 198-213.

Zhou FM, Hablitz JJ (1996c) Postnatal development of membrane properties of layer I neurons in rat neocortex. *J Neurosci* 16: 1131-1139.

Zhu L, Polley N, Mathews GC, Delpire E (2008) NKCC1 and KCC2 prevent hyperexcitability in the mouse hippocampus. *Epilepsy Res* 79: 201-212

Zhu Y, Li H, Zhou L, Wu JY, Rao Y (1999) Cellular and molecular guidance of GABAergic neuronal migration from an extracortical origin to the neocortex. *Neuron* 23: 473-485.

Acknowledgments

Thanks to all students and members of the lab, it has been a pleasure to work with you.

Last, but most importantly, I want to thank my wife, for believing in me and supporting me through my ups and downs.

To them I dedicate this thesis.

Declaration of contribution

This thesis is based on two publications that I coauthored and recent experiments that are not published. Part of the material & methods, results and discussion as well as some figures are directly taken from these publications.

For the publication “Electrophysiological and morphological properties of Cajal-Retzius cells with different ontogenetic origins” by BA Sava, CS David, A Teissier, A Pierani, JF Steiger, HJ Luhmann and W Kilb published in *Neuroscience* 167:724-3 (2010), I participated in the planning of the study, performed and analyzed all electrophysiological experiments, delivered all stained neurons for subsequent morphological analysis, prepared most figures and contributed to the writing of the manuscript. My contribution to this manuscript is approximately 70 %. The Figs. 1-9 were taken from this publication and chapter 3.1 and 4.1 of this thesis are based on this publication.

For the publication “Glycine Receptors Mediate Excitation of Subplate Neurons in Neonatal Rat Cerebral Cortex” by W Kilb, IL Hanganu, A Okabe, BA Sava, C Shimizu-Okabe, A Fukuda, and HJ Luhmann published in *J. Neurophysiol* 100: 698–707 (2008) I participated in planning of some experiment, contributed to the experiments regarding agonists dose-dependency and antagonists pharmacology, performed all experiments regarding cross-desensitization and extrasynaptic taurine/GES actions, contributed to the analysis of these experiments, prepared the figures of the latter two experiments. My overall contribution to this manuscript is about 30%. I was involved in all of the experiments of this study presented in this thesis. The Figs. 10-17 were taken from this publication and chapter 3.2 and 4.2 of this thesis are based on this publication.

Curriculum vitae

Personal Informations:

Name: Aurel Bogdan, Sava

Address: Universitätsmedizin der Johannes Gutenberg-Universität
Institut für Physiologie und Pathophysiologie
Duesbergweg 6, D-55128 Mainz, Germany

Date of Birth: Born in Romania in 1979

Tel: (06131)-39-20442

E-mail: sava@uni-mainz.de

Education:

Since May 2007 PhD student in Neurophysiology at the “Institute of Physiology and Pathophysiology” Medical Faculty, Johannes Gutenberg University, Mainz

Feb 2003 – Jun 2006 Postgraduate studies, fellowship within Max Planck Institute “*Molecular and Cellular Biophysics*“ Friedrich-Schiller University, Germany.

Sep 2001 – Feb 2003 Working at the “ Al. I. Cuza” University of Iasi, Faculty of Physics, in the Spectroscopy Department.

Sep 1997 – Jun 2001 “ Al. I. Cuza” University of Iasi, Romania, Faculty of Physics, Section Medical Physics; graduating mark: 9,37 (in a scale from 1 to 10)

Diploma Thesis “The study of surface properties using the *Contact Angle method* “

Certificate: “Laboratory Animal Science” 40 hours of theoretical and practical training 19-23th July 2010 “ University of Mainz ”

Teaching: Tutor for muscle practicum at Medical Faculty ”Johannes Gutenberg University of Mainz”

Research

- Since 2007: Neocortical development. Under the supervision of PD. Dr. rer. nat. Werner Kilb and Prof. Dr. Heiko Luhmann, Institute of Physiology and Pathophysiology, Medical Faculty, Johannes Gutenberg University, Mainz, Germany.
- 2003-2006: Gating and thermodynamics of EAG potassium channels. Under supervision of Prof. Stefan Heinemann, Max Planck Institute “*Molecular and Cellular Biophysics*“ Friedrich-Schiller University, Jena, Germany.

Publications

- **BA Sava**, CS David, A Teissier, A Pierani, JF Steiger, HJ Luhmann and W Kilb (2010) Electrophysiological and morphological properties of Cajal-Retzius cells with different ontogenetic origins. *Neuroscience* 167:724-3.
- W Kilb, IL Hanganu, A Okabe, **BA Sava**, C Shimizu-Okabe, A Fukuda, and HJ Luhmann (2008) Glycine Receptors Mediate Excitation of Subplate Neurons in Neonatal Rat Cerebral Cortex. *J. Neurophysiol* 100: 698–707

Two others manuscripts are in preparation:

- **BA Sava**, HJ Luhmann, and W Kilb Taurine promotes neocortical excitation by the selective activation of GABAergic subpopulations
- **BA Sava**, C Hügel, K Achilles, HJ Luhmann and W Kilb Cholinergic activity excites Cajal-Retzius cells via activation of neocortical GABAergic interneurons.

Oral presentations

- **Sava, A.B.**, Luhmann, HJ., and Kilb, W., GABAergic networks in the developing cerebral cortex are activated by Taurine, Keynote Lecture at the 88th German Physiological Society, 22-25 March 2009, Giessen, Germany.

Poster presentations

- **Sava, BA.**, CS. David, A Teissier, A. Pierani, JF. Steiger, HJ Luhmann and W. Kilb (2010) Electrophysiological and morphological properties of Cajal-Retzius cells with different ontogenetic origins. *7th FENS meeting*, July 2010, Amsterdam, Holland.
- **Sava, BA.**, CS. David, A Teissier, A. Pierani, JF. Steiger, HJ Luhmann and W. Kilb (2010) Electrophysiological and morphological properties of Cajal-Retzius cells with different ontogenetic origins. *1th rmn2*, Nov. 2010, Oberwessel, Germany.
- **Sava, BA.**, Luhmann, HJ., and Kilb, W., GABAergic networks in the developing cerebral cortex are activated by Taurine, 8th German Neuroscience Society, 25-29 March 2009, Göttingen, Germany

- **Sava, BA.**, Kilb, W. and Luhmann, H.-J Taurine specifically activates GABAergic networks in the developing cerebral cortex. *IAK meeting*, November 2008, Mainz, Germany.
- **Sava, BA.**, Kilb, W. and Luhmann, H.-J., Excitatory Actions of Taurine on Single Neurons and Neuronal Networks of the Developing Cerebral Cortex, *6th FENS meeting*, July 2008, Geneva, Switzerland.